Energy, Mines and Resources Canada
Earth Physics Branch
1 Observatory Crescent
Ottawa Canada
K1A 0Y3

Énergie, Mines et Ressources Canada
Direction de la physique du globe
1 Place de l'Observatoire
Ottawa Canada
K1A 0Y3

Geothermal Service of Canada

Service géothermique du Canada

INVESTIGATION OF MOISTURE MOVEMENTS AND STRESSES IN FROZEN SOILS

P.J. Williams and J.A. Wood

Geotechnical Science Laboratories
Department of Geography
Carleton University

Earth Physics Branch Open File Number 82-20
Ottawa, Canada, 1982

143p & 17p Appendices

Price/Prix: $52.00

Energy, Mines and Resources Canada
Énergie, Mines et Ressources Canada

Earth Physics Branch
Direction de la physique du globe

1 Observatory Crescent
Ottawa Canada
K1A 0Y3

1 Place de l'Observatoire
Ottawa Canada
K1A 0Y3

Geothermal Service of Canada

Service géothermique du Canada

INVESTIGATION OF MOISTURE MOVEMENTS AND STRESSES IN FROZEN SOILS

P.J. Williams and J.A. Wood

Geotechnical Science Laboratories
Department of Geography
Carleton University

Earth Physics Branch Open File Number 82-20
Ottawa, Canada, 1982

143p & 17p Appendices

Price/Prix: $52.00

Abstract

An apparatus has been developed for the measurement of pressure changes in frozen soils during thermally induced moisture migration. The results are analyzed from a thermodynamic perspective, and from that of current theory on the rheological properties of frozen soils. The regelation-transport mechanism was also investigated and the results found to be in close agreement with the values predicted by the Clapeyron equation. A review of recent developments in the concept of frost heaving as well as current theory on the mechanism of water migration in frozen soils completes the report.

Resumé

Un appareil a été développé pour mesurèr les changements de pression dans les sols gelés lors de migrations d'eau induite thermiquement. Les résultâts sont analysés dans une perspective thermodynamique et à la lumière de la théorie actuelle sur les propriétés rhéologiques des sols gelés. Le mécanisme de transport - regélation a aussi été étudié et les résultâts obtenus sont en accord aux valeurs prédite par l'équation de Clapeyron. Une revue des développements récent dans les concepts de soulèvement par le gel aussi que les théories courantes sur les mécanismes de migration d'eau dans les sols gelés complète le rapport.

FINAL REPORT

Investigation of Moisture Movements and Stresses in Frozen Soils

by

P.J. Williams and J.A Wood

to the

Department of Energy, Mines and Resources
Earth Physics Branch

Geotechnical Science Laboratories
Department of Geography
Carleton University
Ottawa, Ontario
K1S 5B6

Contract Serial No. OSU81-00119
DSS File No. 23SU 23235-1-0700

June, 1982

TABLE OF CONTENTS

TABLE OF CONTENTS (continued)

LIST OF FIGURES AND TABLES

Figure

LIST OF FIGURES AND TABLES (continued)

Figure

Table

NOMENCLATURE

P	pressure
T	temperature
s	entropy
v	specific volume
G	specific free energy
μ	chemical potential
L	specific heat of fusion of water, mass transport coefficient
ρ	density
σ_{iw}	surface tension (ice-water interface)
π	osmotic pressure
θ_i	volumetric ice content
θ_w	volumetric water content
R	universal gas constant
r	radius of curvature
σ_e	effective stress
σ_T	total stress
σ_n	neutral stress
C_s	solute concentration
ϕ	osmotic coefficient, total hydraulic potential
τ	film thickness
∇	differential operator
J	flux

Conversion Factors

1 Kilopascal = 10.20 cm. of water

1 Bar = 100 kilopascals

INTRODUCTION

This report describes a further year's research into the fundamental nature and behaviour of frozen ground. In 1973 studies were initiated at the Geotechnical Science Laboratories that demonstrated the migration of water within frozen ground. Discussions in the Berger Inquiry into the Mackenzie Valley pipeline, represented a first and significant practical application for this research. Movement of water within frozen ground means that higher frost heave pressures develop than previously thought, especially over long periods; the realization of this led to the rejection of the geotechnical designs for that pipeline. Subsequently, research has continued under contract to Energy, Mines and Resources directed towards improving knowledge of the rates of water movement and heave in, for example, frozen ground around a pipeline. The movement of water in or out of frozen samples under temperature gradients was demonstrated but various factors appeared to influence the rates of flow. The nature and quantitative effects of these factors have now been examined.

Our report of July 1981 described slightly more than a year's work on these aspects and, in particular, modifications of the apparatus permitting measurement of stresses in the frozen sample. The present report describes measurements with the apparatus. Differences in pressure within the frozen sample are associated with differences of temperature and it now appears that the yield stress of the frozen soil is an important factor controlling the accumulation of ice and thus the migration of moisture within the frozen soil. Thus, to the basic thermodynamic potentials (the driving forces) and the hydraulic conductivities (the transport coefficients), must be added the mechanical properties of the various soil types as a controlling factor in the all-important question of frozen soil heave and pressure effects.

Field evidence from Russia, China and, not least, Canada indicates a wide range of strain rates in frozen ground due to moisure migration. Current designs for the Alaska Highway Gas Pipeline are based on insulation procedures to prevent freezing of the ground by the pipe. The procedure is necessitated by the inability to predict the frost heave. The procedure is costly, and in any case, a fuller understanding of frozen ground behaviour is essential to define the extent of insulation required. The practical implications of the findings described in this report and their complex nature lead to the conclusion that as progress is made, the demonstrable need for further research has increased rather than diminished.

SECTION 1

THERMODYNAMICS OF SOIL FREEZING

1.1 Freezing-Point Depression In Bulk Water

A fundamental equation used in thermodynamics is the Gibbs equation. Expressed in differential form, this is given as:

$$dG = vdP - sdT \tag{1.1}$$

where G = the specific free energy of the system,
P = the pressure,
v = the specific volume,
s = the specific entropy
and T = the absolute temperature.

Equation 1.1 relates changes in the temperature and pressure of any system to changes in its free energy. Figure 1.1 illustrates the temperature dependence of the Gibbs free energy for water at atmosphere pressure p. The breaks in the slope of the curve represent the change in entropy involved in the transition from one phase to the next. If the pressure of the water is raised by an increment Δp, equation (1.1) indicates that free energy will also increase. Note, however, that the freezing temperature decreases. The phenomenon can be attributed to the enhanced molecular movement of the water at higher pressures which increases the tendency for the solid phase to break up at lower temperatures.

The pressure dependence of the temperature at which phase change occurs in any substance is indicated by the generalized form of the Clapeyron equation:

$$\frac{dP}{dT} = \frac{S_2 - S_1}{V_2 - V_1} \tag{1.2}$$

where the subscripts 1 and 2 denote the appropriate phase.

This is an exact result and applies to any phase change provided equilibrium is maintained between the two phases (Atkins, 1978). The quantity S_2-S_1 denotes the change in the specific entropy of the system involved in the transformation from phase 1 to phase 2.

Although the Clapeyron equation, in the form shown above, relates changes in the freezing temperature to the total changes in pressure on the system, it does not specify how the freezing-point changes when the change

Figure 1.1

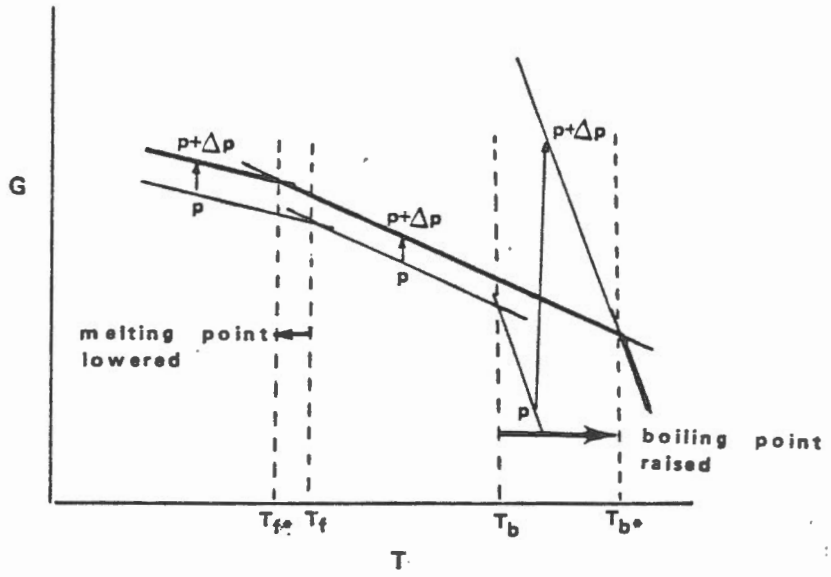

The pressure and temperature dependence of the Gibbs free energy and its effect on the melting and boiling points of water. The phase with the lowest G is the stable phase at that temperature.

after Atkins (1978)

in pressure on two co-existing phases are different. It is well established that in frozen soils, for example, the ice and water are not generally at the same pressure (Koopmans and Miller 1966, Williams 1967). Edlefsen and Anderson (1943) derived a modified form of the Clapeyron equation:

$$v_w dP_w - v_i dP_i = \frac{L dT}{T} \qquad (1.3)$$

where P_i and P_w = the pressure of the ice and water,
v_i and v_w = the specific volume of the two phases,
dT = the freezing-point depression of the water;[1]
T = the absolute temperature of the system,
and L = the specific latent heat of fusion of water at temperature.

Equation (1.3) indicates that for a system of water and ice in thermodynamic equilibrium, freezing-point depression is produced by a rise in the pressure of the ice or a fall in the pressure of the unfrozen water or a combination of both changes.

Hudson (1906) examined three extreme cases of the equation above: (i) If P_i is increased by 1 atmosphere while P_w remains constant, dT = -0.0899K. (ii) If, however, P_i remains constant while P_w is decreased by 1 atmosphere, dT = -0.0824K. (iii) If P_i and P_w are both raised by 1 atmosphere then dT = 0.0075K. The latter value represents the difference in dT in the two cases above.

1.2 Relationship Between The Shape of the Ice-Water Interface and Its Freezing Point

The theory of ice crystal growth in small capillaries and porous media was formally worked out and described by Everett (1961). He investigated the thermodynamic conditions governing the equilibrium and growth of small ice crystals immersed in a bath of their own melt.

For a small ice crystal to exist in equilibrium with its own melt, the free energy of the crystal must equal that of the surrounding water. However, figure 1.1 indicates that at any given pressure the free energy of bulk ice is less than that of water at temperatures below the normal freezing-point. Thus, in order for a small crystal to maintain equilibrium with its own melt, its free energy must exceed that of bulk ice. This is achieved by an increase

---

[1] The freezing temperature of bulk water at 1 atmosphere pressure = 273.15K.

in the pressure of the ice above that of the surrounding melt. The condition is described by the Laplace equation:

$$P_i - P_w = \sigma_{iw} \frac{dA}{dV} \qquad (1.4)$$

where σ_{iw} = the free energy or surface tension of the interface $\simeq 30.5 \times 10^{-3}$ Nm^{-1},

A = the area of the interface

and V = the volume of the crystal[2].

Equilibrium between the crystal and its melt is maintained by adopting a shape for which dA/dV satisfies $P_i - P_w$, the equilibrium condition being determined by P_i, P_w and the temperature T. Assuming a spherical interface, equation (1.4) becomes:

$$P_i - P_w = \frac{2\sigma_{iw}}{r_{iw}} \qquad (1.5)$$

where r_{iw} = the radius of curvature of the interface.

An implicit assumption in equation (1.5) is that the freezing-temperature along a convex interface is less than that along a planar interface as a result of the rise in pressure within the ice. The relationship between the radius of curvature of an ice-water interface and the associated depression in the freezing-point of the water is described by the Kelvin equation:

$$r^* = \frac{2\sigma_{iw} T}{L\Delta T} \qquad (1.6)$$

For the case of an ice crystal growing within a small capillary or a soil pore, r* represents the 'critical radius' of a spherical ice body that is in a stable equilibrium with the surrounding water, at temperature ΔT below the freezing temperature of bulk ice. Note that r* decreases as ΔT increases. Equilbrium between the crystal and the pore water exists when $r_{iw} = r^*$, since the free energy of the two phases is identical. Growth of the ice varies when the temperature is lowered so that $r_{iw} > r^*$. Under these conditions, the free

---

[2] Bulk and volume terms are included in the Laplace equation since the total free energy of a crystal represents the sum of a contribution from the interface as well as one from its volume.

energy of the water exceeds that of the ice and so the crystal grows spontaneously until equilibrium is attained.

Although the Clapeyron and the Laplace equations specify the magnitude of the suction $P_i - P_w$ at any temperature below freezing, the question of the degree to which this condition is satisfied by a rise in the ice pressure and a fall in the water pressure has not yet been satisfactorily answered in the literature. Everett (1961) identified two extreme cases in which the condition is satisfied:

(1) By an increase in the ice pressure above that of bulk ice, the water pressure remaining constant and equal to that of bulk ice.

(2) By a fall in the pressure of the unfrozen pore water below that of bulk ice, the pressure of the pore ice remaining constant and equal to that of bulk ice at that temperature.

In subsequent tests on frozen soils, Williams (1967) and other investigators demonstrated that $P_i - P_w$ is produced, "at least in part,by a fall in the pressure of the unfrozen pure water." Overall,one is generally led to assume that the ice pressure is atmospheric at the surface of the soil and increases according to its hydrostatic value with depth.

1.3 Growth of Ice in Porous Media

Anderson and Hoekstra (1965) using x-ray diffraction techniques demonstrated that most of the unfrozen water in frozen soils is retained as liquid films immediately adjacent to the particle surfaces. The existence of these films implies a freezing-point depression which is produced by the interaction between the water and the soil mineral surfaces. The phenomenon is generally attributed to two mechanisms, (i) direct adsorption of the ice water by the soil mineral matrix and (ii) the presence of solutes in the bulk solution of the soil pores and in the diffuse electric double layer associated with the surface of the particles.[3]

---

[3] The convex nature of the ice-water interface is often erroneously identified as one of the mechanisms responsible for freezing-point depressions in soils. Realistically, however, the shape of the interface should be regarded as a factor rather than a mechanism in itself. The reason for this is that, truly stable ice crystals are never found in bulk water (where the condition is, at best, metastable) and can only exist in capillaries and porous media. The implication is that the freezing-point is depressed somehow, by the interaction with the walls of the pores.

As the temperature of the soil is lowered, pore ice forms spontaneously and the thickness of each film diminshes. Since the adsorptive and osmotic forces increase, in a roughly exponential manner, towards the mineral surfaces, the free energy of the liquid film also increases accordingly. Consequently, one would expect a corresponding increase in the freezing-point depression of the water, towards the particle surfaces. Evidence for this is found in the overall shape of the soil freezing characteristic curves for various soils. (See example Figure 1.2). In all cases, the freezing characteristic curve shows an initially sharp decline in the unfrozen water content at relatively warm temperatures, followed by an attenuation in the slope of the curve at lower temperatures. Eventually the curve tends to level out somewhat, and very large changes in temperature are required to reduce the unfrozen water content significantly.

The presence of significant amounts of unfrozen water in silts as well as clays at low temperatures can be explained by the fact that double layers tend to form spontaneously on particles of all sizes, colloidal as well as non-colloidal (Miller, 1980). In the lower temperature ranges, clays usually contain greater amounts of unfrozen water than silts at the same temperature. This can be accounted for by the fact that silts are composed largely of quartz, which has a lower specific surface area and surface charge density, in comparison with most aluminium silicates (clay minerals). Hence, the thickness of the double layers and their respective ion concentrations will be considerably lower than in most clay soils.

Everett (1961) indicates that the size of the crystals that can grow in a system of rigid pores is restricted by their geometry. Stable ice can only exist where, $r_p > r^*$ (r_p = the radius of the pore). An unstable condition exists when, $r < r^*$. In this case, the ice will be unable to form within the pores.

Everett (1961) also suggests that in freezing soils, ice enters the pores in a manner similar to the intrusion of air in unfrozen soils.[4] As the temperature of the soil is lowered, r^* becomes less than r_{jw} which enables ice to enter progressively smaller pores and to penetrate further into the narrow regions of pores in which ice is directly present. Along the pore walls and in the wedge shaped regions between the soil particles, a liquid film is always present since the osmotic pressure is much greater in these regions than elsewhere due to the presence of the double layer concentration.

---

[4] This assumption has been questioned by a number of authors (Loch, 1975).

Figure 1.2

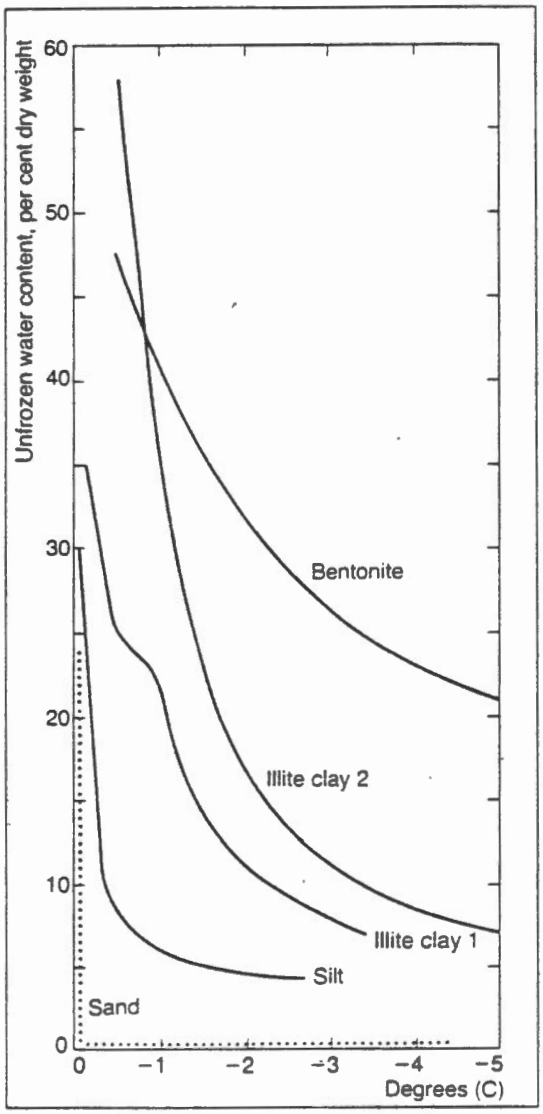

Water contents of frozen soils. Water remains unfrozen as a result of capillary, osmotic and surface adsorption effects, but is progressively replaced by ice at lower temperatures. Thus the water contents depends on temperature and type of soil.

Williams (1979)

SECTION 2

RECENT DEVELOPMENTS IN THE CONCEPT OF FROST HEAVING

2.1 Capillary Model

The term 'frost heaving' describes the condition in which the pore ice within the soil, exceeds the volume of the pores resulting in an ice rich zone or discrete layers of ice called ice lenses. The phenomenon is generally attributed to the redistribution of water and ice within the soil in response to temperature induced gradients of potential within the soil system. The mechanisms governing the migration of water and the formation of ice lenses in freezing soils are not well understood. At least three separate models have been developed in recent years, to explain the process of frost heaving. These are generally referred to as the capillary model, the hydrodynamic model and the secondary frost heaving model. All three models start with the Clapeyron equation. Thereafter, the similarity ends.

The capillary model, originally developed by Everett (1961) remains the most widely accepted of the three models and is the simplest to understand. According to this model, ice lenses form at the frostline, the conditions for growth arising when an advancing ice-water interface is unable to penetrate a pore at a given temperature. The explanation lies in the concept embodied in the Laplace surface tension equation given earlier.

As a freezing-front advances through the soil, either of two conditions will be met:

(i) If the radius of curvature of the ice-water interface (which is defined by the temperature of the soil) is less than the radius of the minimum dimension of each pore at the frost line R, that is $r_{iw} < R$, ice crystals will form immediately within the pores and the frost line will advance. In this situation:

$$P_i > P_w + \frac{2\sigma_{iw}}{R} \qquad (2.1)$$

(ii) If however, the freezing front encounters a series of pores for which $r_{iw} > R$, the ice will be unable to form within the pores.

$$P_i < P_w + \frac{2\sigma_{iw}}{R} \qquad (2.2)$$

Figure 2.1

Growth Of An Ice Lens According To The Capillary Model

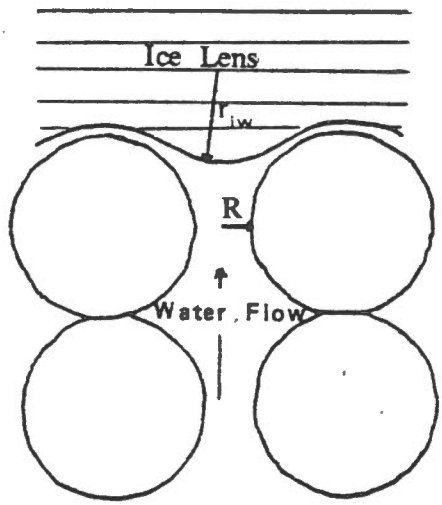

$r_{iw} > R$

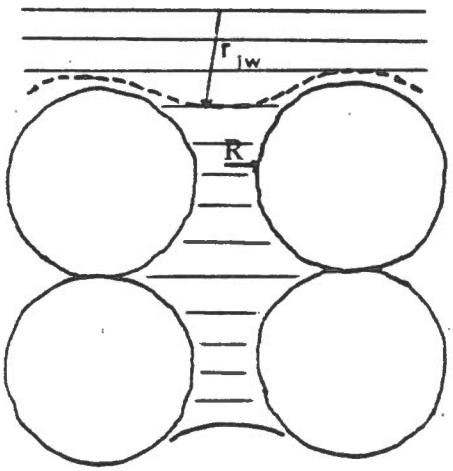

$r_{iw} < R$

Since the unfrozen water at the frost line is under a pressure considerably less than that of the water in the adjacent unfrozen zone, a strong suction gradient is established towards the frost line. This results in water migration towards the freezing-front, water freezing at the frost line and forming on ice lens. Growth of the lens ceases when r_{iw} decreases sufficiently to allow entry of the ice into the pores beneath the lens. This condition may be induced either by a fall in the pressure of the unfrozen pore water beneath the lens or a rise in the overburden pressure.

According to Everett (1961), the maximum heaving pressure that can develop is defined by the Laplace equation:

$$P_{i,max} = P_w + \frac{2\sigma_{iw}}{R} \qquad (2.3)$$

With this model, the rate of growth of an ice lens during heaving is related both to the permeability of the unfrozen soil beneath the lens as well as the rate of extraction of latent heat liberated during the formation of the lens the latter condition imposing restrictions on the rate at which freezing can occur at the frost line.

There are a number of serious drawbacks with the capillary model, the most important of which are outlined briefly below.

First of all, although the model allows prediction of the heaving pressures in a soil where the range of pore sizes is relatively uniform, it is not entirely clear what happens when there is a wide range in pore sizes. Secondly, measurements of heaving pressure obtained by Penner (1967) and Sutherland and Gaskin (1973) for relatively uniform soils, have been found to be roughly twice the value predicted by the Laplace equation. In addition to the above, the capillary model does not allow for the formation of ice lenses in already frozen ground, a phenomenon which has been reported by a number of authors (Washburn 1979). Moreover, recent experimental evidence indicates that in most instances, ice lenses do not form at the frost line as is implied in capillary model but instead form in the partly frozen soil some distance behind the frost line (Penner, 1980; Loch and Kay, 1978). The term 'frozen fringe' was used by Miller (1972) to describe the frozen zone bounded on one side by the frost line and on the other by the ice lens. This being the case, it becomes apparent that the maximum heaving pressure and the rate of heaving will be strongly dependent upon the hydraulic properties and the rate of heat transfer within the frozen fringe. This is explained in the hydrodynamic approach to frost heaving outlined below.

2.2 Hydrodynamic Model

The hydrodynamic model, originally proposed by Harlan (1971, 1973), is based on the continuity equation for frozen soils:

$$\frac{\partial(\rho_i \theta_i)}{\partial t} + \frac{\partial(\rho_w \theta_w)}{\partial t} = -\nabla \cdot \underline{J} \qquad (2.4)$$

where $\rho_i \theta_i$ and $\rho_w \theta_w$ = the mass of the ice and water per unit volume of soil (ρ = density and θ = volumetric water or the content),

$\underline{J}$ = the flow velocity or flux of the water[1]

and t = the time.

The operator ∇ is defined as:[2]

$$\nabla = \left(\underline{i} \frac{\partial}{\partial x} + \underline{j} \frac{\partial}{\partial y} + \underline{k} \frac{\partial}{\partial z} \right) \qquad (2.5)$$

Note that ∇ operates on the flux $\underline{J}$, a vector quantity. The term $\nabla \cdot \underline{J}$ is usually referred to as the divergence of flux. Assuming that Darcy's law remains valid for frozen soils, this term may be expressed as:

$$J = -L_f \nabla \phi \qquad (2.6)$$

where ϕ = the total hydraulic potential

and L_f = the hydraulic conductivity of the frozen soil.

The latter term is expressed as a function of temperature T, since the hydraulic conductivity of most frozen soils has been found to be strongly temperature dependent, especially at temperatures near the freezing-point.

Substituting for the flux in equation (2.4) gives an expression for the conservation of mass in terms of the hydraulic conductivity of the soil and the total hydraulic gradient.

In a somewhat similar fashion, Hallan (1973) derived a generalized heat transfer equation for frozen soils:

$$\frac{\partial(C_a T)}{\partial t} = \nabla \cdot \lambda_{T,t} \nabla T - c_w \rho_w [\nabla (JT)] \qquad (2.7)$$

---

[1] With this model, Harlan (1971) has tacitly assumed that the pore ice remains immobile within the frozen soil.

[2] The terms $\underline{i}$, $\underline{j}$ and $\underline{k}$ are the unit vectors in the x, y and z directions of the Cartesian co-ordinate system.

where λ = the thermal conductivity of the soil (expressed as a function of the temperature and the time),

T = the temperature,

c_w = the specific heat of water

and J = the fluid flux

Equation (2.4) includes terms for both heat transfer by conduction as well as convective heat transfer by moisture migration. C_a is a term which describes the apparent heat capacity of frozen soils:

$$C_a = C_{T,t} - L\ \rho_i\ \left(\frac{\partial \theta_i}{\partial T}\right) \qquad (2.8)$$

where $C_{T,t}$ = the volumetric heat capacity of the soil

and L = the latent heat of fusion of water.

C_a is similar to the volumetric heat capacity of the soil except that it includes a term for the addition or loss of heat to the soil from the freezing or melting of water.

Equations (2.4) and (2.7) indicate that the heat and mass transfer in the frozen soil are interdependent, the total hydraulic gradient being a function of the temperature gradient and the heat transfer being dependent upon the convective transport of water. It is clear that these terms must be linked in some manner. The link is provided by the Clapeyron equation which specifies the relationship between the suction and temperature and thus the total driving force for moisture movement. The Clapeyron equation also provides the criterion which determine whether heat losses from the soil induce changes in phase or temperature within the system (Taylor and Luthin, 1972).

Figure 2.2 summarizes the boundary conditions which prevail during the formation of an ice lens, according to the hydrodynamic model. For explanatory purposes, a number of simplifying assumptions have been made:
(1) that the temperature gradient across the soil is linear,
(2) the soil is saturated and homogeneous throughout the column,
(3) freezing is unidirectional in the vertical (z) dimension.

Moisture flow within the soil proceeds in the direction of colder temperatures where the potential of the soil water is lowest. This follows as a result of the increased suction within the frozen soil as specified by the Clapeyron equation. Note that the hydraulic conductivity of the frozen section decreases with temperature and is very much less than that in the unfrozen soil — the implication being that the flux in the unfrozen soil is much greater than that in the frozen zone (i.e. $J_{uf} >> J_f$). Continuity of mass (equation 2.4), in effect states that, if the moisture flux into a layer

Figure 2.2

Growth Of An Ice Lens According To The Hydrodynamic Model

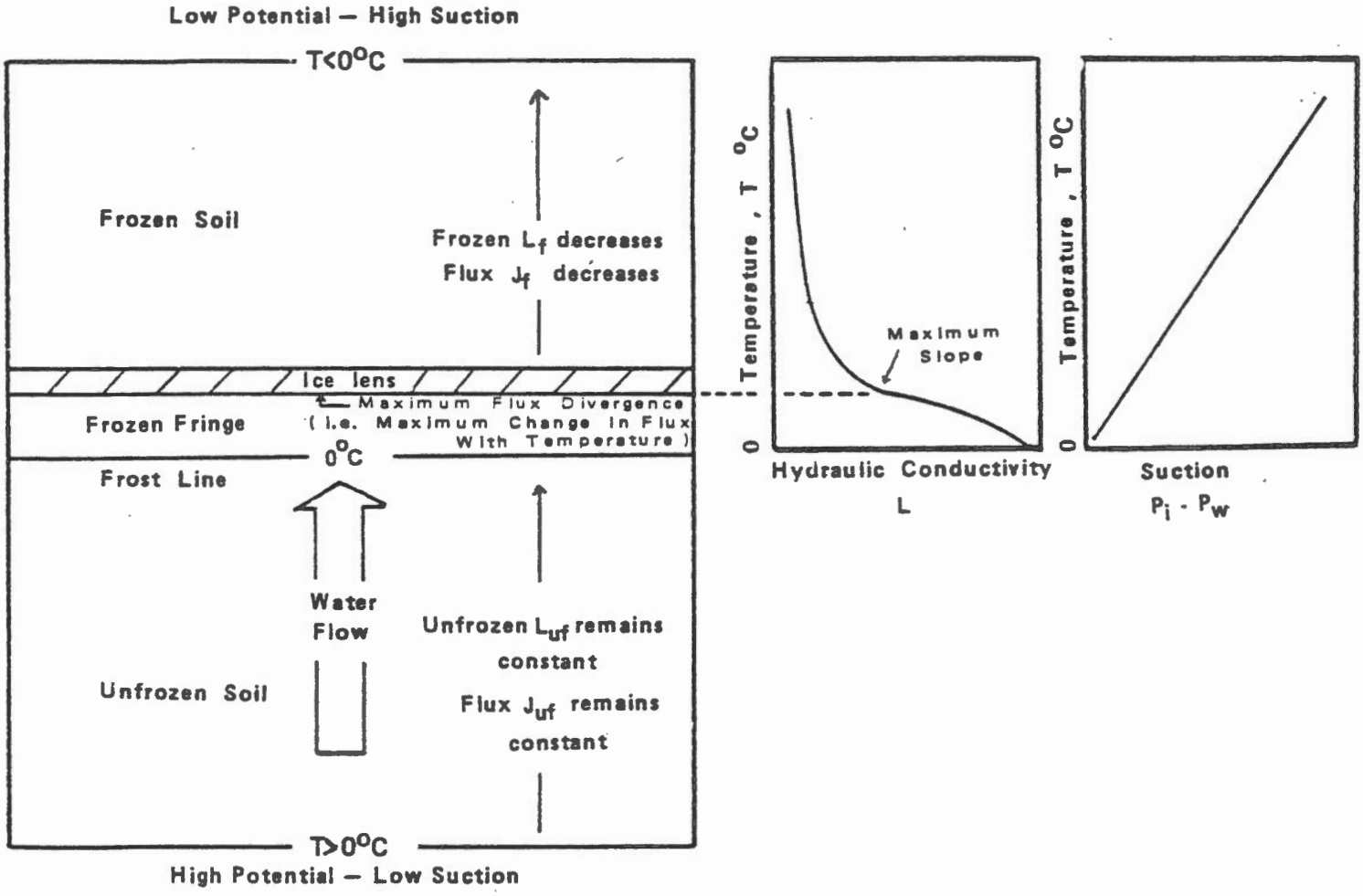

of soil is greater than the flux out, then the soil is storing the excess as ice or water or both. In the case of an actively growing ice lens, then the storage term in equation 2.1 is ice.

According to the hydrodynamic model, the base of an actively growing ice lens is defined as an infinitesimal layer within the frozen fringe where the divergence of flux ($\nabla \cdot \underline{J}$) is maximum. In other words, this occurs where the difference between the flux in and the flux out of the column is maximum. At this point, the rate of change of flux with temperature is also maximum. This condition is met where the temperature change within the soil corresponds with the greatest decrease in the hydraulic conductivity. Figure 2.3 indicates that with most soils the greatest change in the hydraulic conductivity with temperature occurs between 0°C and -0.3°C. In view of this, it would be reasonable to assume that most ice lenses are formed somewhere between the 0°C and -0.3°C isotherms in freezing soils. Evidence supporting this conclusion is provided by Penner (1980) who located the position of ice lenses in freezing soils using x-rays and by Loch and Kay (1978) using a dual energy gamma ray scanning system.

The degree to which the hydrodynamic model realistically simulates the growth of ice lenses is not known, since the model has not yet been rigorously tested against laboratory data (Loch and Kay, 1978). Although the model allows for the growth of ice lenses within already-frozen soil, there are a number of important points which appear to have been overlooked. First of all, the model only indicates the location of an ice lens relative to the frost line, it does not indicate the boundary conditions which initiate and terminate the growth of the lens. Secondly, the model assumes that the ice phase in the frozen fringe is immobile and that moisture flow is restricted to the fluid phase. However, experiments by Horiguchi and Miller (1980) and a recent analysis by Miller, Loch and Bresler (1975) indicate that regelation can form a large fraction of the total moisture transport in frozen soils even at relatively warm temperatures. Another difficulty with the hydrodynamic model is that the ice pressure is assumed to be atmospheric throughout the frozen fringe. No attempt is made to describe the relationship between the stress of the overburden, the pressure of the liquid and ice phases and the intergranular stress with the frozen fringe.

2.3 Secondary Frost Heaving Model

The secondary frost heaving model, proposed by Miller (1972, 1978) is the first attempt to describe the distribution of the overburden pressure between the ice and water phases and the soil skeleton. Miller (1972) distinguished between two different types of frost heaving in soils. These he termed 'primary' and 'secondary' heaving.

Primary heaving refers to the mechanism described by the capillary model. Miller (1978) indicates that the condition probably only occurs naturally during the formation of needle ice. The phenomenon is generally attributed to steady states which have been attained within the soil, so that the formation of ice at the soil surface is sustained by the continuous flow of water towards the freezing plane, the column below remaining saturated and ice free (Loch and Miller, 1978).

Figure 2.3

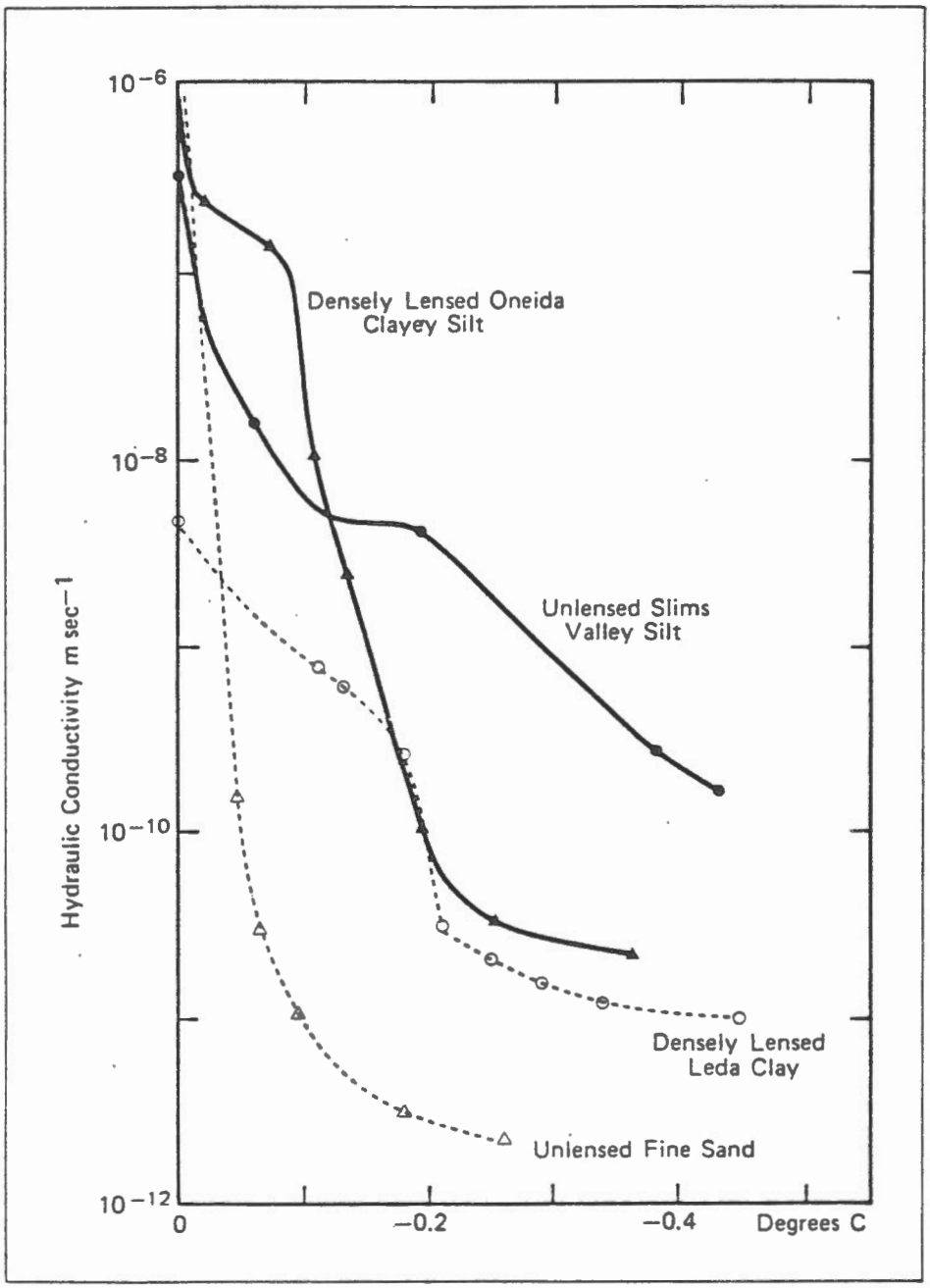

Values of the permeability or hydraulic conductivity coefficient for various soils, over a range of temperatures.

Burt and Williams (1976)

Secondary heaving is associated with non-steady state conditions and describes the process whereby ice lenses form in the frozen soil some distance behind the frost line. Miller (1972) suggested that the pore ice within the frozen fringe would not be immobile, as was believed by many investigators, but instead would move through the soil as an integral part of the ice body, including the ice lens. The driving mechanism for the system is the temperature induced gradients of potential between the 'warm' and the 'cold' ends of the frozen fringe. Moisture movement occurs by a series-parallel transport mechanism involving, (i) transport entirely within the fluid phase; (ii) plug movement of pore ice and (iii) regelation transport. The latter term describes the process in which water traverses the pores in the ice phase, travelling around the soil particles in the fluid films adjacent to each particle. Motion within the pore ice proceeds at a uniform translational velocity and is accompanied by internal exchanges of latent heat between the ice-water interfaces on the upstream and downstream sides of the ice body (Miller, Loch and Bresler, 1975).

Conservation of mass within the frozen fringe is expressed by the continuity equation (2.4). Since the total mass transfer across the frozen fringe represents the sum of the flux in the ice and water phases, equation (2.4) must include terms for regelation transport. Similarily, the equation for heat transport must include terms for convective transport by the movement of pore ice as well as conductive heat transfer and convective transport in the fluid phase.

Miller (1977, 1978) also specified the criteria which define the position of ice lens relative to the freezing-point. These are related to Terzaghi's effective stress equation:

$$\sigma_e = \sigma_T - \sigma_n \qquad (2.9)$$

where σ_e = the effective or intergranular stress between the soil particles,

σ_T = the total normal stress

and σ_n = the neutral stress

The total stress represents the stress that is produced by the weight of the overlying material (this acts to increase the intergranular stress). The neutral stress term describes the stresses acting on the particles that are generated by the pore contents of the soil. These may operate in a manner which increases or decreases the intergranular stress, depending upon the nature and the amount of the pore contents.

Following Bishop and Blight's (1963) example for unsaturated soils, Miller (1978) proposed that for frozen soils:

$$\sigma_n = P_i - \chi_\gamma (P_i - P_w) \qquad (2.10)$$

where P_i and P_w = the pressure of the pore ice and the unfrozen pore water respectively

χ_γ was defined as a stress partition parameter with specifies the relative importance of the suction $P_i - P_w$ in determining the neutral stress. χ_γ varies chiefly with the amount of unfrozen water in the soil. Since empirical values of χ vs. θ have not been determined, it was assumed that the relationship could be approximated by:[3]

$$\chi_\gamma = \frac{\theta_\gamma}{n} \qquad (2.11)$$

where θ_γ = the unfrozen water content of the soil (volumetric basis)

and n = the porosity

The term γ was used by Miller (1978) to specify the degree of freezing or the state of the soil water at any particular temperature:

$$\gamma = \frac{P_i - P_w}{\sigma_{iw}} = \frac{2}{r_{iw}} \qquad (2.12)$$

This represents the mean curvature of the liquid phase of an ice-water interface at any particular temperature below freezing.

Miller (1977) indicates that in the frozen fringe below an actively growing ice lens, there are two principal components of force operating on the soil particles that are generated by the pore contents:

(i) A large downward component produced by the gradient in the pressure of the pore ice (this acts to increase the integranular stress). Associated with this phenomenon is an additional element of force (also downward) arising from the asymmetry of the unfrozen pure water retained between the soil particles.

---

[3] $\chi = 1$ when the pores are completely filled with water and $\chi = 0$ when they are completed filled with ice.

(2) A second component of force is produced by the hydraulic gradient in the unfrozen porewater. This decreases from a maximum at the frost line, to a minimum value at the ice lens, the magnitude of the force depending upon the magnitude of the gradient in P_w. As a result of this gradient, the particles in the frozen fringe experience a strong upward force which reduces the intergranular stress.

The swelling pressure of an adsorbed film P_{sw} represents the difference between the film pressure at the ice-water interface P_i and the pressure of the bulk pore water P_w (Miller, Loch and Bresler, 1975):

$$P_{sw} = P_\tau - P_w \tag{2.14}$$

According to Miller (1978), the liquid pressure in an unfrozen film exceeds that of the pore ice by an amount:

$$P_\tau = P_i + \frac{2\,\sigma_{iw}}{R+\tau} \tag{2.15}$$

where R = the radius of the soil particle

and τ = the film thickness

If the film thickness is negligible in comparison with the radius of the particle, the film pressure gradient becomes equal to the gradient in the pressure of the pore ice. Combining this result with the Clapeyron equation gives an expression relating the temperature gradient within the frozen fringe to the gradient in the pressure:

$$\frac{\partial P_\tau}{\partial z} = \frac{\partial P_i}{\partial z} = \frac{L}{v_i T}\,\frac{\partial T}{\partial z} \tag{2.16}$$

The effect of the ice pressure gradient on the soil matrix is restricted to those areas on the particle surfaces where the adsorbed films are symmetrical. This is defined by diameters subtending angles ϕ, where,

$$\phi_2 > \phi > 0 \tag{2.17}$$

In the areas beyond this zone, there is an additional component of force caused by asymmetry of the pore water imbibed between adjacent soil particles (see Figure 2.4). This refers to the regions circumscribed by,

Figure 2.4

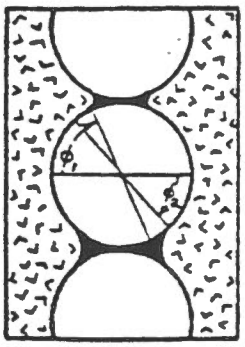

Sketch illustrating vertical gradient of pore contents (liquid water in black) in static column, showing angles of latitude ϕ_1 and ϕ_2.

$$\phi_1 > \phi > \phi_2 \qquad (2.18)$$

"At the upper (colder) ends of such diameters, the particle experiences a surface force due to the swelling pressure of the film .... At the other end, it experiences a surface force due to the pore water pressure alone; the result is a net downward component of force" (Miller, 1978).

The balance between the upward and downward components of force at any point within the frozen fringe are described by the effective stress equation. Substituting for σ_n in equation (2.9), rearranging terms and differentiating with respect to depth z, we obtain:

$$-\frac{\partial \sigma_e}{\partial z} = \chi_\gamma \frac{\partial P_w}{\partial z} + [1-\chi_\gamma]\frac{\partial P_i}{\partial z} + [P_i - P_w]\frac{\partial \chi_\gamma}{\partial z} \qquad (2.19)$$

This describes the change in the effective stress in the frozen fringe in terms of the hydraulic gradient, the ice pressure gradient and the gradient associated with asymmetry of the unfrozen pore contents. A schematic diagram illustraing the physical significance of each of these components is shown in Figure 2.5. The negative sign on the left side of the equation (2.19) signifies that the effective stress decreases with distance above the frost line.

Boundary conditions during the initiation and growth of an ice lens, according to the secondary frost heaving model, are summarized in Figure 2.6. Miller (1978) demonstrated that during regelation the soil particles in the frozen fringe would remain stationary rather than move with the ice phase. The explanation for this lies in the relative magnitude of the surface forces acting in this zone. If the forces operating downwards exceed those acting upwards, a part of the load is always borne by the solid matrix and the particles will remain stationary. This is described by the condition $\sigma_e > 0$. Since the soil particles above a growing ice lens are being displaced upwards, the forces acting upwards must exceed those operating downwards. Hence, the upper boundary of a growing ice lens is defined as the point where $\sigma_e \leq 0$.

Figure 2.6a illustrates the stress distribution in the frozen fringe at the initiation of an ice lens. Note that P_w decreases in an exponential fashion across the frozen fringe. Miller (1978) argues that the exponential decrease in P_w follows as a result of the roughly exponential decay in the hydraulic conductivity of the frozen fringe with temperature.

In the lower part of the frozen fringe, P_i increases at a decreasing rate passing through a maximum and then decreases at an increasing rate. The change in the slope of the curve implies that the film force reverses direction above the maximum, further reducing the intergranular stress.[4]

[4] The difference between P_i and P_w at any point within the frozen fringe is fixed by the Clapeyron equation. Thus, the reversal in the gradient in P_i can be explained by the fact that, in order for the suction $P_i - P_w$ to increase linearly in this region when P_w decreases exponentially, P_i must begin to decrease at some point (Miller, 1981).

Figure 2.5

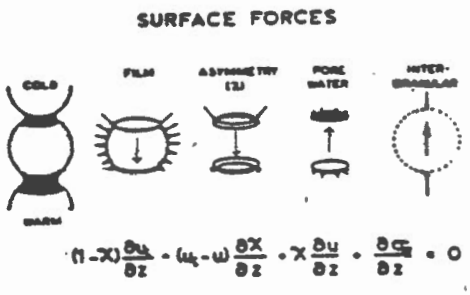

u = pore water pressure
u_i = pore ice pressure

Schematic diagram of surface forces acting on a particle in the frozen fringe.

Miller (1977)

Above the frost line, σ_n converges towards σ_T and σ_e towards 0 both along S-shaped curves. This follows as a result of the rapid divergence between P_i and P_w in the colder regions of the frozen fringe. If the ice phase is continuous throughout the frozen fringe, P_i must also be continuous. Since the ice lens bears the full load of the overburden, at a moment in time just prior to the initiation of a new lens, the base of the antecedent lens is specified by:

$$(P_i)_{z_3} = \lim_{z \to z_3} P_i = \sigma_T \qquad (2.20)$$

The implication is that P_i cannot exceed σ_T at the base of the lowest lens. Once a new lens has been established, P_i suddenly drops to σ_T at the base of the new lens. This is accompanied by a corresponding decrease in P_w, the amount being defined by the Clapeyron equation. The abrupt changes in P_i and P_w result in a slight increase in the intergranular stress immediately below the new lens and this suppresses the growth of further lenses in this region temporarily (Miller, 1978). As the new lens grows, the frozen fringe continues to extend itself downward into the soil, σ_n increasing all the while until $\sigma_n = \sigma_T$. At this point, the old lens ceases to grow and a new lens is initiated.

According to Miller (1977), "monotonic freezing will result in heaving of any load, no matter how large, at some rate, which may be vanishingly small if one waits long enough and if the surface temperatures are cold enough. The theoretical limit is fixed only by the temperature at which the liquid phase cease to be mobile .... Fluctuations in the load, water table and temperature, by inducing premature lens initiation at too low a level, thereby excising the high pressure stages, may arrest or even temporarily reverse the heaving process."

Miller (1978) indicates that the maximum heaving pressure that can develop during secondary frost heaving depends solely upon the temperature ΔT_b and the pore water pressure $P_{w,b}$ at the base of the ice lens:

$$P_{i,max} = \frac{1}{v_i} \left[v_w P_{w,b} + \frac{L \Delta T_b}{T} \right] \qquad (2.21)$$

Comparing equation (2.21) with equation (2.3), it is evident that the values predicted by this model are considerably greater than those predicted by the model contemplated by Everett (1961).

Although preliminary experiments by Loch and Miller (1975) and Loch and Kay (1978) lend credence to the concept of secondary frost heaving, confirmation of the model awaits further testing. Refinements to the model should include extension of the boundary conditions to allow for

Figure 2.6

Sketch profiles in heaving column. a. A moment before a new lens is initiated. b. Immediately after a new lens has been established. c. A moment before another new lens is initiated.

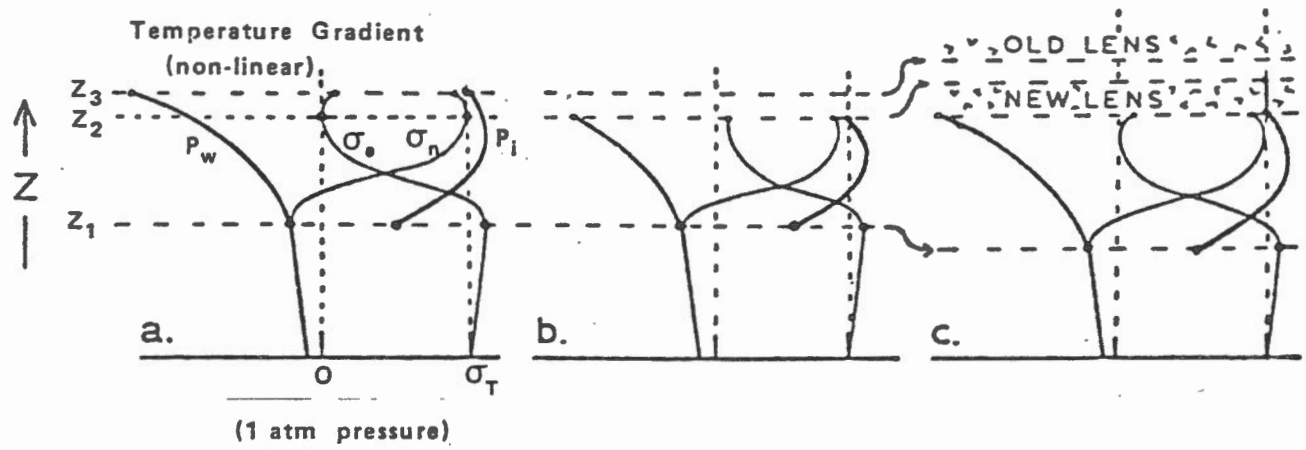

Z_1 Freezing Front

Z_2 Upper Boundary Of Growing Ice Lens

Z_3 Lower Boundary Of Antecedent Ice Lens

P_i Ice Pressure

P_w Water Pressure

σ_e Effective Stress

σ_n Neutral Stress

σ_T Normal Stress

after Miller (1978)

possible tertiary heaving.[5] This describes a condition in which growth of overlying ice lenses occurs at the expense of the lowest lens. Heaving pressures produced by this mechanism should not develop until the lowest lens has vanished. According to Miller (1972), "the ultimate maximum heaving pressure could turn out to be a constant that correponds to the temperature at which unfrozen films disappear (or cease to conduct water) or the surface temperature, if it is above this limit. It seems unlikely that the ultimate heaving pressure will be established experimentally in a reasonable length of time unless the rates of equilibriation are faster than expected."

---

[5] Some clarification of the terms 'primary', 'secondary' and 'tertiary' frost heaving is necessary since Miller (1978) uses the terms with an apparently different meaning than most other investigators. Although there are no official definitions of the terms, most investigators refer to any form of heaving of an initially unfrozen soil as 'primary' frost heaving, regardless of the particular mechanism by which it occurs. In general, the term 'secondary' frost heaving is used to describe further heaving of already frozen ground. This corresponds with the condition which Miller (1978) calls 'tertiary' heaving.

SECTION 3

HEAT AND MASS TRANSFER IN FROZEN SOILS

3.1 Role of Osmotic Forces In Thermally Induced Moisture Migration

Miller (1972) envisaged the frost heaving process as one whereby moisture migration within the frozen fringe is sustained by the continued osmotic recharge of the liquid films surrounding the soil particles. Römkens and Miller (1980) suggest two possible mechanisms by which water moves under temperature gradients in frozen soils. These are referred to as the 'diffusion' model and the 'double layer' model. Both models attribute the movement to temperature induced gradients in the equilibrium concentration of the ions in the fluid films surrounding the soil particles.

With the diffusion model, the coulombic forces emanating from the particle surface are assumed to be weak enough to permit the lateral mobility of the ions in the unfrozen film, yet sufficient to prevent separation of ions from the particle. Diffusion of solutes from the 'cold' end of the particle towards the 'warm' end, proceeds according to Fick's law. Transport of solutes is matched by an equal transport of water in the opposite direction. In the frozen fringe, the concentration gradient is maintained during diffusion by the continuous addition of solutes to each film, from the preceding film located at a slightly warmer temperature.

With the double layer model, the solutes are assumed to form part of the electric double layer and are restrained from lateral movement by the electric charges emanating from the particle surface. Under these conditions, the gradient in solute concentration between the 'warm' and 'cold' ends of each particle generates an osmotic pressure which increases with colder temperatures. This is countered by an equal but opposite gradient in the partial pressure of the water, resulting in fluid transport.[1]

Studies by Römkens and Miller (1980) on the migration of glass beads in ice, suggest the prevalence of the diffusion mode of transport, particularly at relatively 'warm' temperatures (near 0°C). Evidence for this is also provided by Sheeran and Yong's (1975) observation that frost heaving is usually accompanied by the expulsion of salts away from the frozen zone.

---

[1] The total pressure of a solution represents the sum of the partial pressures of the ions and water.

Figure 3.1

Schematic Diagram Of Series - Parallel Mass Transport In The Frozen Fringe During Secondary Frost Heaving

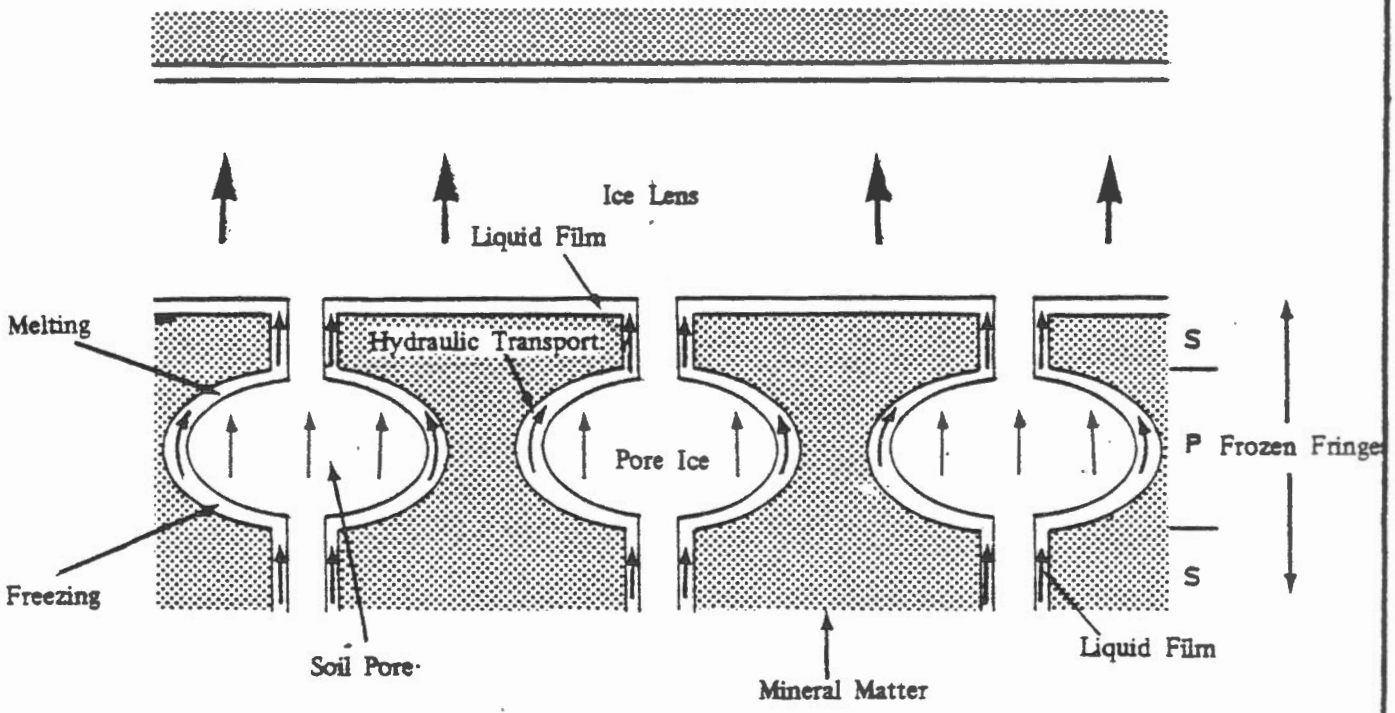

S = series transport

P = parallel transport

Source: Loch (1975)

3.3 Mass Transport In a Frozen Soil

Miller, Loch and Bresler (1975) derived expressions for ice and film water transport in a simplified soil system, taking into account momentum exchange between the liquid and solid phases. They assumed that the soil consists of a plate of mineral matter containing uniform cylindrical pores of radius R, filled with ice, which is separated from the walls of each pore by an adsorbed film of water of thickness τ (see Figure 3.1). Assuming laminar viscous flow in the liquid phase, the flux of film water is given by:[3]

$$J_\tau = -\left(\frac{2\rho\theta_i}{3\eta R}\right)\tau^3 \frac{\Delta p_f}{\ell_f} - \left(\frac{\rho\theta_i}{2\eta}\right)\tau^2 \frac{\Delta p_i}{\ell_f} \qquad (3.1)$$

where $\frac{\Delta p_f}{\ell_f}$ and $\frac{\Delta p_i}{\ell_f}$ = the gradient in liquid and ice pressure respectively,

η = the viscosity of water,

θ_i = the volumetric ice content of the soil

and ρ = the density of the film water

If the ice moves at a uniform translational velocity (that is, by plug flow), the flux in the ice phase is given by:

$$J_i = -\left(\frac{\rho_i\,\theta_i}{2\eta}\right)\tau^2 \frac{\Delta p_f}{\ell_f} - \left(\frac{\rho_i\theta_i R}{2\eta}\right)\tau \frac{\Delta p_i}{\ell_f} \qquad (3.2)$$

Note that in the equations above, film flow is reduced by the viscous drag of the pore ice, while ice transport is enhanced by the flow of film water.

Adding J_τ to J_i and dropping terms with the higher powers of τ, the total flux of mass within the soil becomes:

$$J = -\left(\frac{\theta}{6\eta}\right)\left[\rho_i\,\tau^2 \frac{\Delta p_f}{\ell_f} + \rho R\tau \frac{\Delta p_i}{\ell_f}\right] \qquad (3.3)$$

If transport is assumed to occur entirely within the fluid phase, equation (3.1) reduces to:

---

[3] Note that equation (3.2) ignores the possibility of internal deformation (plasto-viscous) flow within the pore ice. Miller, Loch and Bresler (1975) indicate that, an exception to the assumption of uniform translational velocity within the ice, can be imagined if the pressure gradient within the ice becomes large enough to cause significant creep deformation. This probably occurs at temperatures near 0°C and may be significant in limiting the pressures that can be produced during secondary frost heaving.

$$J = -\left(\frac{\rho\theta_i}{6\eta R}\right) \tau^3 \frac{\Delta p_f}{\ell_f} \qquad (3.4)$$

Comparing equations (3.3) and (3.4), it is evident that ice movement forms a very large component of the total mass transport within a frozen soil.

3.4 Measurement of the Mass and Heat Transfer Coefficients For Frozen Soils

Until very recently, few attempts had been made to measure the thermal and hydraulic properties of frozen soils directly. The first attempt at measuring the mass transfer coefficient of frozen soils under isothermal conditions was made by Burt and Williams (1976). The apparatus used in the experiments was similar to the 'ice sandwich' apparatus used by Miller (1970). A frozen soil sample confined to a perspex ring was interposed between two reservoirs (also made of perspex), containing lactose solution. The soil sample was separated from the solution by membranes whose pores were permeable to water but impermeable to lactose. The lactose maintains a freezing-point depression in the water, the concentration being adjusted so that the chemical potential of the water in the reservoirs, equals that of the pore contents of the adjacent soil.

Miller, Loch and Bresler (1975) describe equations for coupled heat and mass transfer in a permeameter containing a frozen soil. These appear to be based on the Onsager reciprocity relations which are utilized extensively in irreversible thermodynamics (see Appendix A):

$$J = -L_m \left(\frac{1}{\rho}\right) \frac{\Delta p}{\ell_f} - L_{mh} \left(\frac{1}{T}\right) \frac{\Delta t}{\ell_f} \qquad (3.5)$$

$$j = -L_{hm} \left(\frac{1}{\rho}\right) \frac{\Delta p}{\ell_f} - L_h \left(\frac{1}{T}\right) \frac{\Delta t}{\ell_f} \qquad (3.6)$$

where $\frac{\Delta p}{\ell_f}$ = the total hydraulic gradient across the soil sample,

$\frac{\Delta t}{\ell_f}$ = the temperature gradient across the sample

and L_m, L_{mh}, L_{hm}, L_h = phenomenological directional cross coefficients for heat (h) and mass (m) transfer

According to Onsager's reciprocity principle $L_{mh} = L_{hm}$. The flux of mass, J, is measured as the total input or output of water from the soil sample, while the quantity j describes the flux of heat (in one dimension), as would be measured by a heat flux transducer placed at the end of the soil sample (see Figure 3.2). Heat and mass transfer coefficients for the soil itself must be separated from measured coefficients for the permeameter and the soil-permeameter system.[4] Note that the mass transfer coefficient represents the combined transport in the fluid and solid phase within the soil.

Burt and Williams (1976) believed that they were measuring the hydraulic conductivity of the liquid phase within the frozen soil.[5] At that time, it was not fully realized that water movement within the soil occurs in the ice phase as well as the fluid phase. Moreover, they were also unaware of the degree to which heat and mass transfer are coupled in frozen soils. Unfortunately, since analytic expressions for the direct and cross-coefficients are not yet available and since Burt and Williams (1976) did not measure the heat flux in their permeameter, L_m and L_{mh} cannot be computed from their results. In retrospect, it seems clear that the hydraulic conductivity values that they obtained, represent the combined mass transfer in the solid and liquid phases and these are dependent upon, and may even be limited by, the heat transfer within the soil, and between the soil-permeameter system and the surroundings. Because of this, it is suggested that the term 'apparent' hydraulic conductivity be used in association with the results obtained from this type of experiment.

Attempts to measure the mass transfer coefficients of frozen soils have also been made by Horiguchi and Miller (1980) and Aguirre-Puente (1982). The apparatus used by Horiguchi and Miller (1980) is similar to Burt's apparatus except that supercooled water is used in the end reservoirs rather than lactose solution. Equilibrium between the supercooled water and the pore contents of the soil is achieved by a rise in the pressure of the pore ice. Results of tests on a fine silt appear to be very similar to those obtained by Burt and Williams (1976) with the same type of soil.

The apparatus used by Aguirre-Puente (1982) is somewhat more sophisticated than the simple permeameter described above. Frozen soil is confined to a central metal cylinder with hollow walls, which allow the circulation of cooling fluid. The cylinder is located between two adjacent metal cylinders (also hollow) in which the soil is maintained at a temperature slightly above freezing (see Figure 3.3). Sandwiching the

---

[4] Radial heat flow from the soil is restricted by placing an insulating sleeve around the permeameter.

[5] Burt and Williams (1976) used Darcy's law to compute the hydraulic conductivity coefficients.

Figure 3.2

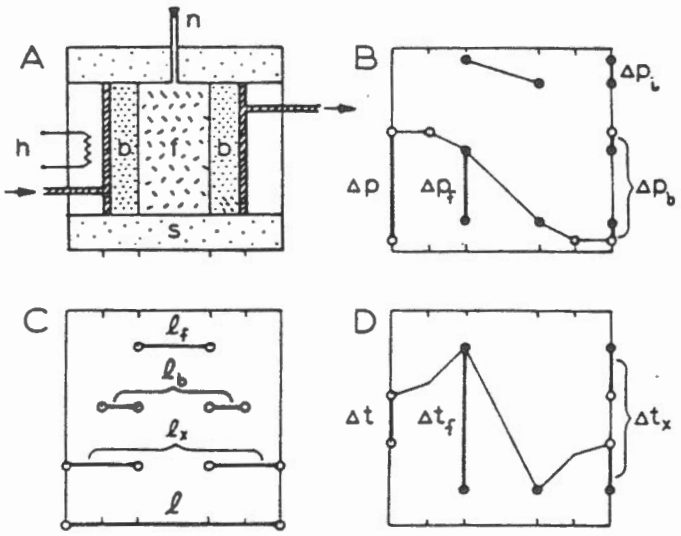

Schematic frozen soil permeameter in insulating sleeve (*s*), with rigid porous phase barriers (*b*), separating supercooled water (*hatched*) from frozen soil (*f*). A heat flux sensor (*h*) is required. Freezing of a supercooled specimen is nucleated by means of a side arm (*n*). (*B*) Schematic pressure profile for the permeameter. Upper segment represents ice pressure; lower transect represents liquid pressure. (*C*) Lengths identified in derivations. (*D*) Schematic temperature profile for the permeameter.

Figure 3.3

Schematic Diagram Of The Permeameter Currently Being Developed By Aguirre - Puente (1982)

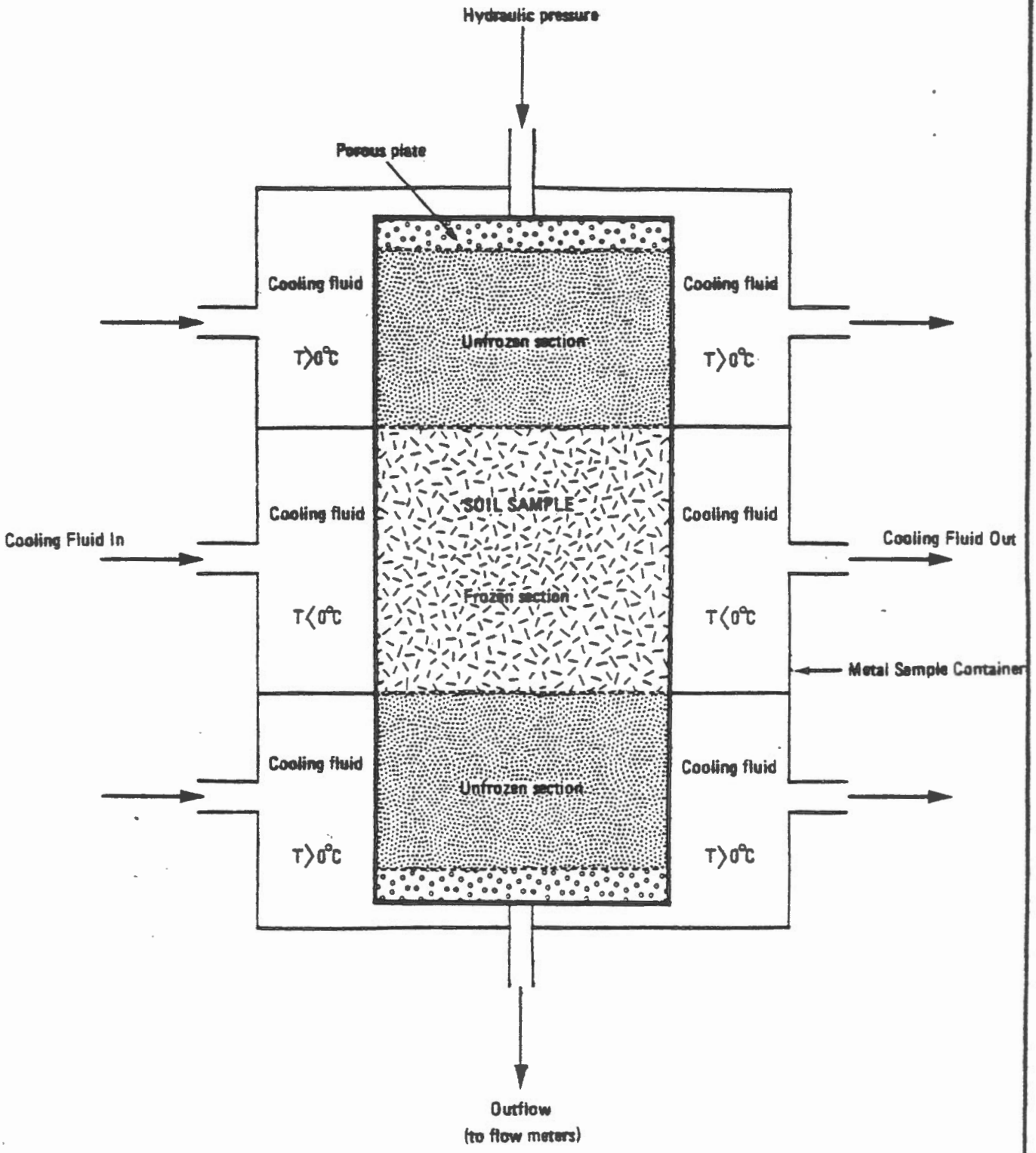

frozen soil between two unfrozen layers avoids many of the difficulties associated with the use of lactose and supercooled water, but presents problems of its own.[6] Results of experiments from Aquirre-Puente's permeameter await the further development of the apparatus.

3.5 Direct Measurement of Temperature Induced Moisture Migration in Frozen Soils

Recently, Williams and Perfect (1980) developed an apparatus for measuring directly moisture migration in a frozen soil subjected to a temperature gradient. The apparatus consists of a perspex sample container that is sandwiched between two aluminum end plates, the temperature of which is controlled by Peltier (thermoelectric) cooling. Inflow and outflow from the soil are observed by the movement of menisсii in capillary tubes attached to small reservoirs,which are located in the end plates. Temperatures within the sample are monitored with thermistors mounted at various locations throughout the column. Semipermeable membranes at either end of the sample, act as phase barriers between the soil and the water in the reservoirs.

As in the case with Burt and Williams (1976) experiment, lactose solution was used in the end reservoirs. The lactose concentration should have been adjusted so as to produce chemical equilibrium between the water in the end reservoirs and the pore contents of the adjacent soil. Unfortunately, however, the same lactose concentration was used in both reservoirs, with the result that the thermal gradient at the 'warm' end of the sample was counteracted, in part, by a local osmotic gradient. Results from the experiments are as follows.

In some of the experiments, although not all, once a linear temperature gradient was attained (which indicates steady state heat flow conditions), a constant flux of water was observed at the 'cold' end of the sample. In some instances, inflow was observed at the 'warm' end of the sample, although in other cases, no flow occurred at all, or there was outflow.

---

[6] With lactose solution, the chief difficulty is that the membranes are not completely impermeable to the sugar and so there is a slow diffusion of lactose molecules into the soil with time. This compromises interpretation of the results to an unknown degree.

With supercooled water, the main problem is that it is difficult to maintain its metastable state for long periods of time. In addition to this, the probability of freezing increases as the temperature decreases and so experiments are limited to the warmer temperature ranges (0°C to - 0.25°C).

In all of the experiments where inflow occurred, the flux at the 'warm' end of the sample was observed to be less than the outflow at the 'cold' end. This was explained by the fact that the lactose concentration at the 'warm' end of the sample was too high, the result being a local osmotic gradient which reduced the rate of inflow.

Williams and Perfect's (1980) results indicate the dominant influence of the permeability of the soil on the rate of flow through the system. For a series of infinitesimal layers in which the permeability is continuously changing, the overall permeability of the soil K is given by:

$$K = \frac{\ell}{\int_{x_1}^{x_2} \frac{1}{k(x)}\, dx}$$

where ℓ = the length of the soil sample
and $k(x)$ = the permeability of the soil expressed as a function of distance (Loch and Kay, 1978)

In general, considerably greater amounts of flow were observed at relatively warm temperatures (near 0°C). Under these conditions, the flow rates were also strongly influenced by the magnitude of the temperature gradient. In contrast, at colder temperatures (approximately - 0.4°C), flow rates remained small despite large changes in the temperature gradient. These results were attributed to the fact that near 0°C, the permeability of the soil is strongly temperature dependent and may be several orders of magnitude greater than at colder temperatures.

SECTION 4

REGELATION - TRANSPORT EXPERIMENTS

4.1 Apparatus And Materials

The apparatus used in the experiments consisted of a disc of ice confined to a plexiglass sample holder, which was interposed between two reservoirs containing supercooled water. An o-ring maintained a seal between each reservoir and the sample container. The reservoirs were sprayed with a polytetrafluroethylene compound (a water repellant substance) to inhibit nucleation of the supercooled water caused by the plexiglass walls.

Schleicher and Schuell cellulose acetate AC-61 membranes were used as phase barriers, separating the ice from the water. These were supported by porous plexiglass plates which were inserted in the end reservoirs. The membranes have an average pore size of about 0.005 μm which, in theory, should restrict the entry of ice down to temperatures as low as - 10°C although in practice, freezing usually occurred at - 6°C. (The physical properties of the membrances are described in Table 5.2).

The entire assembly was held together with a brass clamp and immersed in a modified 'Hotpack' refrigerated bath circulator containing methanol (see Figure 4.1). Modifications to the bath included substitution of a Duncan 2252Ω 10-turn potentiometer with vernier guage, for the original pot. This arrangement allowed temperature control constant to within ±0.005° C of the desired temperature for extended periods of time. The temperature of the bath was monitored with a mercury in glass thermometer (estimated limit of accuracy of ±0.01° C - see calibration report, Appendix C). As a check against the thermometer, the temperature of the bath was also recorded with a 3000Ω thermistor.

Flow through the system was produced by a constant hydrostatic pressure which was applied to one reservoir. Outflow was recorded with small capillaries (internal diameter 0.03325 cm) mounted on a finely divided scale.

Most of the experiments were conducted using a larger diameter cell (1.0 cm long x 5.40 cm internal diameter, wall thickness = 1.0 cm). The volume of each reservoir was approximately 58 cm^3. In some of the experiments, the apparatus was outfitted so that ice pressures could be measured as well as flow. In this case, an elongated but smaller diameter cell was used instead (3.02 cm long x 3.80 cm internal diameter, wall thickness = 1.0 cm). The internal volume of each reservoir was approximately 40 cm^3.

Pressures within the cell were monitored with a Kulite XTM-1-190 sealed guage pressure transducer (rated pressure = 100 psi - see Appendix C). Since the transducer could not be immersed in methanol, the device was

Figure 4.1

SCHEMATIC DIAGRAM OF THE APPARATUS USED TO MEASURE REGELATION-TRANSPORT COEFFICIENTS

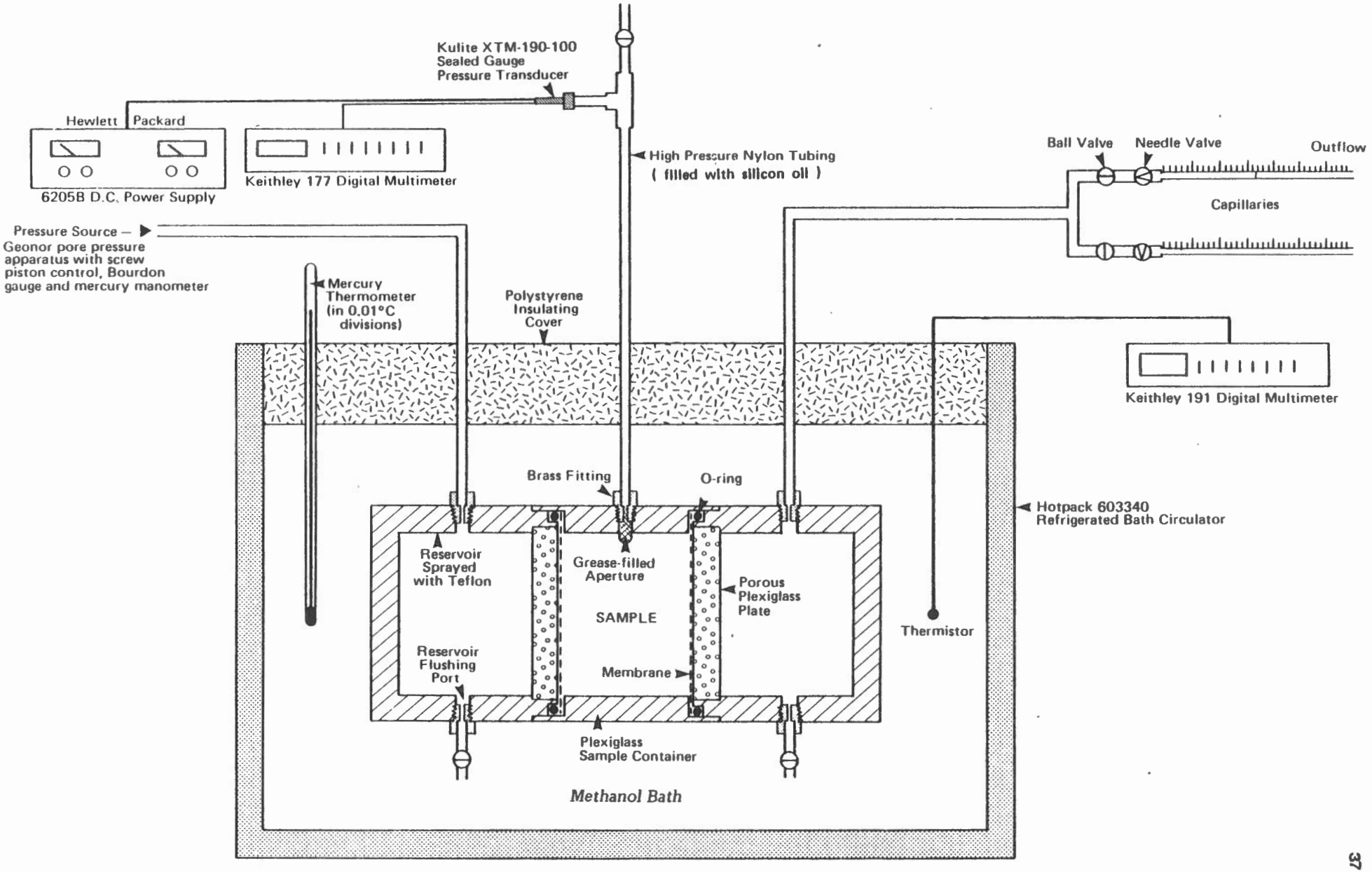

The clamp used to hold the cell and the end reservoirs together is not shown.

connected to the sample container via a length of high pressure tubing filled with silicon oil. To prevent seepage of the oil into the ice chamber, a quantity of silicon grease was inserted into the brass fitting, mounted in the wall of the sample container. Extra care was taken to remove any bubbles that were present in the grease or the oil. This precaution ensured the effective transmission of pressure from the ice sample to the transducer diaphragm.

4.2 Experimental Procedure

Whenever water is exposed to the atmosphere, a certain quantity of air is dissolved in the water, the equilibrium concentration depending upon the temperature of the water as well as the air pressure above the interface. Since ice and air are immiscible substances, when water freezes, the air will come out of solution forming small bubbles around nucleation sites at the ice-water interface. If water is frozen very slowly, impurities, such as air and other solutes, are rejected in front of the advancing interface. As ice is progressively formed, the concentration of the air in the remaining liquid increases until a critical level of supersaturation is reached, and air bubbles begin to form as a result of heterogeneous nucleation.[1] If the rate of freezing is slow enough, and if the concentration of the ice in the water remains below the critical level, a column of pure polycrystalline ice will form.

This principle was utilized to grow bubble free ice for the present experiments. The cell was filled with doubly deionized water (conductivity = $1.0 \times 10^{-4}\ \Omega^{-1}\,m^{-1}$) and mounted on a freezing plate. Once freezing had commenced, the temperature of the plate was adjusted so that the ice-water interface advanced at a rate of about 1 mm every hour. Periodically, the remaining water was replaced with fresh water. A thin foil barrier separated the ice from the freezing plate and facilitated removal of the cell once the ice column had finished growing. The sample was then placed in a freezing chamber (temperature ≈ - 20°C) for a period of about 24 hours.

Prior to assembly of the cell, the ice was scraped down with a blade until flush with the ends of the sample container. Before placing the membranes on the ice surface, the sample was allowed to warm up to a temperature of about - 4°C.

Flow readings were made at temperature decrements between 0°C and - 0.35° C. At temperatures lower than this, tests were limited by the tendency for nucleation to occur in the reservoirs. At each temperature, the ice was allowed to equilibriate with the supercooled water for a period of about 48 hours, before applying pressure to the system.

---

[1] The term 'heterogeneous nucleation' refers to nucleation that is initiated by foreign particles within the liquid.

4.3 Flow Properties and Transport Coefficients For Ice During Regelation

Examples of the results obtained using the larger diameter cell are shown in Figures 4.2 a-e, experiment no. A4. (Additional results from experiment no. A8 are shown in Appendix E.) Best fit curves for the data are plotted in addition to the measured values for outflow. Comparing Figures 4.2 a,c and e, it is evident that at relatively warm temperatures (- 0.05°C), the flow rate increases dramatically with stepwise increments in the hydrostatic pressure. Note, however, that the flow rate diminishes markedly with colder temperatures and much larger increments in hydrostatic pressure are required to produce any significant change in the rate of flow.

Results of the experiments were analyzed to determine whether the regelation mechanism obeys a linear transport type equation similar to many of the laws which are used in classical physics (i.e. Ohm's law of electrical conduction, Fourier's law of heat conduction, Fick's law of diffusion). Since the present experiment involves fluid transport, results were compared against Darcy's law which describes fluid transport in a porous medium. For the case of one dimensional flow, Darcy's law takes the form:

$$J = - L \frac{dH}{dx} \qquad (4.1)$$

where $\frac{dH}{dx}$ = the hydraulic gradient

and L = the hydraulic conductivity or mass transport coefficient of the medium.

Equation 4.1 states that the fluid flux through a medium is direclty proportional to, and in the direction of, the driving force for fluid transport, and a constant which describes the ability of the medium to transmit the fluid. According to Darcy's law, if the flux is plotted against the hydraulic gradient, the relationship should be linear, the slope of the line representing the hydraulic conductivity of the medium. [2]

---

[2] The term 'permeability' is often used instead of the hydraulic conductivity to describe the ability of a soil to transmit fluid. Strictly speaking, however, the terms are not the same. In theory, the conductivity L is separated into two components:

$$L = pf$$

where p = the intrinsic permeability of the soil

and $f = \frac{\rho g}{\nu}$ = the fluidity of the fluid (ν = the viscosity, ρ = the density and g = the acceleration of gravity).

Thus the conductivity depends upon the properties of both the soil and the fluid.

Figure 4.2a

Cumulative Outflow vs Time for Ice During Regelation Transport

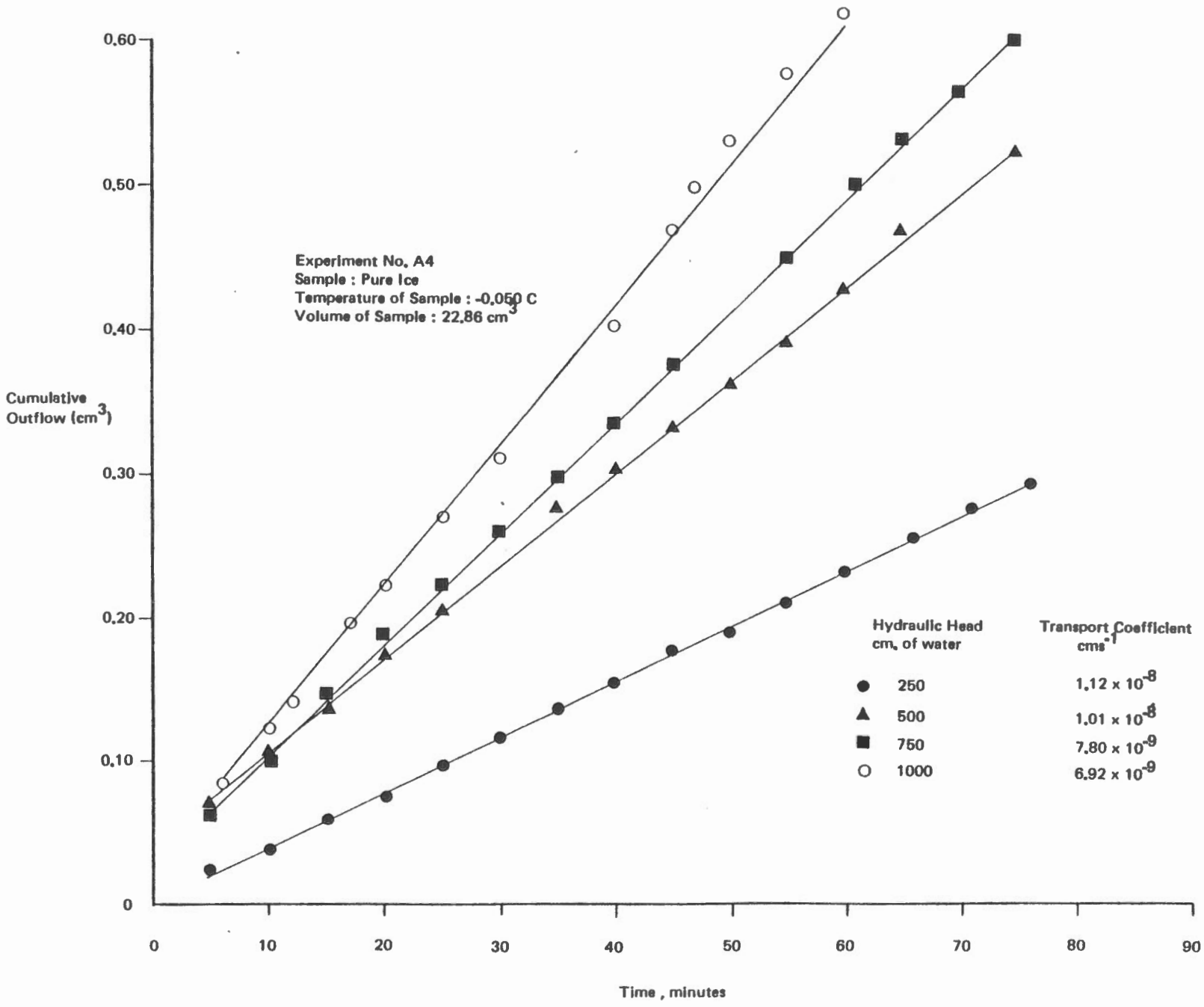

Figure 4.2b

Cumulative Outflow vs Time for Ice During Regelation Transport

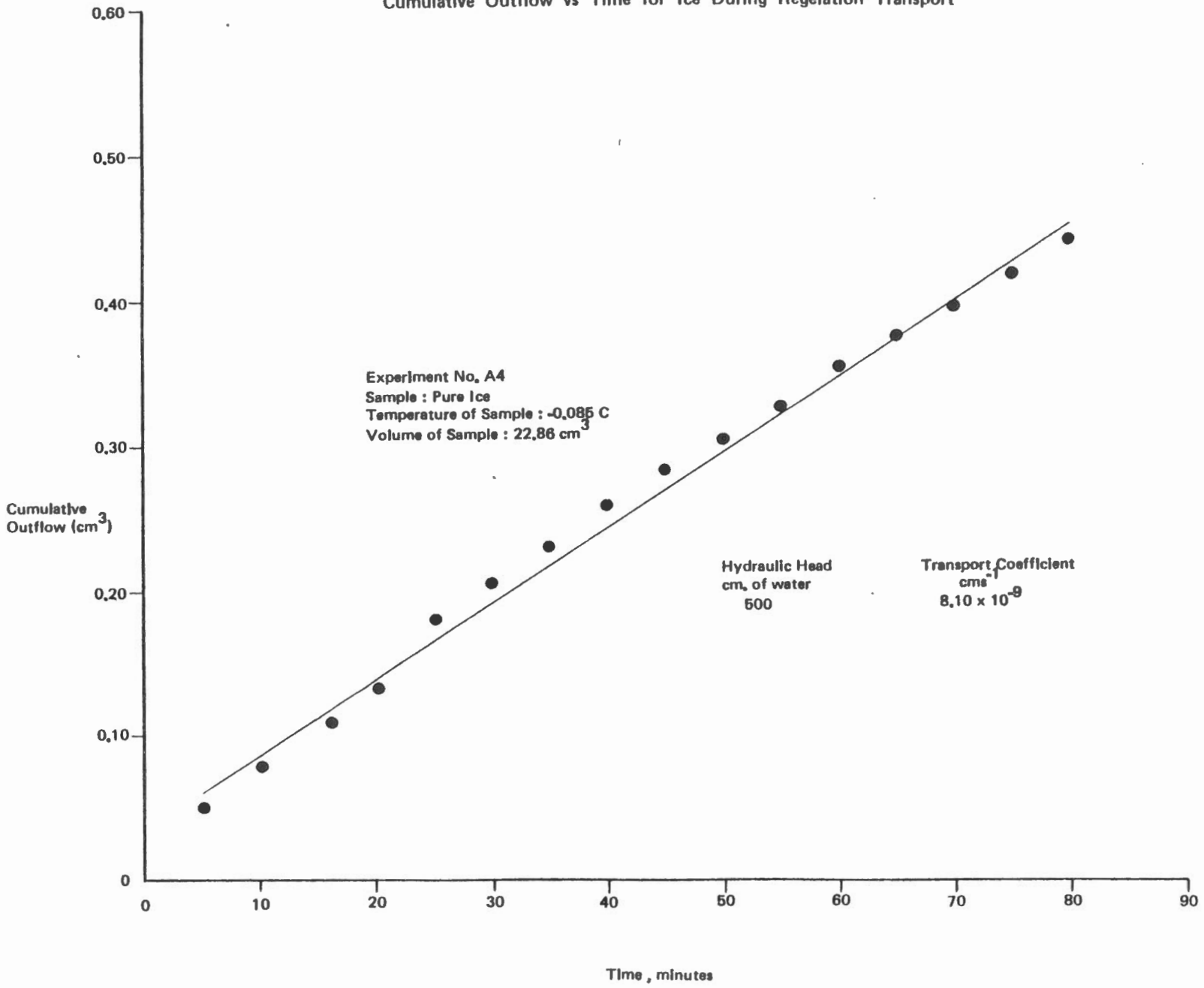

Figure 4.2c

Cumulative Outflow vs Time for Ice During Regelation Transport

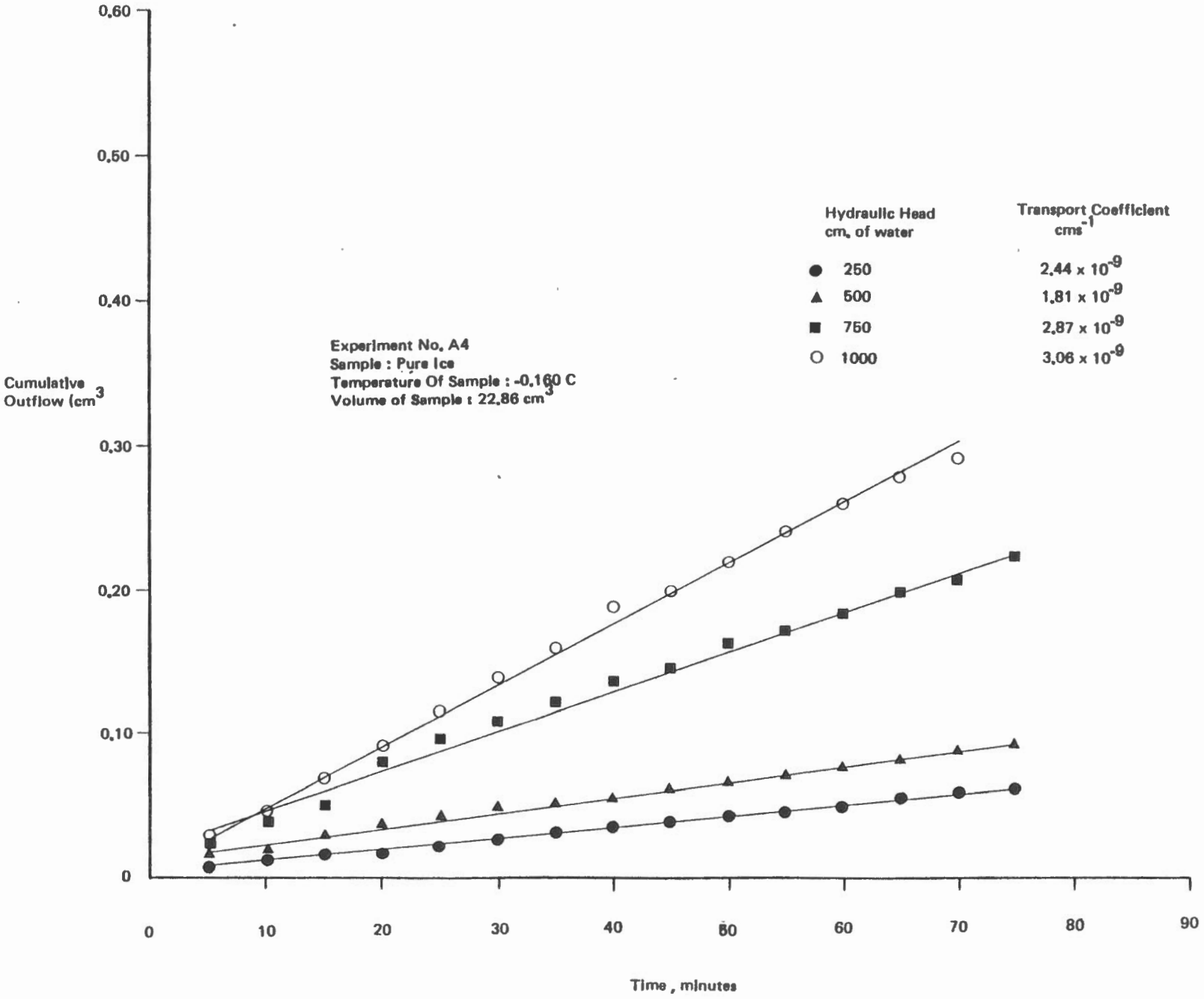

Figure 4.2d

Cumulative Outflow vs Time for Ice During Regelation Transport

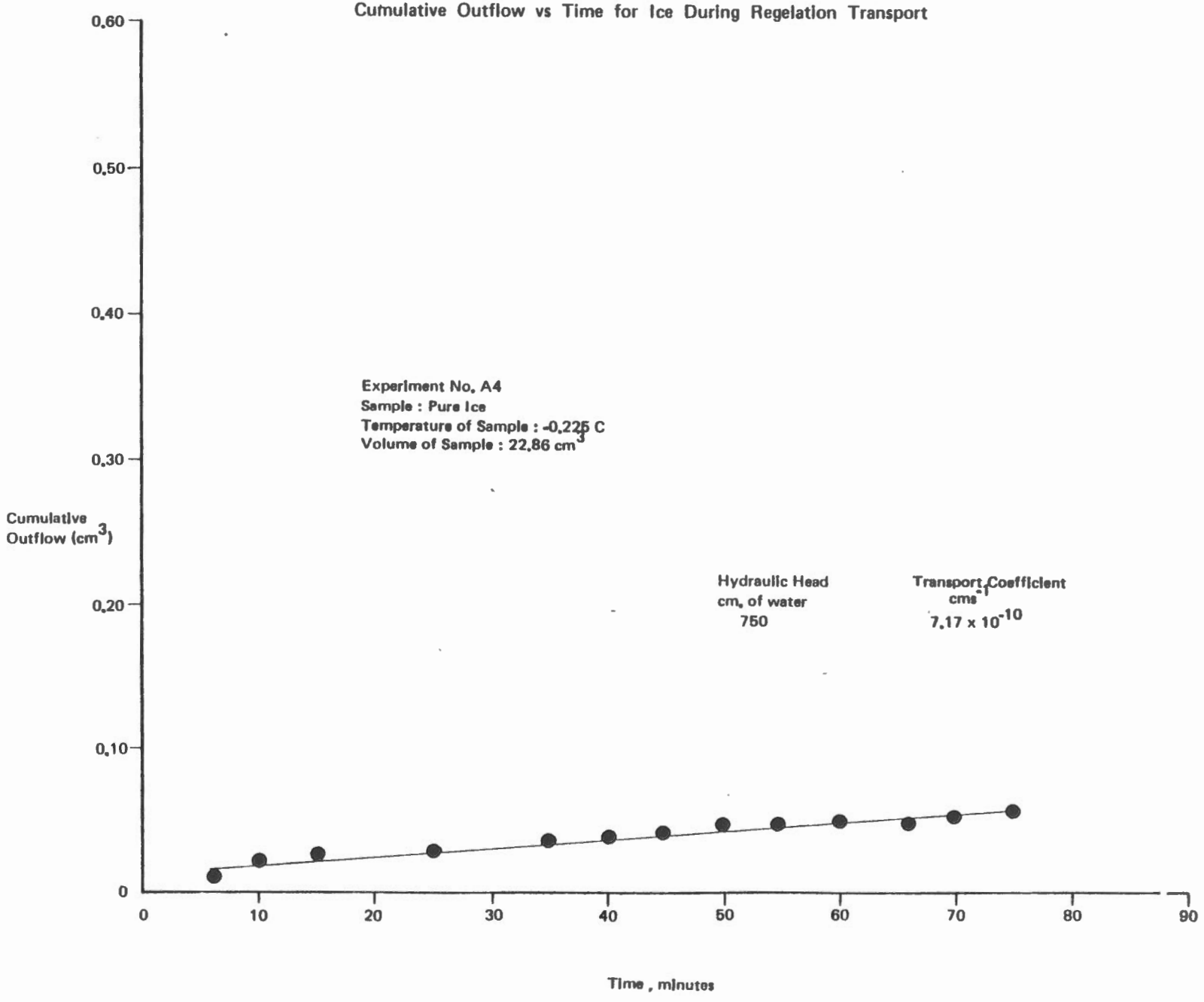

Figure 4.2e

Cumulative Outflow vs Time for Ice During Regelation Transport

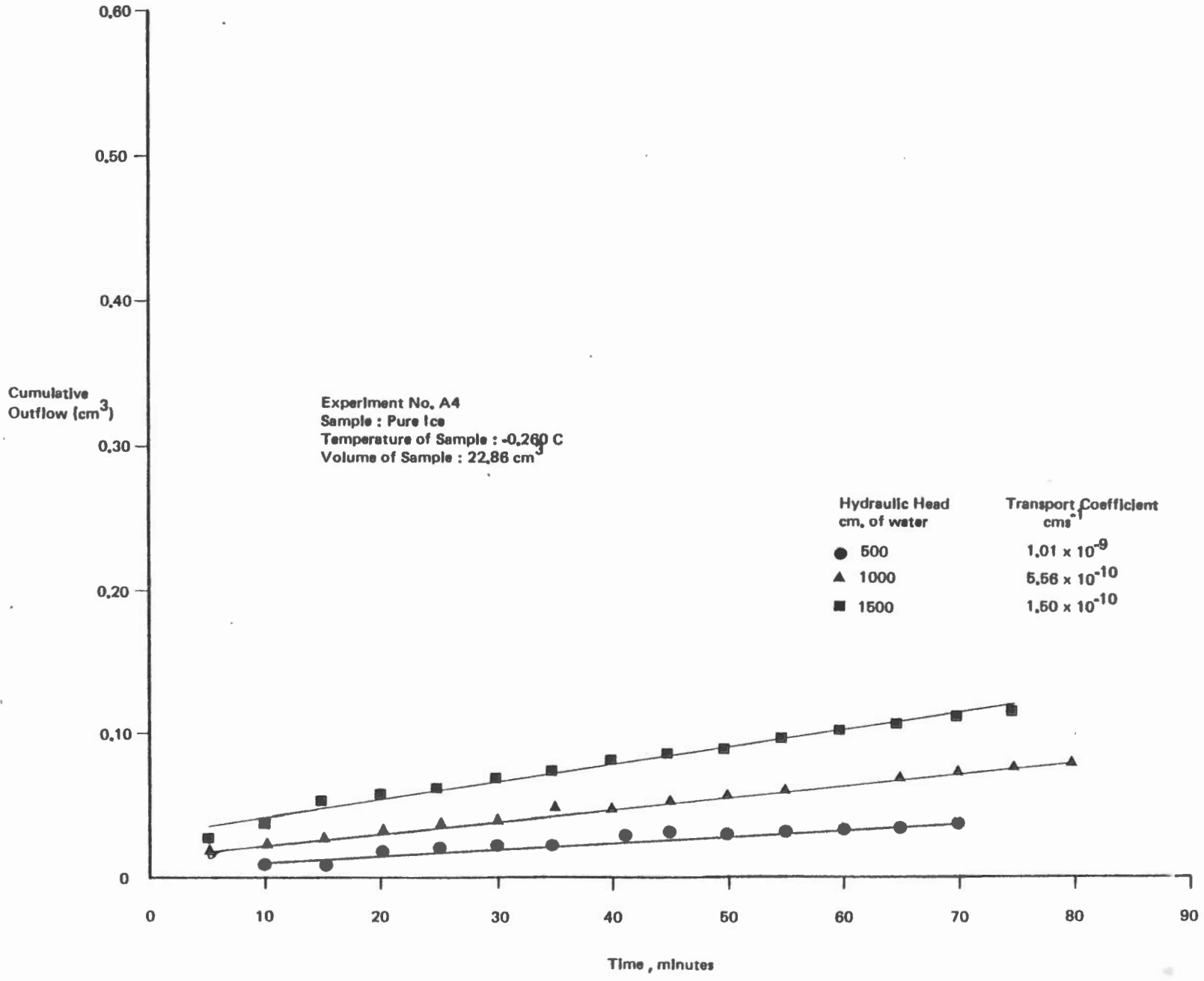

Figure 4.3 shows a plot of the flux against the hydraulic gradient at various temperatures for the results obtained in experiment no. A4. Note that in all three cases, the flux appears to increase more or less linearly with the hydraulic gradient, which indicates that regelation does conform to a linear transport type of equation. Similar findings were also reported by Horiguchi and Miller (1980), using their 'ice sandwich' apparatus (see Figure 4.3b). In the present case, there was some tendency for deviations from linearity to occur particularly at warmer temperatures. This may be a result of the increasing tendency for the ice to move by anistropic flow rather than simple plug flow in the warmer temperature ranges.[3]

Since water flow associated with regelation does appear to correspond to Darcian behaviour, at least in the temperature range that was investigated, it is evident that the flux of the ice is related to the hydraulic gradient by a constant transport coefficient. Horiguchi and Miller (1980) suggested the use of the term 'apparent' hydraulic conductivity to describe this coefficient. A plot of the regelation transport coefficient as a function of temperature is shown in Figure 4.4a. Note the close correspondence in the general rate of decline of the transport coefficient between values obtained from experiment no. A4 and A8. This demonstrates that the experiment is, in fact, reproducible and that the results are not unique to a single ice sample.

Figure 4.4a also indicates that the regelation transport coefficient L_i declines exponentially with temperature. This is described by an equation of the form:

$$L_i = c\, e^{bT} \qquad (4.2)$$

where c and b = constants

L_i = regelation transport coefficient

and T = the temperature

Taking the common logarithm of both sides, equation (4.2) becomes:

$$\log_{10} L_i = \log_{10} c + T\,(b \log_{10} e) \qquad (4.3)$$

This plots as a straight line on semi-log graph paper with slope $b \log_{10} e$ and intercept $\log_{10} c$. For the present example:

$$b \log_{10} e = 5.703,$$

therefore $$b = \frac{5.703}{\log_{10} e} = 13.13$$

and $$\log_{10} c = -7.729$$

thus $$c = 1.868 \times 10^{-10} \text{ cm s}^{-1}$$

---

[3] The term 'plug' flow identifies the condition when the ice deforms at a uniform translational velocity throughout its entire cross-sectional area.

Figure 4.3a

Plot of the Flux vs. the Hydraulic Gradient at Various Temperatures During Regelation Transport

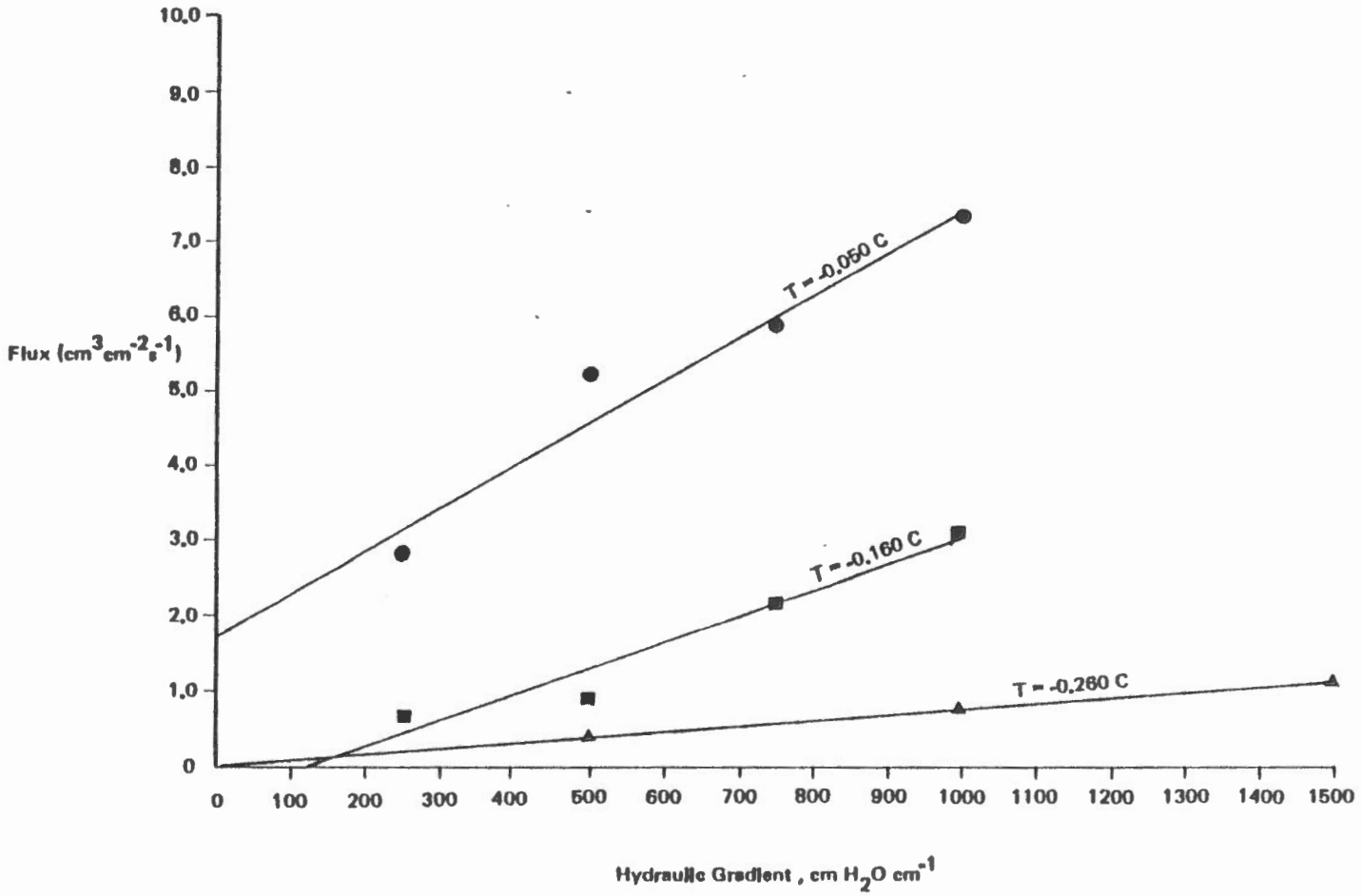

Figure 4.3b

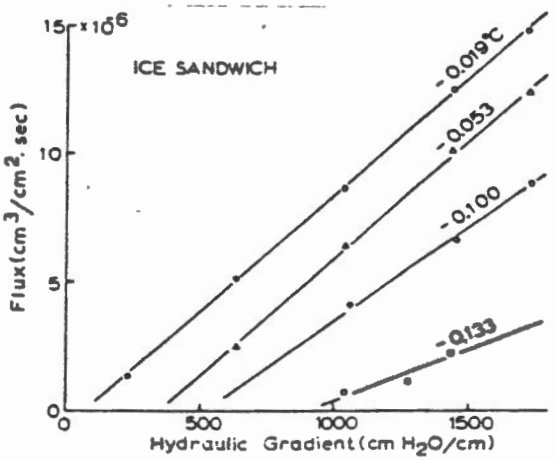

Transport data at various temperatures and hydraulic gradients in ice sandwich mode.

Horiguchi and Miller (1980)

Figure 4.4a

Mass Transport Coefficients for Ice During Regelation Flow as a Function of Temperature

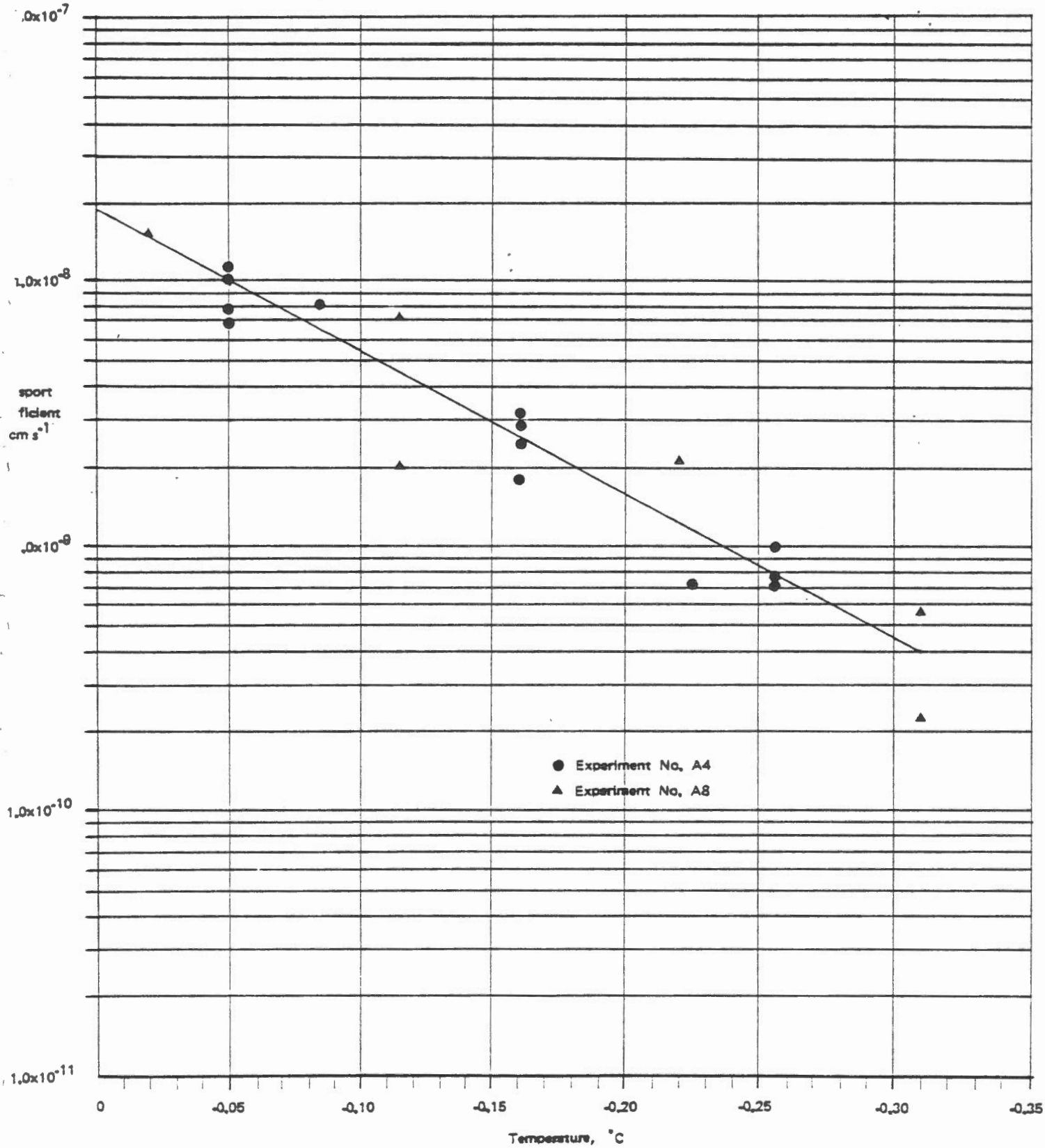

Figure 4.4b

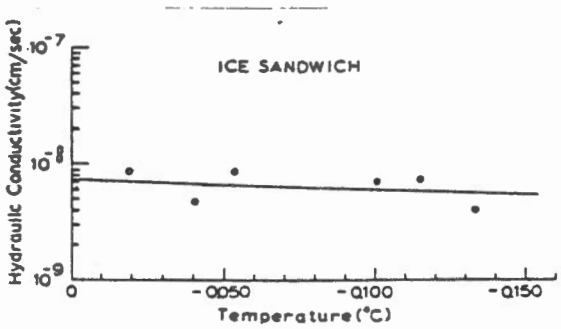

"Apparent hydraulic conductivity" of ice in ice sandwich as a function of temperature.

Horiguchi and Miller (1980)

Hence, the relationship between the ice flux during regelation, the hydraulic gradient and the temperature is described by the expression:

$$J_i = -L_i \frac{\Delta H}{\Delta x} \qquad (4.4)$$

where $L_i = 1.868 \times 10^{-8} e^{13.13T}$

In general, the results shown in Figure 4.4 appear to be in agreement with those of Horiguchi and Miller (1980), although in the present example, the transport coefficient shows a much greater temperature dependence (Horiguchi and Miller's results indicate an overall decline of about 1.5×10^{-8} cm s^{-1} for every 0.1°C change in temperature. Our results indicate that the rate of change is an order of magnitude greater, i.e. 1.5×10^{-7} cm s^{-1} for every 0.1°C). Note also that the transport coefficients were investigated at much lower temperatures (0°C to -0.3°C) than the experiments conducted by Horiguchi and Miller (1980).

4.4 Measurement of Threshold Pressure Required to Initiate Flow

Horiguchi and Miller (1980) predicted that the flux of ice in an 'ice sandwich' type apparatus would commence only when the applied hydrostatic pressure became sufficient to overcome the static friction between the ice and the sidewall of the cell. Examples of the threshold pressures required to initiate flow in experiment No. A4 and A8 are shown in Figure 4.5. The values were obtained by slowly increasing the hydrostatic pressure on one reservoir until outflow from the other became perceptible. Usually, once the threshold barrier had been crossed, further increases in the hydrostatic pressure resulted in large changes in the flow.

As can be seen from the diagram there is a considerable degree of variation in the absolute magnitude of the threshold pressure from one experiment to the next. The explanation for this phenomenon is not fully understood. If static friction is the cause, it seems reasonable to assume that the magnitude of the threshold pressure is related to both the nature of the bond between the ice and the sidewall of the cell, as well as the orientation of the ice crystals relative to flow.

However, it is doubtful whether the static friction is the cause since at pressures lower than the threshold value, although instantaneous flow was not observed, over an extended period of time, flow did occur, and this gradually increased with time. This is probably a result of a gradual transition from an elastic mode of deformation to a viscous deformation (see Section 4.9).

The pressure required to sustain flow in the dynamic state is less than the static threshold value. In other words, once the threshold barrier had been crossed, flow through the sample continued even after the pressure is reduced below this limit. This is probably due to the tendency for strain softening to occur as the ice deforms. Strain softening describes a condition in which the rate of deformation increases as the ice moves.

Figure 4.5

Plot of the Threshold Pressure Required to Initiate Flow as a Function of Temperature

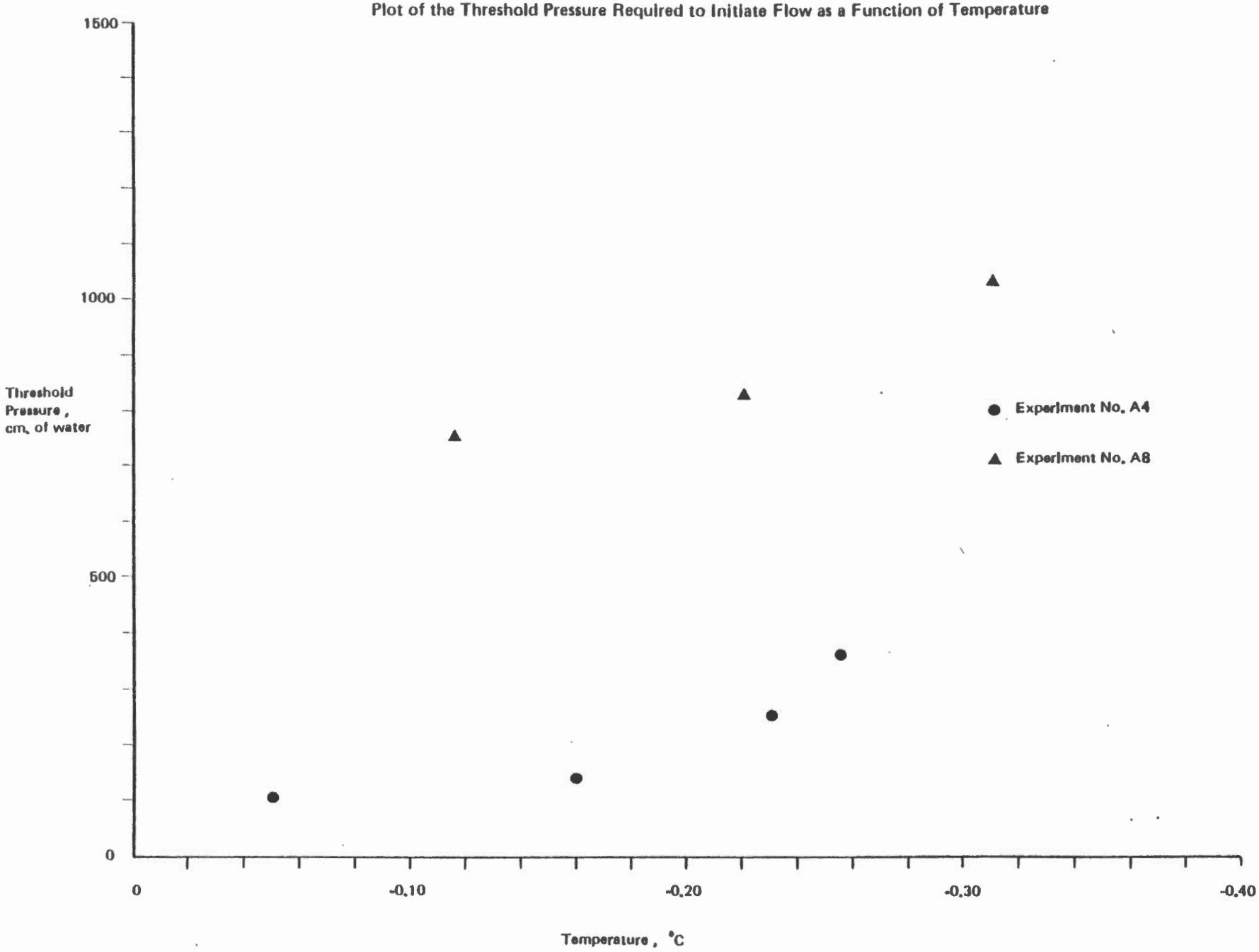

It is generally attributed to the migration of crystal boundaries as well as the recrystallization of ice under stress. (A discussion of this phenomenon is provided in section 4.8.)

4.5 Static Equilibrium of the Ice and Water Phases

Experiments were also conducted in which the ice pressure was measured as well as the flow. (In this case, the smaller diameter cell was used). At each decrement in temperature, the ice sample was allowed to equilibrate with the supercooled water for a period of 48 hours or more before applying hydrostatic pressure to the system. During the equilibriation period, a small amount of inflow was observed at both ends of the ice sample, the ice pressure slowly rising to a constant value about 24 hours after the temperature had been changed.

At any temperature below the normal freezing temperature of water, the Gibbs free energy of ice is less than that of liquid water (see Figure 1.1). In order for equilibrium to occur, the free energy of the two phases must be equal. This is ahieved by a rise in the internal pressure of the ice, the amount being specified by the Clapeyron equation. In the present example, since the pressure of the water in the reservoirs remains at atmospheric pressure Pa, the Clapeyron equation takes the form:

$$P_i - P_a = \frac{L \Delta T}{v_i T} \qquad (4.5)$$

where $P_i - P_a$ = the amount by which the ice pressure exceeds the water pressure.

Measured values of $P_i - P_a$ at various temperatures are plotted in Figure 4.6a. The solid black line represents the values predicted by the Clapeyron equation. (Similar findings are also reported by Buil and Aguirre -Puente (1981) using a somewhat more complicated apparatus - see figure 4.6b.) Note that, there is close agreement between measured and predicted values of $P_i - P_a$ at relatively warm temperatures (greater than -0.2° C.) Thereafter, the difference between the two progressively increases.

One possible explanation for this discrepancy is that, at temperatures lower than about -0.2° C, the ice pressure exceeds the yield stress required for elastic deformation of the cell and the clamping device used to hold the apparatus together.

A second possible explanation is that ice pressures may not be isotropic. The initial build-up of stress within the ice phase may be greater in the axial dimension or may tend to concentrate along the ends of the ice sample. Since polycrystalline ice is not known to have any measurable yield stress, ultimately stresses within the cell should become isotropic via a gradual internal deformation of the sample. This, however, may take longer than the time that was allowed for equilibrium to be reached between the ice and the supercooled water, particularly at colder temperatures. Thus, the pressures being measured by the transducer may be

Figure 4.6a

Equilibrium Ice Pressures in the Permeameter as a Function of Temperature

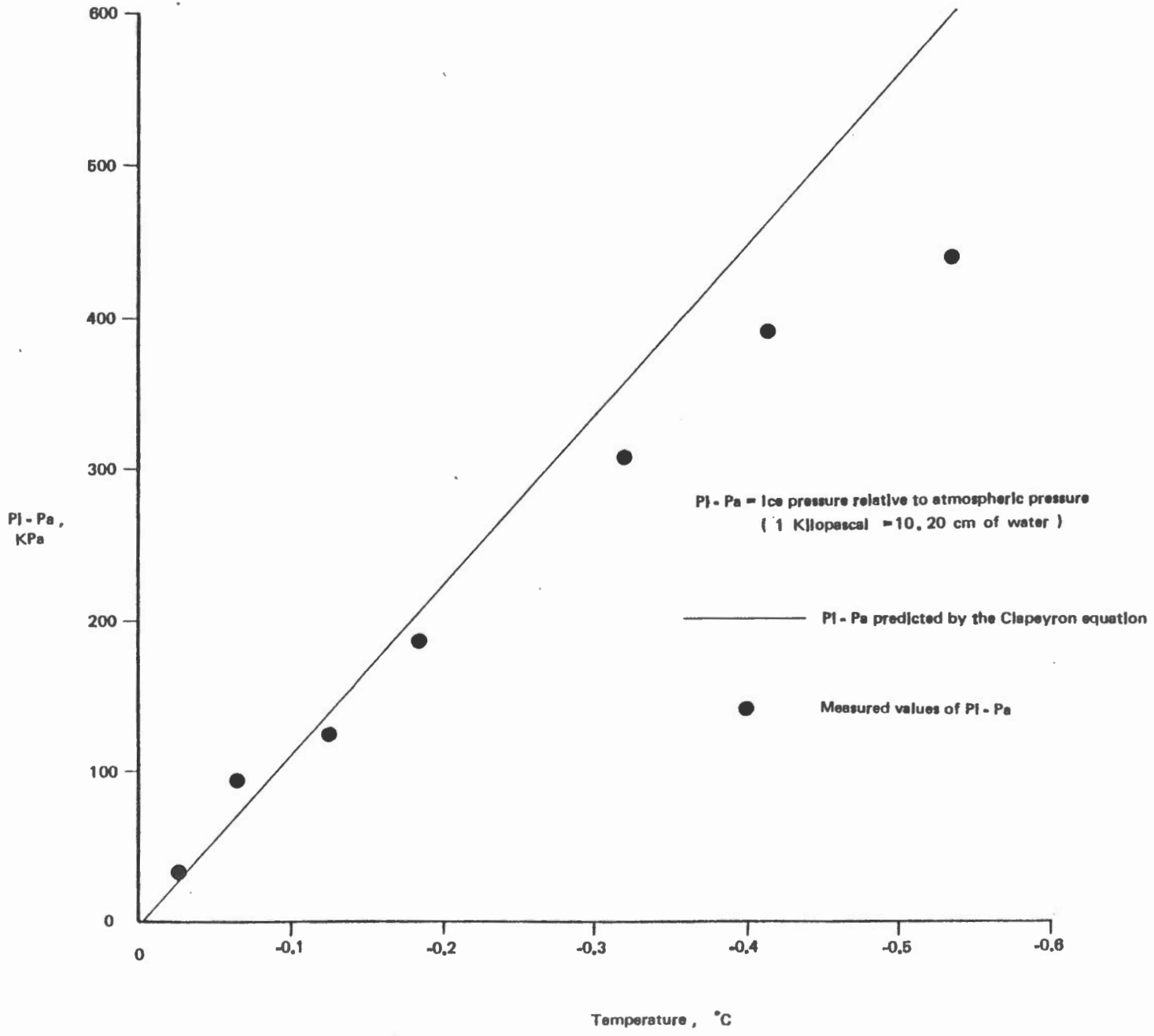

Figure 4.6 b

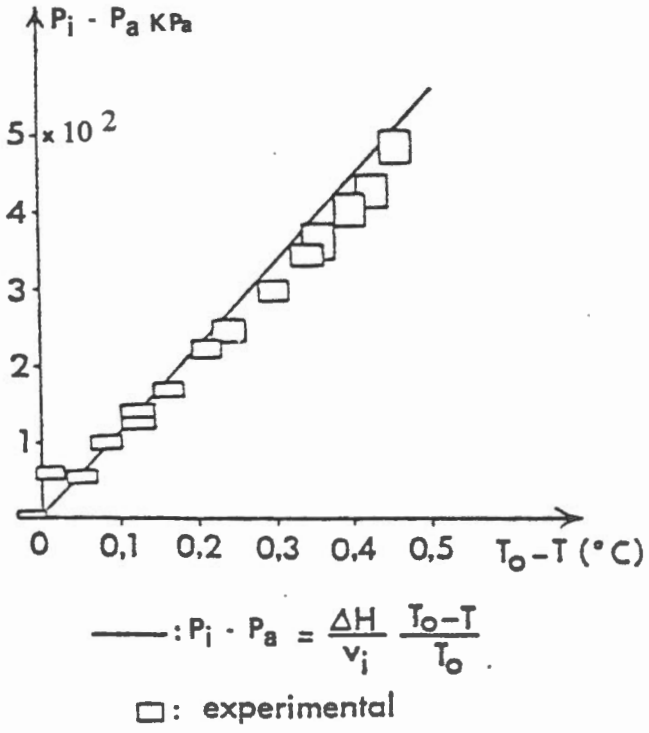

Equilibrium Ice Pressure As A Funtion Of Temperature

Buil and Aguirre-Puente (1981)

somewhat lower than the final equilibrium value when isotropic conditions are fully established.[4]

4.6 Dependence of the Flow Rate on the Heat Conducting Properties of the Ice-Permeameter System

Examples of the results obtained using the elongated, smaller diameter cell at -0.185 ° C and -0.320° C are shown in Figure 4.7a and b. If these results are compared with the results of tests at similar temperatures using the larger diameter cell, it becomes apparent that the dimensions and other physical properties of the permeameter have a rather profound influence on the flow rates and the transport coefficients that are obtained. With both cells, the cumulative flow initially increases a a declining rate, the flow rate levelling off after a period of time to a constant value. However, with the shorter cell, usually steady-state conditions are established within 10 minutes following the application of pressure to the system. In contrast, with the longer cell, much longer periods of time (about 60 minutes) are required before the flow rate becomes constant.

The explanation for this phenomenon lies in the production and transfer of sensible heat within the sample. Once flow has been initiated, a temperature gradient is established within the ice as a result of the absorption/liberation of latent heat at the ends of the sample (See Section 4.7.) Since the system is initially at a uniform temperature, after pressure is applied, the temperature gradient takes time to be established, the amount depending upon the rate of flow and the length of ice as well as the heat conducting properties of the permeameter. The latter governs the rate at which thermal equilibrium is achieved with the surrounding bath. In the present example, the smaller diameter cell takes 6 times longer for steady-state conditions to be established than the larger diameter cell, although its length is only 3 times greater. The difference clearly lies in the cross-sectional area of the sample which is twice as large in the larger diameter cell, thus, twice the rate of heat production. To generalize, the time for steady state mass transfer conditions to be established within the system varies in direct proportion to the length of the sample and inversely with its cross-sectional area.

---

[4] Buil and Aguirre-Puente (1981) point out that, at equilibrium, the free energy of a solution and a non-hydrostatically stressed solid may be a function of the orientation of the crystals within the solid relative to the solid-liquid interface. This may explain the tendency for recrystallization to occur under stress or for crystals to develop a preferred orientation. The subject remains a matter of controversy. In the present example, this would account for greater axial stresses within the ice sample even though equilibrium between the ice and the supercooled water has been fully established.

Figure 4.7a

Cumulative Outflow vs Time for a Layer of Ice During Regelation Transport

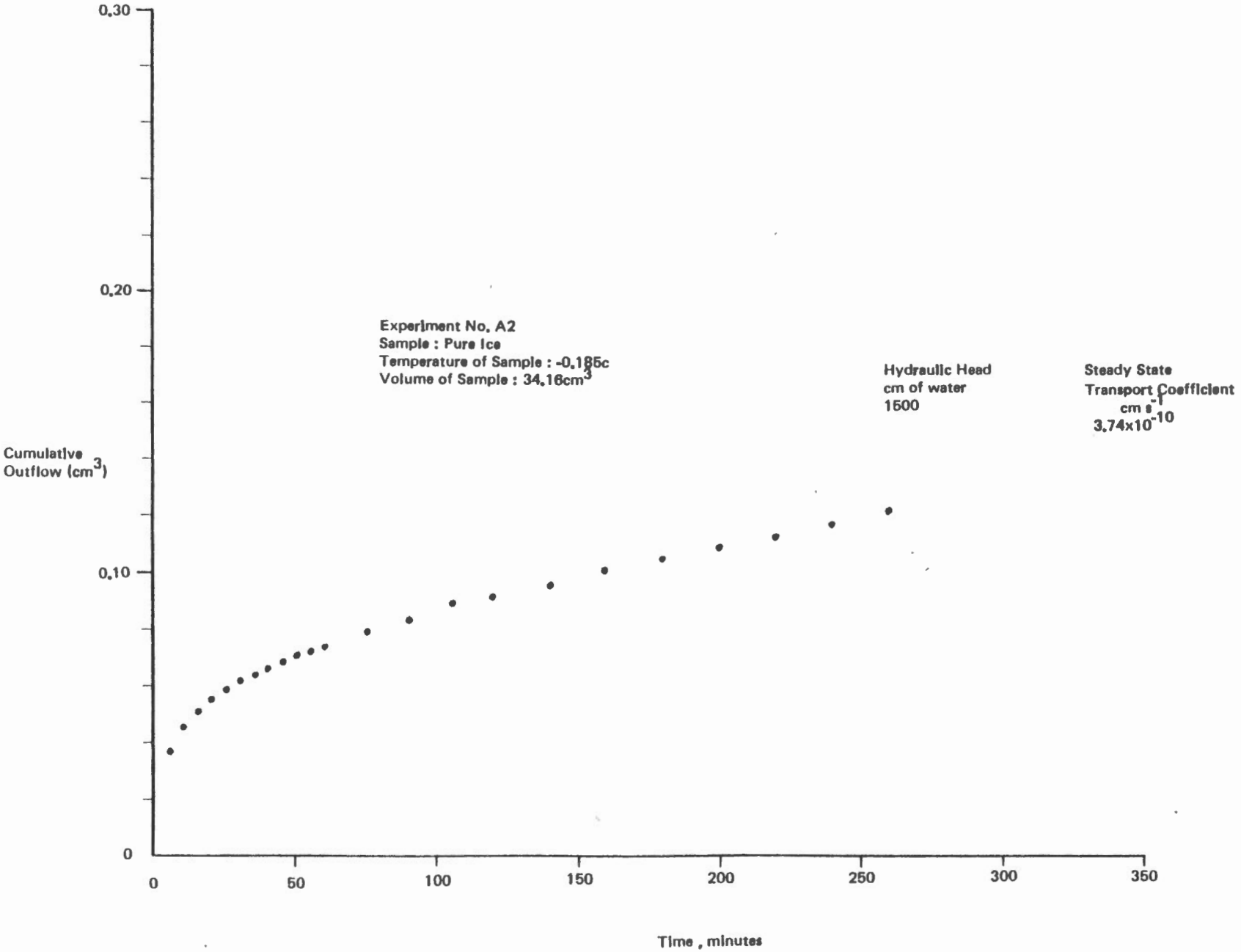

Figure 4.7b

Cumulative Outflow vs Time for a Layer of Ice During Regelation Transport

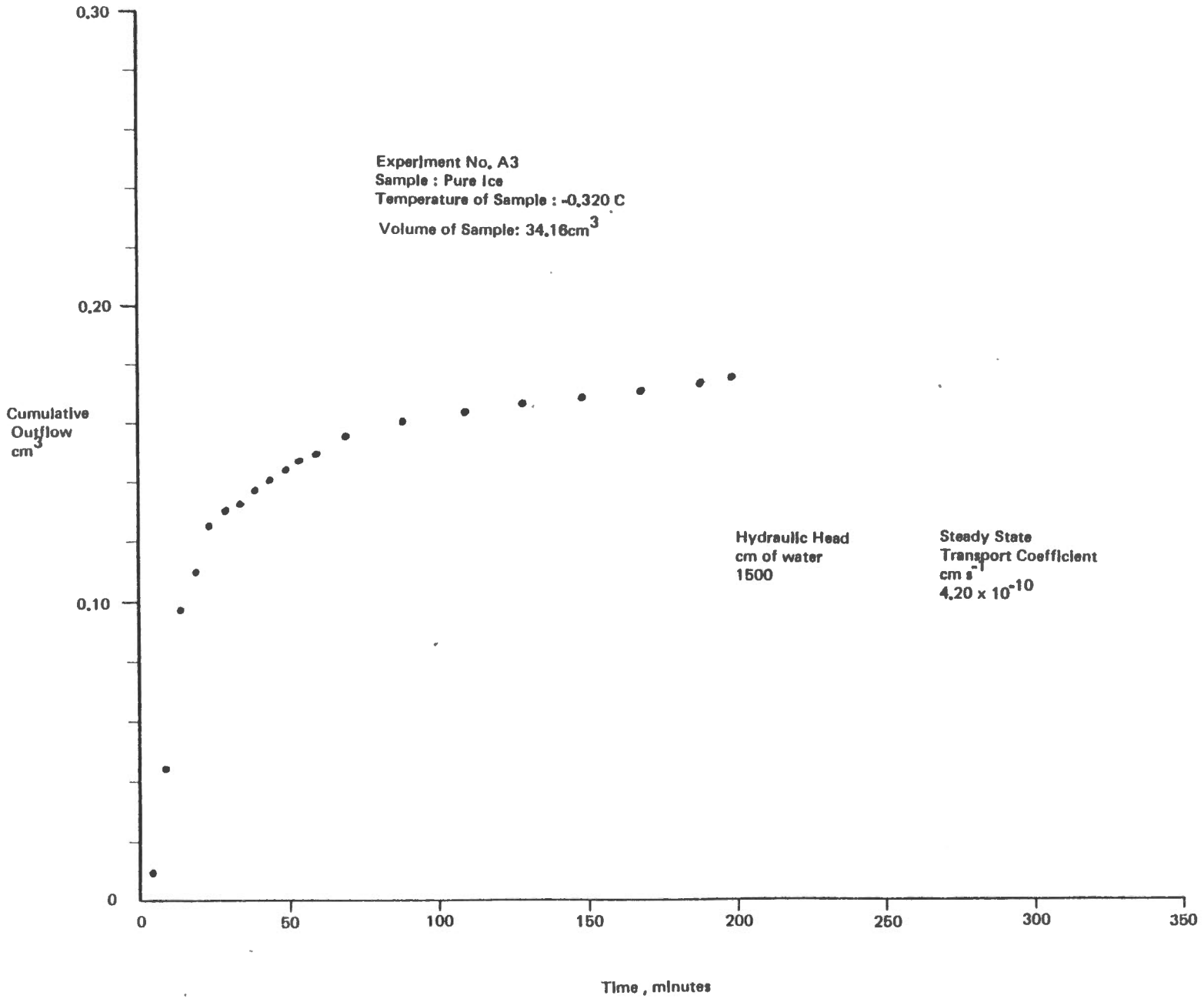

The phenomenon of declining flow rates has also been observed in permeability tests on frozen soils, (Burt and Williams, 1976, Williams and Wood, 1981.) Williams and Wood (1981) suggested a number of possible explanations for the phenomenon. In light of the findings mentioned above, it seems almost certain that the problem of declining flow rates arises as a result of the approach to steady-state heat transfer conditions in the soil-permeameter system. The induced temperatures gradient is in a direction which diminishes transport through the permeameter.

It is recommended that in future permeability tests, the problem can be largely eliminated by shortening the length of the sample and increasing its cross-sectional area as much as possible. The effect of the heat conducting properties on the flow rates through the soil should also be investigated. Comparing flow rates, under identical conditions, between permeameters made of materials with completely different heat conducting properties (for example, copper as opposed to teflon) should provide an indication in quantitative terms of the restrictions that the thermal properties of the permeameter imposes upon the measured transport coefficents. Installation of temperature sensing devices in the walls of the permeameter should enable direct measurement of the heat exchange with the surroundings.

4..7 Thermodynamic Explanation For Regelation-Transport

An important question which remains to be answered, concerns how the regelation mechanism actually works in the present experiment. Miller, Loch and Bresler (1975) suggested the following explanation.

Initially at equilibrium, the ice pressure exceeds the water pressure by an amount specified by the Clapeyron equation. If, however, the hydrostatic pressure on one side is raised above atmospheric pressure, the Clapeyron equation indicates that the equilibrium temperature of the ice and water increases by $\Delta T = -0.0824^\circ$ C/atm above the existing temperature. Since the system is now colder than its equilibrium temperature,according to the Clapeyron equation the ice pressure must rise to a new equilibrium value. Thus, water freezes along the upstream side of the ice-water interface. At the other side of the system, where P_w remains at atmospheric pressure, the increase in P_i reduces the equilibrium temperature below ambient by an amount $\Delta T = -0.0899^\circ$ C/atm. This causes melting along the downstream phase boundary. The net result is the movement of ice in the direction away from the reservoir with higher pressure.

It should be pointed out that during regelation transport, the ice temperature does not remain constant. Peaks and troughs in the temperature of the ice occur along phase boundaries and are proportional to the rate of mass transfer within the system. (See Figure 4.8.) These arise as a result of the liberation of latent heat by freezing at the inflow phase boundary and the absorption of latent heat by melting along the outflow boundary.

Thus, the rate governing process for regelation-transport may well be heat conduction.[5]

Flow rates during regelation-transport are proportional to the following variables:

(1) The temperature of the ice, which affects its rheological properties,
(2) The threshold pressure required to initiate and sustain flow within the ice,
(3) The hydraulic gradient between the end reservoirs,
(4) Pressure decrements which are sustained by the membranes,
(5) The rate of heat transfer within the ice itself and between the ice and its surroundings.

The latter term will depend upon the dimensions of the sample as well as the thermal properties of the permeameter.

Contrary to expectations, no significant rise in ice pressure was observed after hydrostatic pressure had been applied to the system. Even when hydrostatic pressures of more than 2000 cm of water were applied to the inflow reservoir, the ice pressure did not rise more than 10-20 KPa (1.0 - 2.0 cm of water) above its original value, although large amounts of outflow were observed. In all cases, tests were conducted over extended periods of time (several hours), to ensure that the pressure did not rise slowly as a result of a gradual creep within the ice.

It was expected that, since the pressure sensing apparatus was positioned about midway along the length of the cell, the ice pressure would be approximately half the value of the applied hydrostatic pressure (i.e. 1000 cm of water for an applied pressure of 2000 cm). However, further consideration of this matter and the results should not seem so surprising. First of all, the ice is moving as a result of the continuous freezing/thawing at the ends of the sample and so the pressure within the cell is not able to rise significantly. In other words, it is the continuous movement of the ice which prevents the pressure from building up within the cell. It also seems likely that the ice pressure is inversely related to its velocity of flow, in much the same manner that Bernoulli's principle describes the pressure-velocity relationship in fluids.

Secondly, the membranes may act as an effective barrier in limiting the transmission of the hydrostatic stress to the ice. This may be a result of the low permeability of the membrane which limits the diffusion of water molecules through the pores. Hence, the membrane sustains a large pressure decrement across its thickness.

---

[5] Philip (1980) presented a convincing analysis which demonstrates that this is almost certainly the case in frozen soils.

4.9 A Flow Law For Polycrystalline Ice

The mechanical behaviour of polycrystalline ice is complex since it exhibits elastic and plastic properties as well as those of a viscous fluid. A plot of the deformation or strain of a material (at constant stress) as a function of time, is usually referred to as a creep curve. A schematic diagram of the creep curves for polycrystalline ice under various stresses at constant temperature is shown in Figure 4.9.

At low stress (curve III), the creep shows an instantaneous elastic deformation followed by a period in which the strain rate declines to a constant value. At higher stresses the strain rate starts to increase again and may eventually stabilize at a greater rate of strain (curve I and II). The initial decline in the strain rate is referred to as primary or transient creep. The strain at this stage of the deformation is bimodal with a reversible elastic component as well as a visco-elastic component which is only partly reversible. The term 'secondary' or quasi-viscous creep describes the stage in which the strain rate achieves a steady-state. The stage where the strain rate increases is called tertiary creep. Secondary creep represents the transformation from visco-elastic creep to plasto-viscous creep. The change in the rate of strain is a result of the transition from strain hardening to strain softening. Strain hardening is believed to be caused by interference between crystals with different orientations as well as the accumulation of dislocations at nodes within the ice. Strain softening is attributed to fracture as well as the recrystallization of ice under stress (Glen, 1975).

A similar set of curves would describe the creep of polycrystalline ice at various temperatures under constant stress, curve III corresponding to the creep at cold temperatures and curve I at warm temperatures.

Creep curves for polycrystalline ice at stresses up to 10 bars (= 1000 KPa) and temperatures between - 0.02°C and - 12.8°C are shown in Figure 4.10.[6] At cold temperatures and moderately cold temperatures, creep behaviour is dominated by transient processes and secondary creep is never fully established. Under these conditions, the primary mode of deformation is probably the movement of dislocations. In contrast, at relatively high stress and warm temperatures, secondary creep is overtaken and dominated by tertiary creep. In this case, the dominant mode of deformation is the migration of crystal boundaries.

The temperatures and stress dependence for the deformation of ice during secondary creep can be summarized in a simple flow law. The most commonly quoted analytic form for the flow law is the power function:

$$\dot{\varepsilon} = A \sigma^n \qquad (4.6)$$

where n is a constant,

σ = the normal stress, Nm^{-2},

and $\dot{\varepsilon}$ = the strain rate, s^{-1}

---

[6] 1 bar = 100 KPa

Figure 4.10

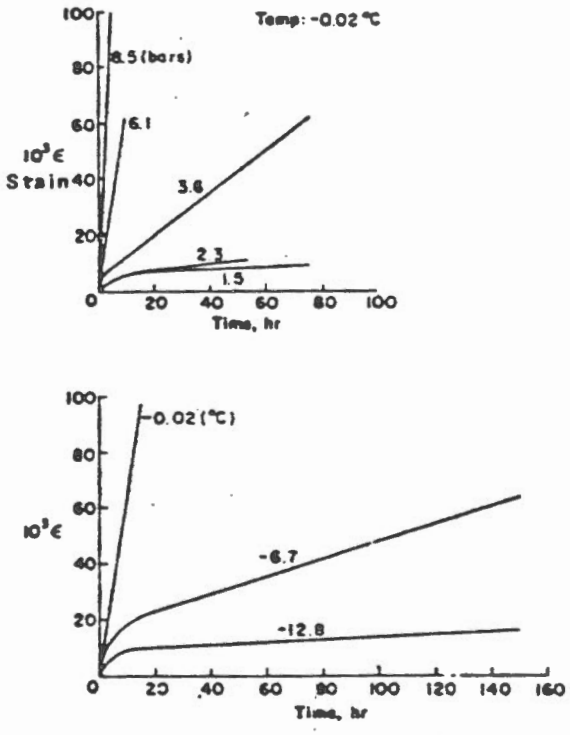

Creep curves of randomly oriented polycrystalline ice (above) at -0.02°C under various stresses (below) at various temperatures under 6 bars. ϵ

1 bar = 100 KPa

The parameter A is given as:

$$A = K \exp(-Q/RT) \qquad (4.7)$$

where T = the temperature,
R = the universal gas constant,
Q = an activation energy constant,
and K = Boltzmann's constant.

Glen (1975) gives a value of n = 3.5 at stresses above about 100 KPa. At lower stresses n falls off and approaches unity.

Note the exponential dependence of the strain rate on the temperature which is compatible with the present findings in the regelation experiment. However, our results indicate that the relationship between the applied stress (hydraulic head) and the strain rate (flow rate) is linear rather than a power function. The discrepancy is probably due to the limitations imposed upon the rate of freezing/thawing within the system and thus the rate of ice deformation, by the heat transfer within the ice and between the ice and the surrounding bath.

Gold (1973) indicates that the creep of ice contains a large delayed elastic component. Because of this, in cases where the stress is relatively low, such as occurs in the 'ice sandwich' experiment, it may take an exceptionally long time before the deformation becomes viscous rather than elastic. This may explain the apparent enigma of the threshold pressure which was observed in the present experiments. It is difficult to conceive that friction along ice-sidewall interface could be sufficient to prevent the movement of the entire ice sample except possibly in a thin layer adjacent to the walls of the cell. What is more likely is that the threshold value represents the pressure that is required for the instantaneous deformation within the ice to become viscous rather than elastic. If one waits long enough, it is doubtful whether there would be any threshold pressure at all, since the initial elastic component of deformation would gradually become viscous in nature over time.

4.10 Experiments in Osmotically Induced Regelation-Transport

In the experiments discussed above, regelation was induced by the application of a hydrostatic pressure to the ice. In frozen soils, however, regelation transport is induced by gradients in the osmotic activity of the solutes in the liquid films surrounding the soil particles. To demonstrate that regelation transport can be induced by an osmotic gradient, a number of experiments were performed in which the apparatus shown in Figure 4.1 was employed as an osmometer rather than as a permeameter. Instead of using hydrostatic pressure the chemical potential of the water in the reservoirs was adjusted to a precise level using lactose solution.

Ice samples were prepared in the same manner discussed earlier. The sample was 3.02 cm long and had a diameter of 5.40 cm. No provision was made for measuring ice pressures during the experiment. After the apparatus was assembled, the system was allowed to equilibriate for about

48 hours before flushing the reservoirs with lactose solution. Flow readings commenced immediately after flushing and continued for a period of 6 hours a day for 2-3 days.

Results of the experiment are shown in Figures 4.11 and 4.12. In experiment no. A9, lactose solution was used in one reservoir. This resulted in a continuous flow of water towards the solution. Figure 4.12 shows a simple osmometer analog for the system. During the initial equilibriation period, supercooled water is drawn into the sample container from both reservoirs, changing phase upon contact with the ice, the ice pressure slowly rising. Equilibrium is attained when the chemical potential of the ice (μ_i) and the water (μ_w) are the same. The Clapeyron equation indicates the amount by which the ice pressure exceeds the water pressure at equilibrium (for pure water). In this particular case, T = - 0.110°C, therefore, $P_i - P_w$ = 1257 cm of water (≙ 123.2 KPa).

When reservoir 1 is flushed with solution, the lactose (concentration = 52.94 g l^{-1}) lowers the chemical potential of the water below that of pure free water by an amount:

$$\mu_w = \mu_w^\circ (T,p) - \phi RTV_w \sum_s C_s \qquad (4.8)$$

where $\mu_w^\circ (T,p)$ = the chemical potential of pure free water at the same temperature and pressure,

R = universal gas constant,
T = the temperature,
V_w = the volume of the water,
ϕ^w = the osmotic coefficient of the solute,

and C_s = the molar concentration of the solute[7].

Since the chemical potential of the ice is now greater than that of the water in the solution, this causes the ice to melt, passing through the membrane, which raises the pressure of the solution. The fall in ice pressure, in turn, disturbs the equilibrium between the ice and the water in the second reservoir (R2). Since the value of $P_i - P_w$ is fixed at any temperature, as the ice pressure falls, the pressure of the supercooled water undergoes a corresponding change, water passing through the membrane and changing to ice (see Figure 4.12b). Flow through the system ceases when the pressure of the solution increases to a value in which the

---

[7] The relationship between the solute concentration C (g l^{-1}) and the molar concentration C_s (g -mol l^{-1}) is:

$$C = \frac{C_s}{M}$$

where M = the molecular weight of the solute.

Figure 4.11a

Cumulative Flow vs. Time for a Layer of Ice During Osmotically Induced Regelation

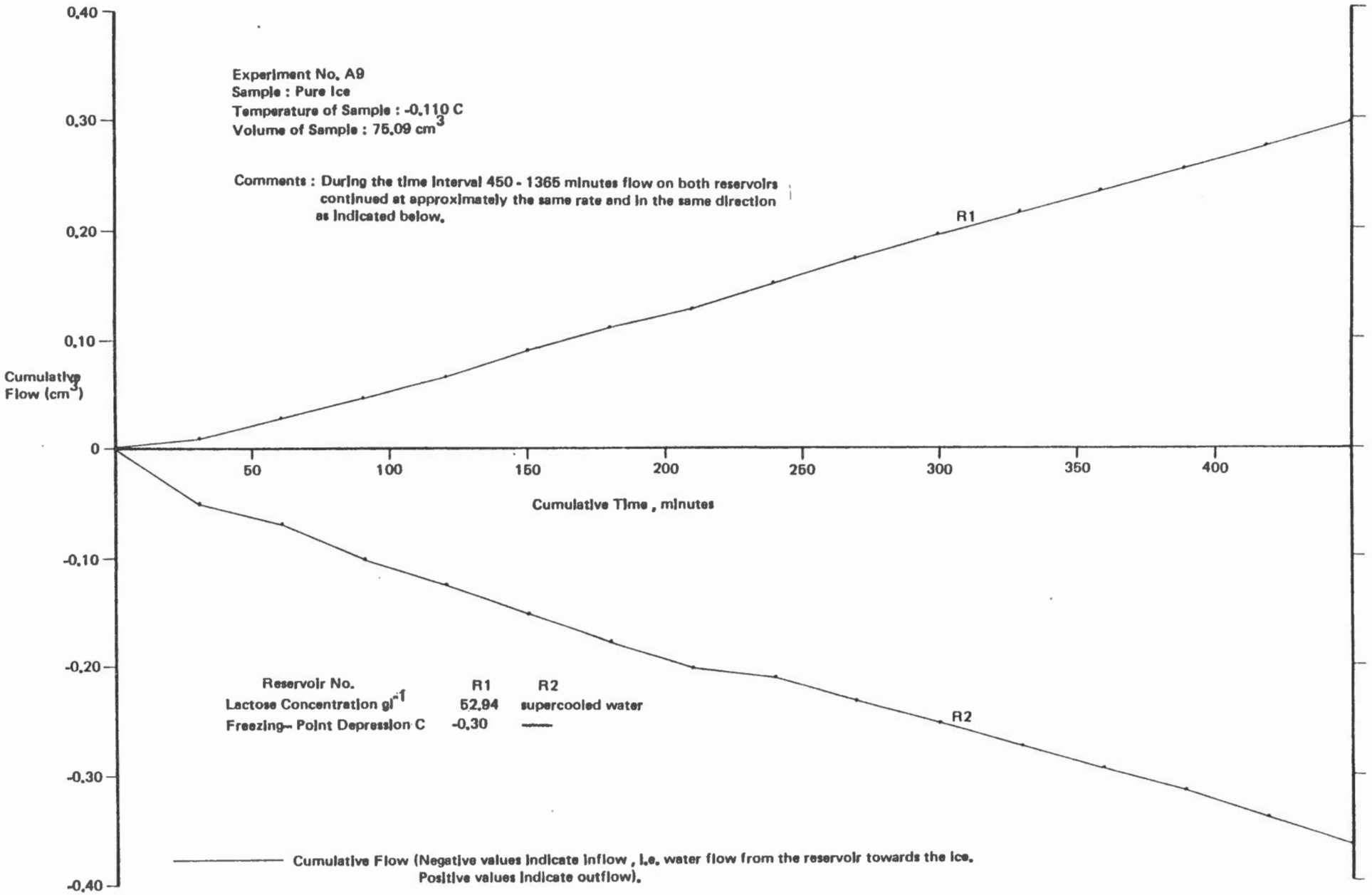

Figure 4.11b

Cumulative Flow vs. Time for a Layer of Ice During Osmotically Induced Regelation

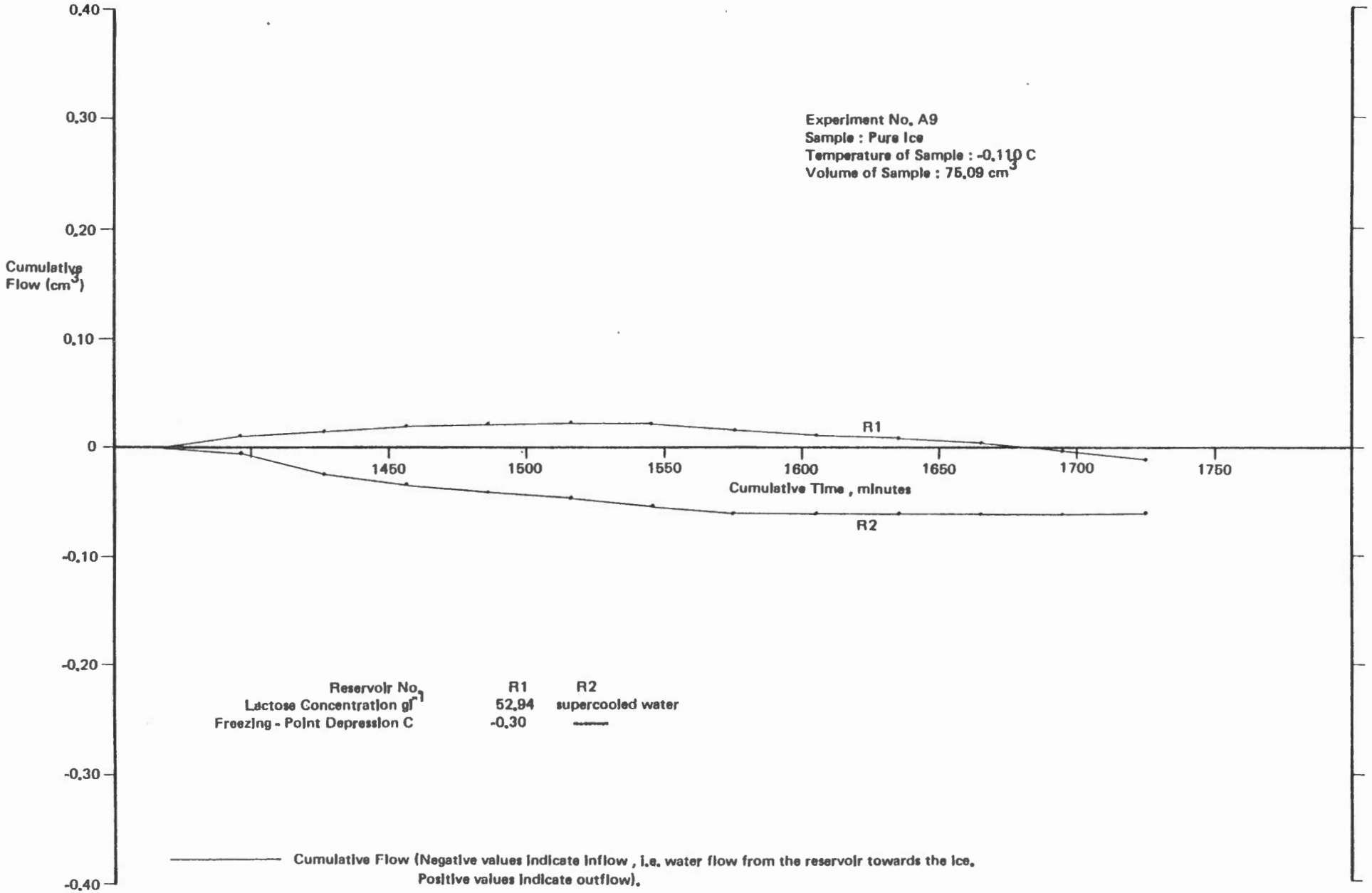

Figure 4.11c

Cumulative Flow vs. Time for a Layer of Ice During Osmotically Induced Regelation

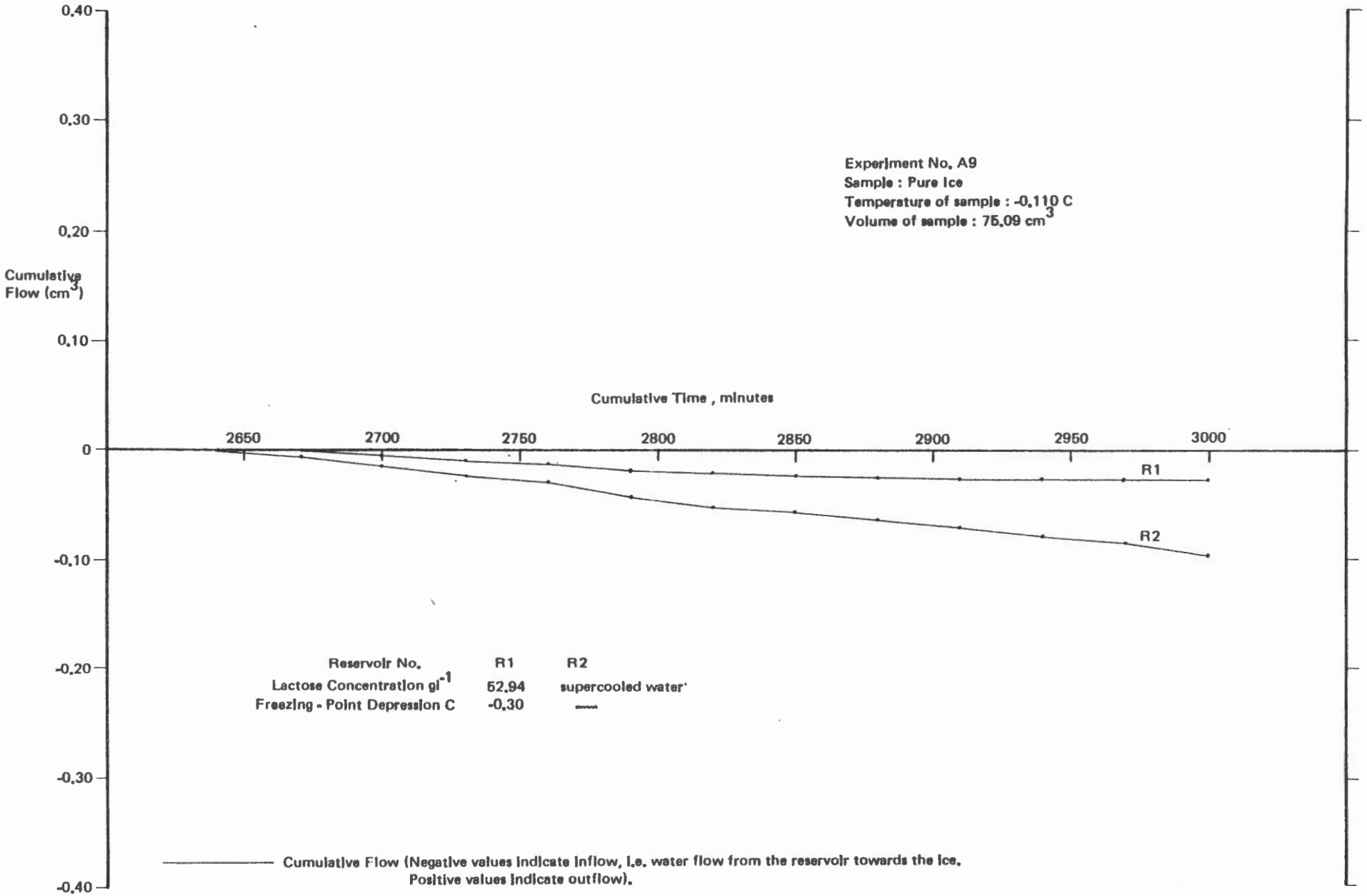

Figure 4.12

Osmometer Analog For Experiment No. A9

a
Initial equilibrium

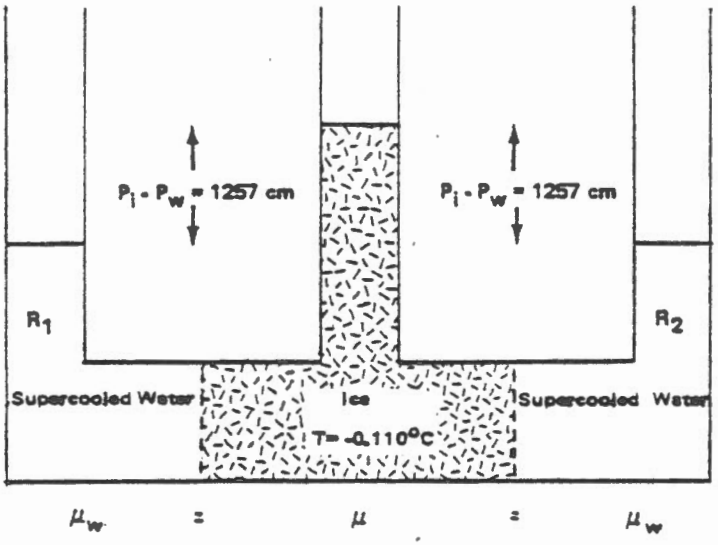

b
Reservoir 1 flushed with lactose solution

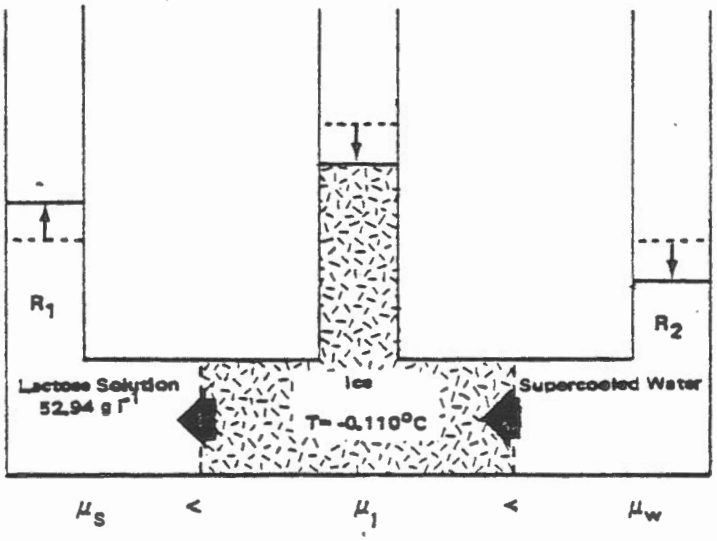

μ =Chemical Potential

All pressures given in cm of water

c
Final equilibrium condition

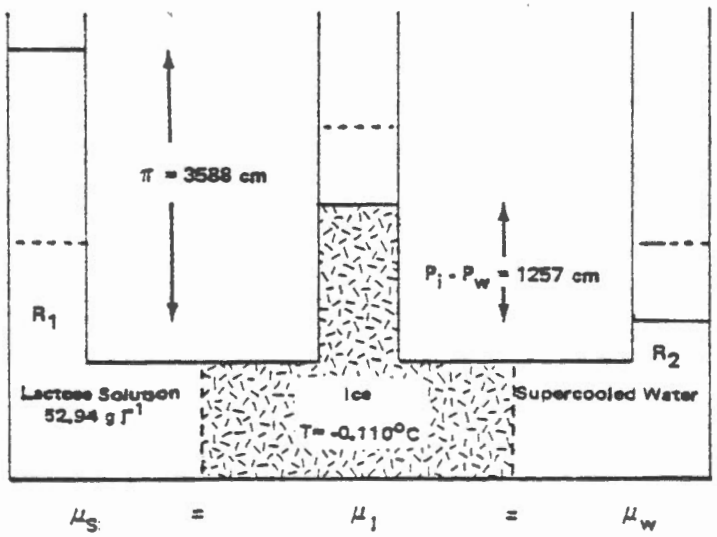

chemical potential of the water in reservoir 1 becomes equal to that of the ice. This value represents the osmotic pressure for the system at that temperature (see Figure 4.12c). For a dilute solution, the osmotic pressure is given by the Van't Hoff equation:

$$\pi = \frac{\phi\ RT}{V_w} \sum_s C_s \qquad (4.9)$$

Assuming in the present case that the solution is ideal, ϕ drops out and π = 3588 cm of water.

In experiment no. A9, equilibrium is never attained since the pressure of the water in reservoir 1 is not allowed to rise.[8] Thus flow through the system is continuous and should be equal in both reservoirs. Examining Figure 4.11a, it is apparent that this does in fact occur, at least in the initial stage of the experiment. Note, however, that this condition does not remain stable for long. During the second reading session, the rate of flow was much smaller than on the previous day and flow reversal was observed on reservoir 1. A small but steady rate of inflow on both reservoirs continued to occur throughout the third reading session (see Figures 4.11b and c). The phenomenon is attributed to the gradual diffusion of lactose molecules through the membranes which causes the ice to thaw. At the end of the experiment, a thawed layer 0.25 cm thick was observed on the side of the ice facing the lactose solution. As the ice thaws, its pressure begins to fall and this disrupts the equilibrium at the other end of the cell. This results in a slow but continuous flow of water towards the ice from reservoir 2.

The situation in experiment no. A10 was somewehat more complicated than in the previous case, since lactose solution was used in both reservoirs. An osmometer analog for the experiment is shown in Figure 4.14.

At T = - 0.295°C, equilibrium between the supercooled water in the reservoirs and the ice is achieved when $P_i - P_w$ = 3372 cm of water (= 330.6 KPa). Flushing the reservoirs with lactose solution should produce outflow from both reservoirs, the amount varying directly with the concentration in each reservoir (see Figure 4.14b). This causes the ice pressure in the cell to fall, thereby lowering its chemical potential. Eventually the ice pressure falls to a sufficiently low value that its chemical potential becomes equal to that of the water in the reservoir with the less concentrated solution (R2). At this point, outflow from reservoir 2 ceases. As the ice pressure continues to fall (due to outflow from reservoir 1), its chemical potential becomes less than that of the water in reservoir 2 and the flow direction in R2 reverses (see Figure 4.14c). Flow should proceed in the direction of the reservoir with the more concentrated

---

[8] If reservoir 1 was sealed, the water pressure would eventually rise to its equilibrium osmotic value, provided lactose did not cause thawing of the ice.

Figure 4.13a

Cumulative Flow vs. Time for a Layer of Ice During Osmotically Induced Regelation

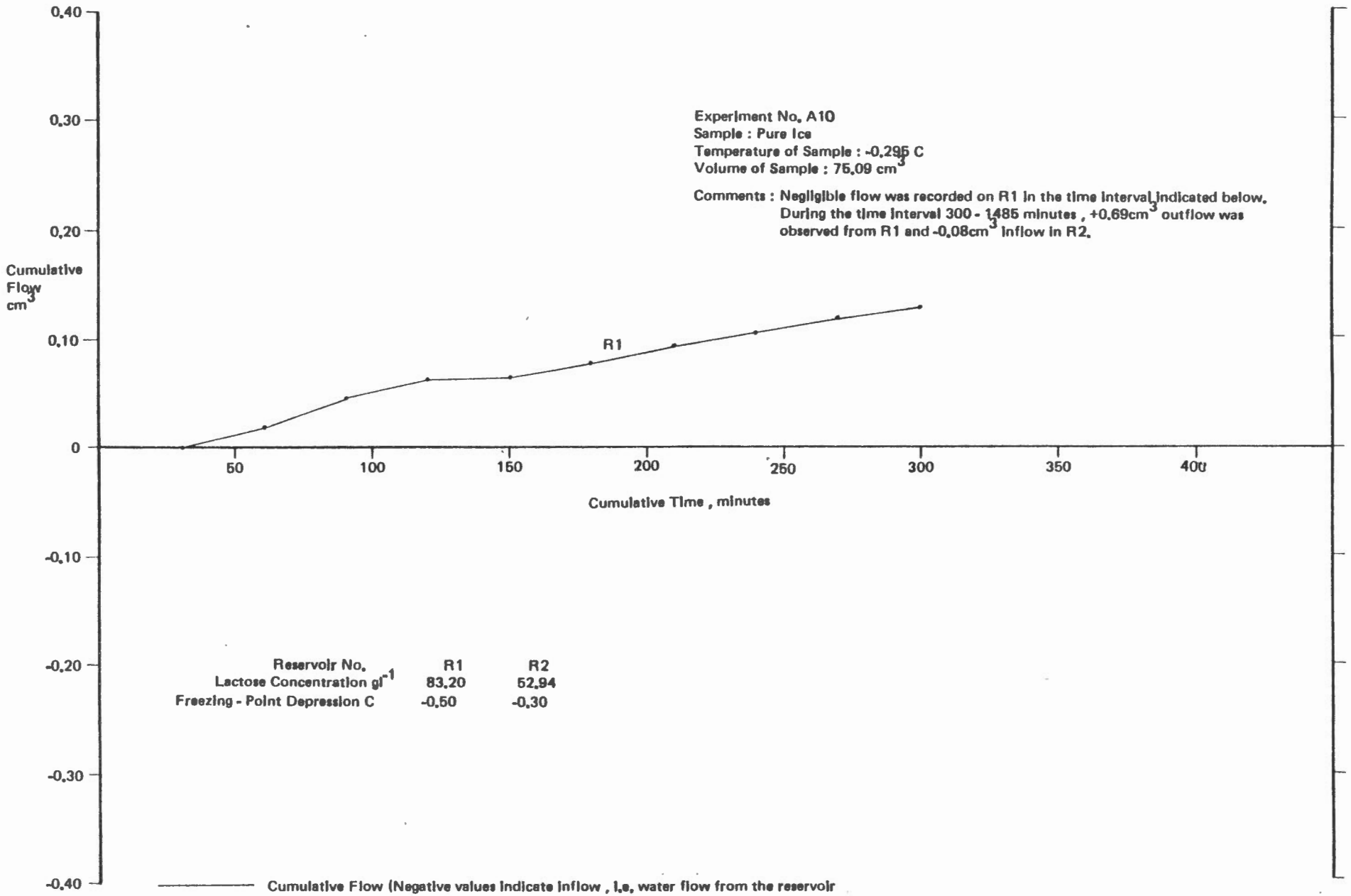

Figure 4.13b

Cumulative Flow vs. Time for a Layer of Ice During Osmotically Induced Regelation

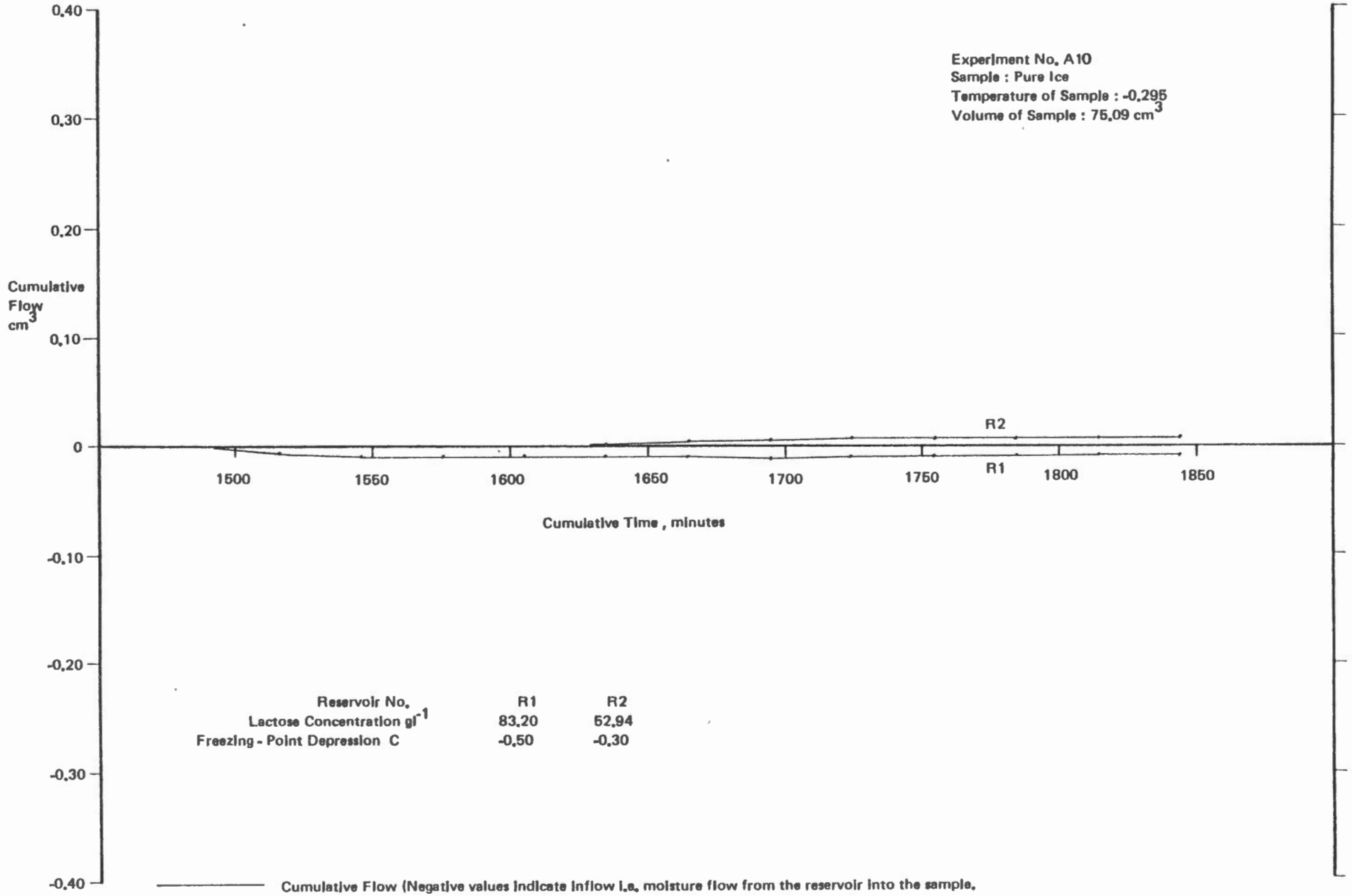

solution until the pressure in this reservoir becomes large enough that equilibrium is again established. The osmotic pressure required to produce equilibrium represents the difference between the osmotic pressures of the two solutions. In the present case, since C_1 = 83.20 g l^{-1} and C_2 = 52.94 g l^{-1} π = 2046 cm of water. Since the freezing-point depression of the lactose concentration in reservoir 2 is - 0.30 C (= the temperature of the system), ultimately equilibrium with the ice will occur when the pressure of the ice and the solution is identical.

Results obtained from experiment no. A10 differed somewhat from what was expected (see Figures 4.13a and b). Although outflow was observed from the reservoir with the more concentrated solution (R1),no flow was recorded on the other reservoir. Obviously, for one reason or another, equilibrium is maintained between the ice and reservoir 2. This may be due to the fact that the gradient in the chemical potential between the ice and reservoir 2 is countered exactly by a pressure gradient within the ice which is caused by flow towards reservoir 1. In other words, the tendency for outflow to occur at R2 is neutralized by the greater rate of outflow at R1, at least in the time period in which the flow was recorded.

4.11 Thermally Induced Regelation

Several experiments were also attempted in which regelation flow was produced by temperature induced gradients in the chemical potential of the water in the reservoirs. The apparatus used in the experiments was similar to that used by Perfect and Williams (1980) to measure water flow in frozen soils under temperature gradients (see Figure 5.1). The ice sample was confined to a plexiglass cell which was sandwiched between two metal end plates containing reservoirs, the temperature of which was controlled by thermoelectric cooling. After assembly, the reservoirs were flushed with supercooled water and the system was set at a uniform temperature of about - 0.1°C and allowed to equilibriate for about 24 hours. Following this, the temperature of one reservoir was lowered slightly, to about - 0.3°C. Since the difference between the chemical potential of the water and ice is greatest at the 'cold' end of the system, this should ultimately induce flow in the direction of warmer temperatures. The situation is similar to that shown in Figure 4.12, the chief difference being that the chemical potential of the water is greater than that of the ice. This explains the tendency for flow to proceed towards the 'warm' reservoir.

Although the explanation outlined above is corroborated, at least to some degree, by experimental results, in general, the results were of such poor quality that they will not be presented in this report. The chief difficulty with the experiment was the failure to prevent nucleation of the supercooled water in the reservoirs. Despite repeated attempts, freezing usually occured within a few hours after the apparatus was assembled.

SECTION 5

PRESSURE CHANGES IN FROZEN SOILS DURING TEMPERATURE INDUCED WATER MIGRATION

5.1 Apparatus and Materials

The soil sample is confined to a plexiglass sample holder, 3.50 cm long with an internal diameter of 5.40 cm and wall thickness 1.90 cm, which is sandwiched between two aluminum plates containing small end reservoirs (see Figure 5.1). The soil is separated from the reservoirs by cellulose acetate membranes (pore size 0.005 μm). The membranes are supported by porous brass or aluminum plates which are inserted in the end reservoirs. The system is cooled by peltier modules attached to the aluminum end plates.[1] Current is supplied by a thermoelectric cooling control unit which maintains temperatures constant to within $\pm 0.01°C$. Inflow and outflow from the reservoirs are measured with small capillaries which are mounted on a finely divided scale. A rigid network of copper tubing, brass ball valves, needle valves and tee junctions enables continuous flow readings to be made over extended periods of time.

Temperatures within the soil and the end plates are monitored with five 3000 Ω thermistors.[2] These are calibrated to an accuracy of $\pm$ 0.01°C (see Appendix B). The thermistors are housed in small copper tubes 3.0 cm long, which are sealed at one end. A small O-ring maintains the seal between the copper tubing and the sample container. The thermistor housings are positioned so that only a small fraction of their length (0.7 cm) is in thermal contact with nylon retaining nuts which press against a copper flange welded to the open end of each tube. These precautions eliminate any significant thermal disturbances due to heat conduction along the copper housings.

To minimize radial heat exchange with the surroundings, the cell is wrapped in a jacket of foam rubber insulation approxiamtely 6 cm thick and placed in a 'Precision' low temperature incubator. The air temperature within the incubator is adjusted so that it remains constant to within $\pm$ 0.1°C of the mean temperature of the soil sample.

---

[1] A peltier element consists of a group of p and n-type semi-conductors connected in series by metal junctions. Passage of a current through the circuit results in heat losss at one junction and the absorption of heat at the other (Gray and Issacs, 1975.)

[2] YIS precision thermistors, model no. 44030, resistance 3000 Ω at 25°C.

Figure 5.1

CROSS-SECTION OF THE EXPERIMENTAL APPARATUS

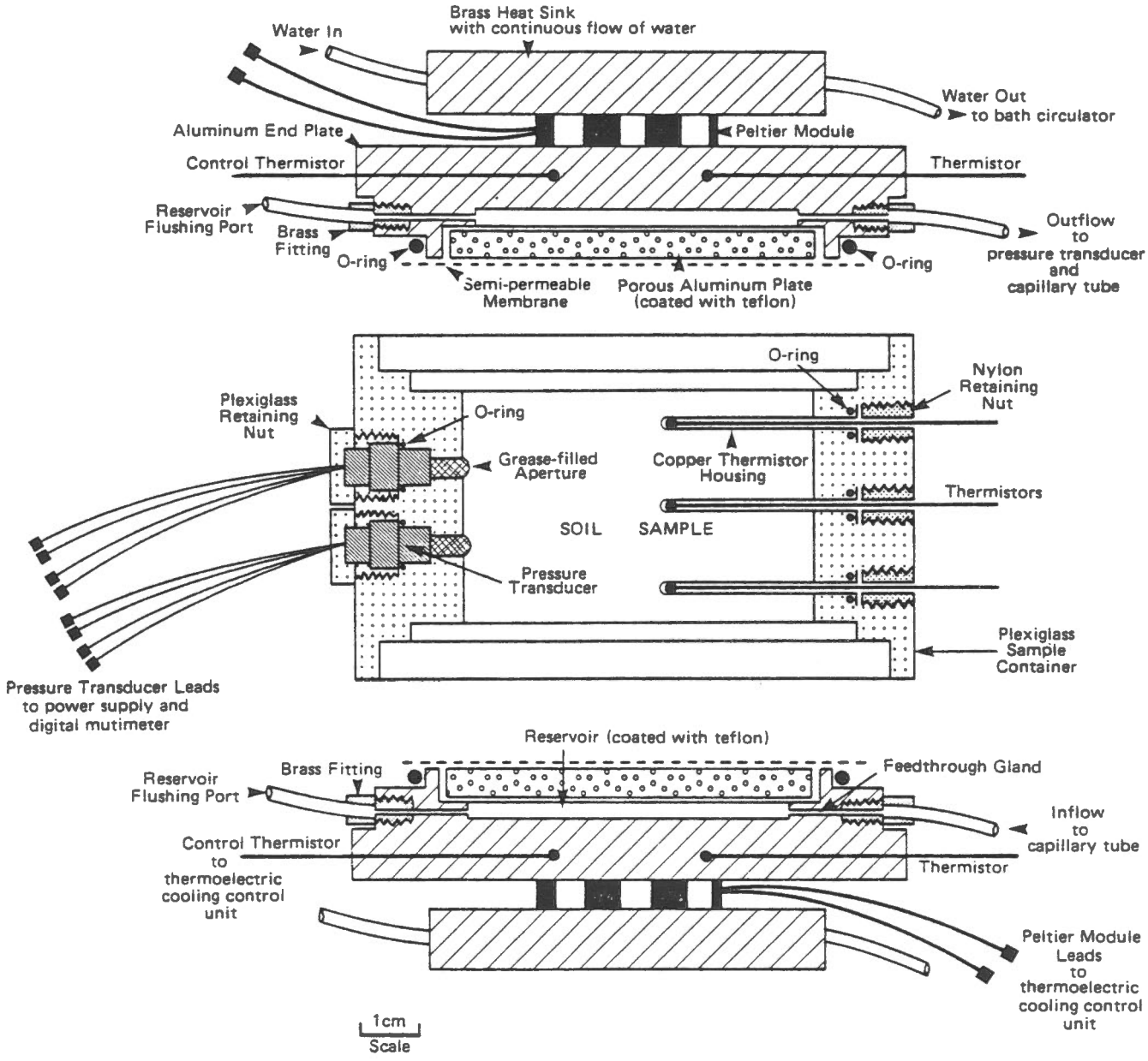

The nylon screws used to hold the apparatus together are not shown.
Brass fittings, and plexiglass retaining nuts are not drawn to scale.

Figure 5.2

SCHEMATIC REPRESENTATION OF THE ENTIRE EXPERIMENTAL ASSEMBLY

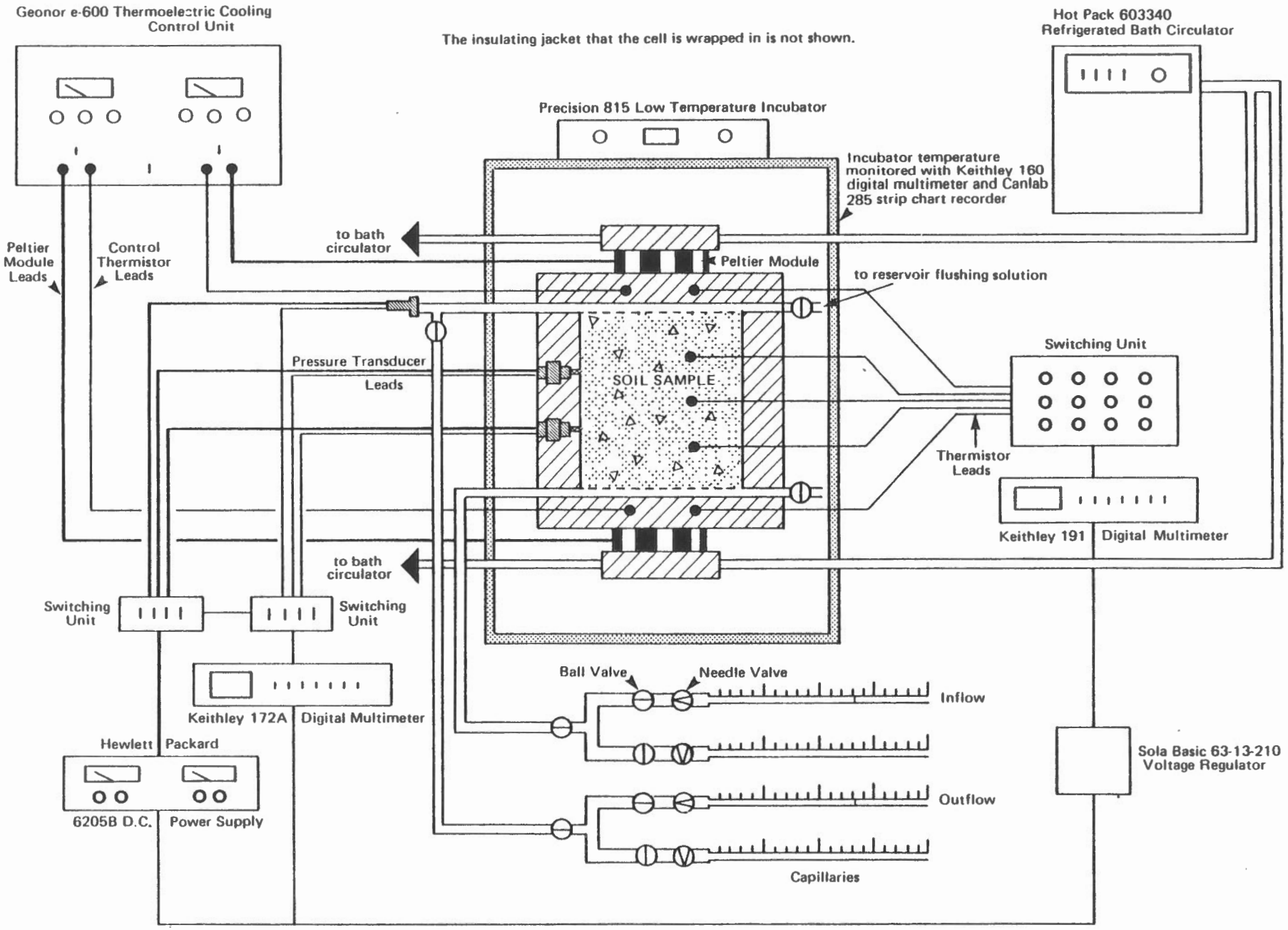

Pressures within the soil sample are monitored with two Kulite VQS-250 sealed guage pressure transducers (rated pressure 50 psi) spaced 1.20 cm apart. This arrangement not only enables the measurement of pressure changes within the frozen soil but also any pressure gradients which might exist as well. This is an important consideration in determining the magnitude and direction of moisture movement in frozen soils. The pressure transducers are held in place by plexiglass retaining nuts 1.00 cm long with an outer thread diameter of 1.90 cm. Owing to the size of the retaining nuts, the transducers were offset from each other in the radial dimension by about 4 cm.[3]

Since moisture flow in frozen soils usually proceeds in the direction of colder temperatures, if outflow from the 'cold' reservoir is arrested, the pressure of the water in the reservoir should increase. Measurement of the total rise in pressure within the reservoir over an extended period of time should provide an indication in mechanical terms, of the thermally induced driving head within the soil. The appartus is shown in Figure 5.2. A brass ball valve was attached via a length of high pressure nylon tubing to the outlet port on the 'cold' reservoir. Closing the valve enables the flow to be shut off at any time during an experiment. Pressure within the reservoir is measured with a Kulite XTM-1-190 sealed gauge pressure transducer (rated pressure 100 psi), which is connected to the nylon tubing via a stainless steel tee junction.

5.2 Experimental Procedure

Soil samples were prepared as slurries using deionized deaired water and gently spooned into the plexiglass cell. To remove any excess air trapped within the soil, the sample container was placed in a vacuum dessicator for approximately 20 minutes. The soil was then frozen rapidly to a temperature of -22°C for about 24 hours. Prior to assembly, the ends of the sample were scraped down until flush with the plexiglass container. To prevent damage to the membranes by freezing, the sample was allowed to warm up to a temperature of about -4°C, before placing the membranes on the soil surface. Following this, the end plates were attached to the sample container with nylon screws and the cell was wrapped in insulation and placed in the incubator. Once the system had been connected to the thermoelectric cooling control unit, a temperature gradient was established within the soil sample by adjusting the current suppled to the peltier modules. The reservoirs were then flushed with the appropriate lactose concentration. In most cases, a linear temperature gradient was fully established in about 12-18 hours, although near linear gradients were usually observed after about one hour.

---

[3] Placing the pressure transducers in an aligned position would have required further extension of the test cell. Not only would this decrease the rate of moisture flow through the soil, it would also reduce the magnitude of the temperature gradient which could be established.

Temperature pressure and flow readings were made at 30 minute intervals, for a period of about 6 hours every day. Usually experiments were run for a period of about 3 days, the duration of each test being limited by the gradual thawing of the soil sample as a result of lactose diffusion through the membranes. With the Allendale soil lactose diffusion was less rapid, and so, tests were run for periods of up to one week.

After the apparatus was dismantled, the length of the remaining frozen section was measured and the bulk density and moisture content of the sample were determined.

5.3 Operation of Pressure Transducers

In principle, the transducer circuit is fairly simple consisting of a wheatstone bridge with a temperature compensating module mounted on a silicon diaphragm which acts as the pressure sensitive area. Operation of the transducers requires external excitation from a constant voltage source (5 V d.c. is used). This is provided by a Hewlett Packard 6205 B d.c. power supply. Output from the transducers is in millivolts and is read from a Keithly 1191 digital multimeter.

To prevent damage to the diaphragms the transducers are separated from the soil by a small gap 0.5 cm deep and 0.3 cm diameter which is filled with silicon grease. To minimize potential arching effects around the orifice, the grease protrudes outwards into the soil for about 0.2 cm. (see Figure 5.1). Extra care is taken to ensure that no air is present within the grease which might cause significant errors in the pressure measurements.

Pressure of the soil sample is determined relative to atmospheric pressure using the simple conversion factor:

$$P = \frac{V_f - V_i}{s} \qquad (5.1)$$

where P = the pressure of the soil sample relative to atmospheric pressure, KPa,
s = sensitivity of the transducer, mV KPa^{-1}
V_i = output of the transducer in mV, at current atmospheric pressure Ai,
V_f = output of the transducer in mV, at soil pressure P.

The total pressure within the soil is obtained by adding the pressure indicated by the transducer to the atmospheric pressure (A_i) in the laboratory at the time of the reading. The atmospheric pressure reading is obtained from a mercury barometer mounted on the wall of the laboratory. (Estimated limit of accuracy = ±0.01 Kpa.) The zero reading for each transducer is obtained by simply determining the initial output in mV before the soil sample is placed in the container. Since the air pressure within the transducer remains constant, a small correction must be made for the effect that changes in the atmospheric pressure have on the zero

reading (V_i) of the transducer:

$$V_i = V + (A_i - A)\, s \qquad (5.2)$$

V = initial output of transducer at atmospheric pressure A,
V_i = corrected zero reading of transducer,
A_i = atmospheric pressure at the time of soil pressure reading.

Excitation of the transducer circuits does produce a significant heating effect. In most instances, after power is applied, the output voltage rises rapidly for a minute or two and then stabilizes at a constant value. This is believed to be due to the thermal expansion of the silicon grease and the plexiglass walls of the sample container. Over an extended period of time, it is likely that heating effects could produce a significant thaw bulb within the soil itself.

To minimize potential heating effects, power is applied to the transducers for the briefest possible period (about 2 seconds) when pressure readings are taken. In addition to this, the excitation voltage has been lowered from 10V d.c., which had originally been used, to 5V d.c. This results in a slight loss in the sensitivity of the transducer.[4]

5.4. Properties of the Soils used in the Study

Two locally obtained soils, Castor sandy loam and Allendale silty clay were used in the study. The Allendale is a colloidal material containing slightly less than 50% clay. In the dry state, it is well flocculated having shperoidal aggregates about 0.1 cm in diameter. Rapid freezing of the soil produces a dense pattern of fairly thick ice lenses (up to 0.2 cm wide) which are randomly oriented throughout the sample.

The Castor soil exhibits the opposite properties of that of the Allendale. It is a non-colloidal soil with less than 3% clay present. In structure, it is granular, having no cohesive strength and resembles a coarse silt in texture. Usually no ice lenses are apparent when it is rapidly frozen. All of the ice occurs as pore ice although the volume of the ice may exceed the pore volume slightly.

The physical properties of both soils are listed in Table 5. Soil freezing characteristic curves were determined by D. Patterson using time domain reflectometry (see Figure 5.3). Mass transport coefficients for both soils in the frozen state are plotted as a function of temperature

---

[4] The sensitivity decreases linearly with the excitation voltage, although lower excitation voltages could have been used, 5V d.c. represents the optimum value, minimizing the heating effects while retaining a high sensitivity.

TABLE 5.1

Grain Size Characteristics of Soils Used in Study*

	% Sand (> 50μm)	% Silt (50-2μm)	% Clay (<2μm)	Classification (USDA system)
Castor	44.2	52.8	2.9	sandy loam
Allendale	17.7	33.9	48.5	silty clay

Mineral Composition**

Allendale	Illite and chlorite present in large amounts. Smaller amount of quartz, plagioclase and orthoclase feldspar and traces of amphiboles are also a pparent.
Castor	Principal mineral is quartz with smaller quantities of orthoclase and plagioclase feldspar also present. Small amounts of chlorite, amphiboles and hydrous micas are also apparent.

Physical Properties

	Castor	Allendale
ρ_B	1.55	1.25
ρ_s	2.73	2.68
ω_{sat}	27.0	42.7
θ_{sat}	42.0	53.4
K_{uf}	1.2×10^{-2}	8.2×10^{-3}

ρ_B = bulk density, g cm^{-3}

ρ_s = particle density, g cm^{-3}

ω_{sat} = saturated moisture content (% dry weight)

θ_{sat} = saturated moisture content, volumetric (% total volume $\theta = \omega\rho_B$)

K_{uf} = unfrozen hydraulic conductivity, saturated state, cm s^{-1}

* Data courtesy of Mr. D. Patterson, Carleton University

** Data obtained from analysis of x-ray diffraction peaks

Figure 5.3

Freezing Characteristics of Soils Used In Study

—— Castor Sandy Loam
- - - Allendale Silty Clay
• Average of 3 Values

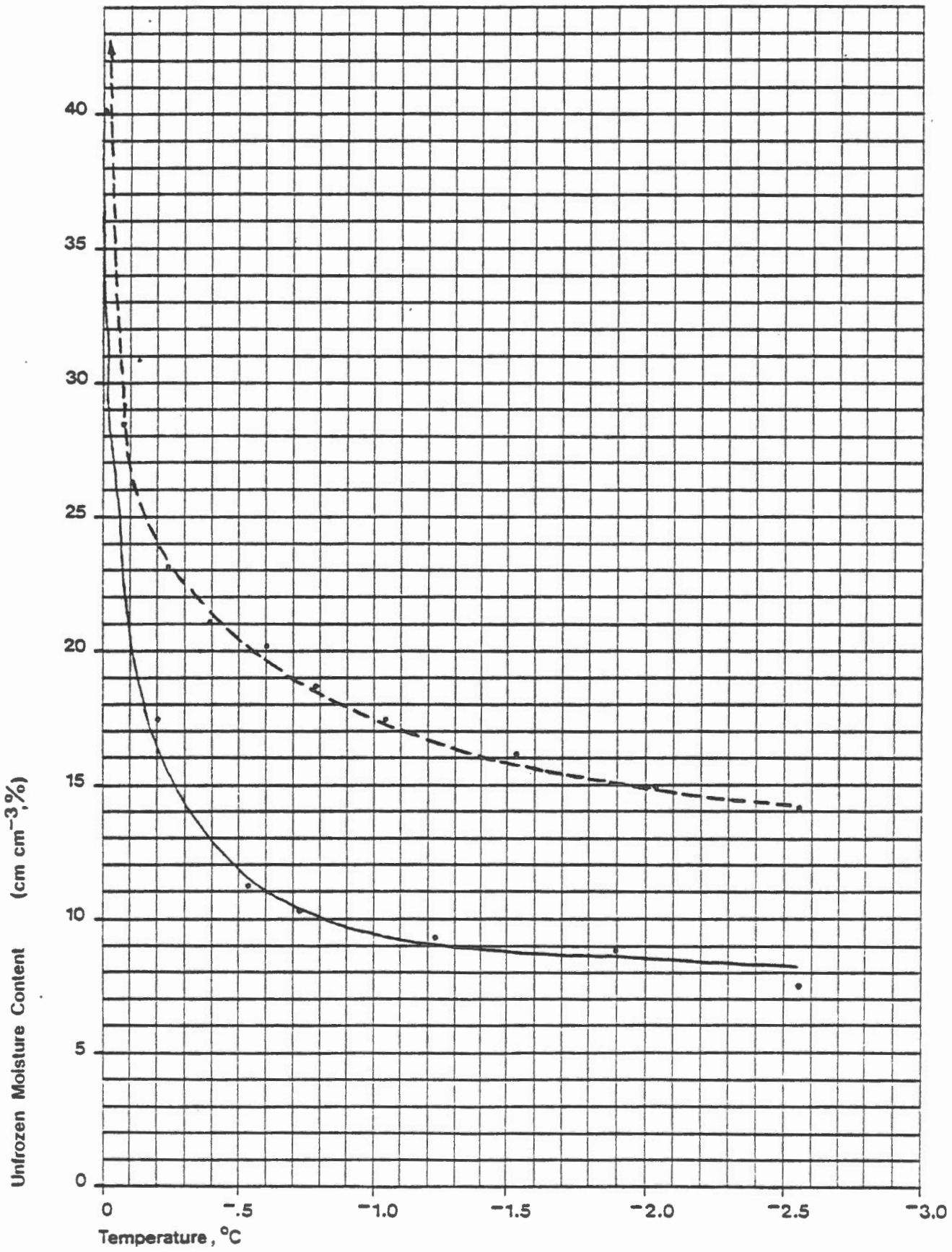

Figure 5.4a

Variation In Mass Transport Coefficient Of Castor Sandy Loam With Temperature

Experiment No. H1,H2

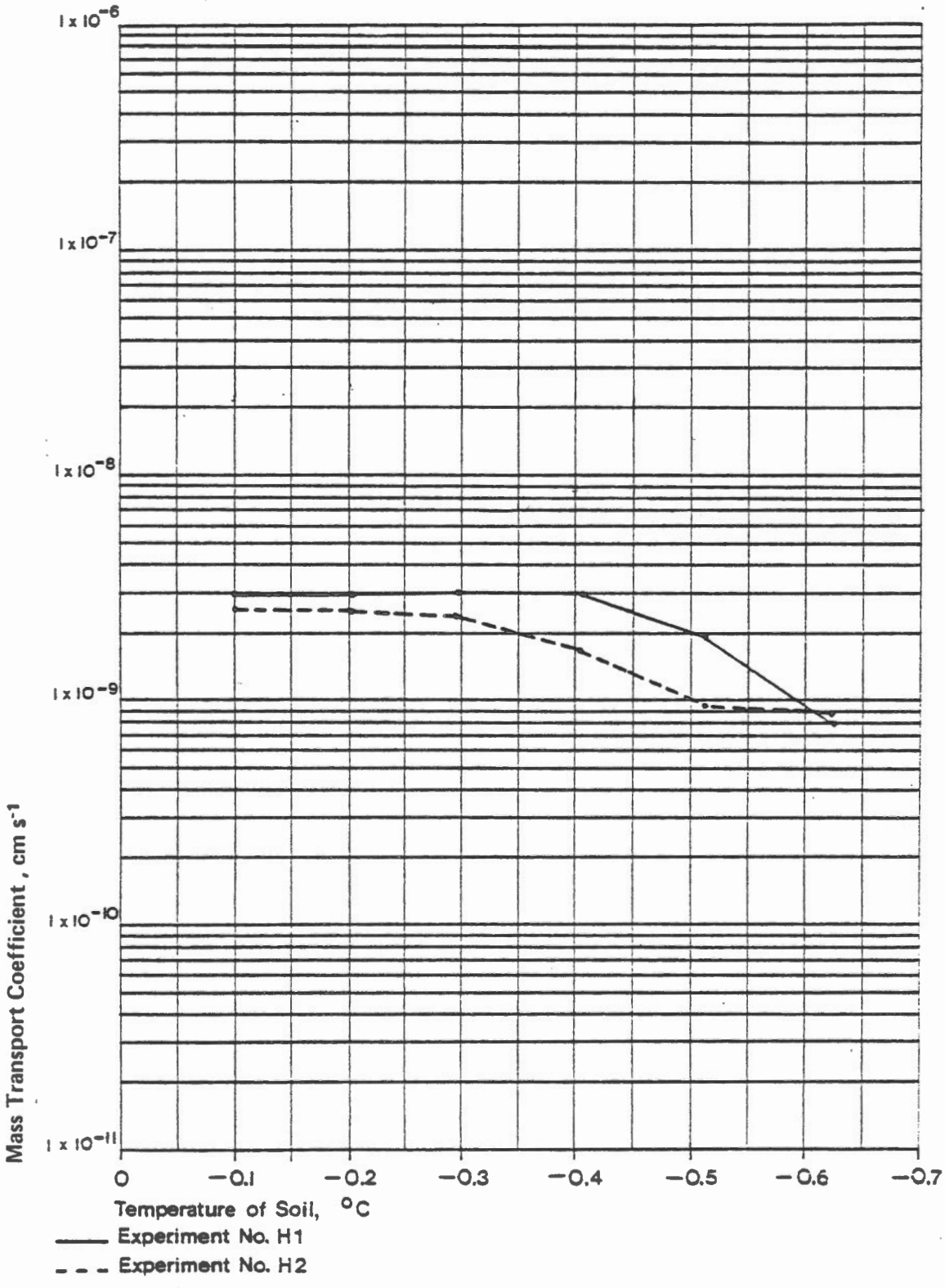

Figure 5.4b

Variation In Mass Transport Coefficient Of Allendale Silty Clay With Temperature

Experiment No. I1,I2

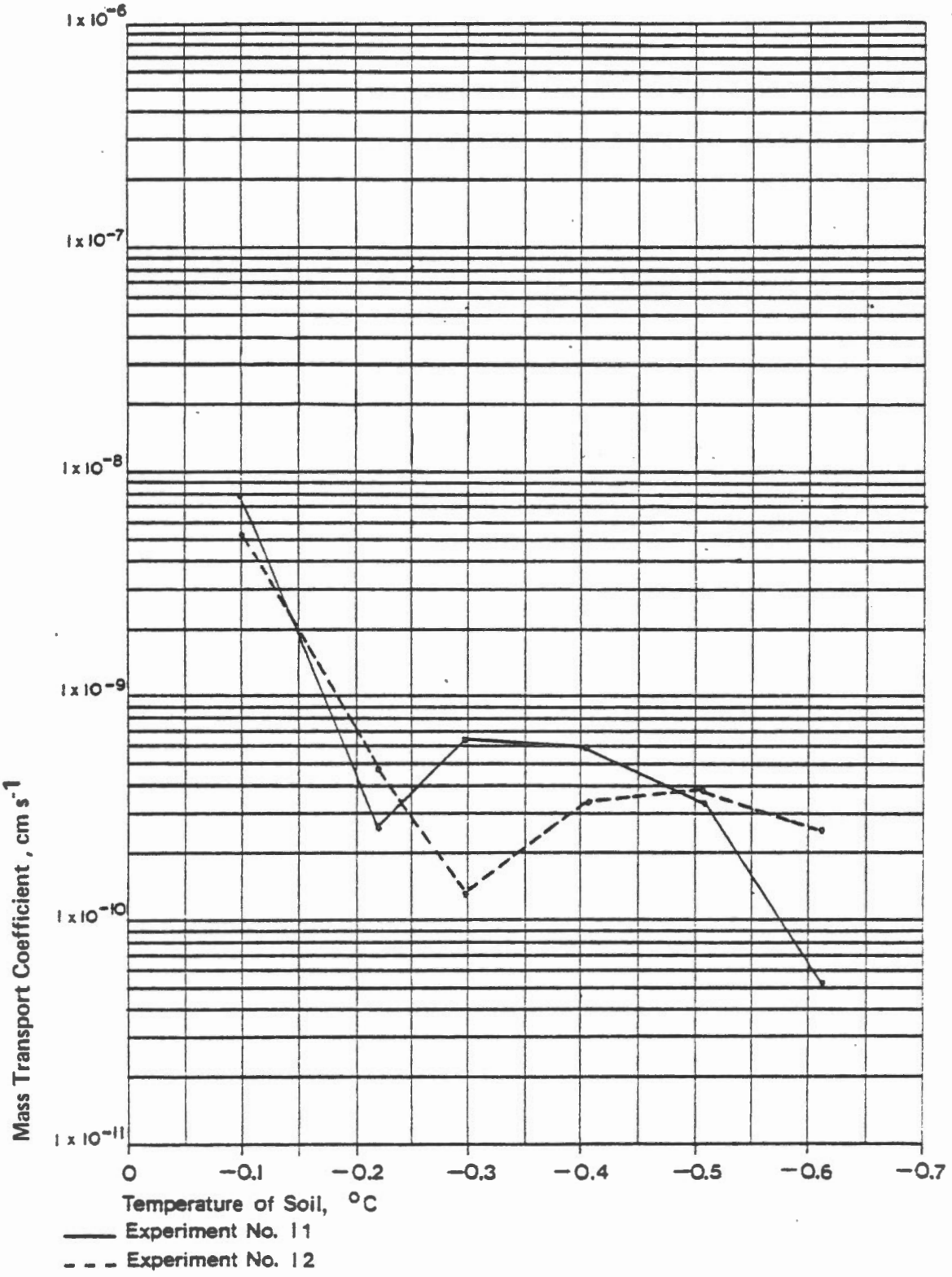

in Figure 5.4. The results were obtained using the same apparatus as in the study of regelation transport (Figure 4.1). The values plotted represent the transport coefficients which were obtained after steady-state heat and mass transfer conditions were established within the soil. The coefficient for the Castor soil shows a very weak dependence upon temperature although both the liquid flow and regelation transport are known to decrease rapidly with colder temperatures. This suggests that some consolidation of the sample occurred during the experiment, offsetting to some degree, the effect of warmer temperatures on its permeability.

5.5 Equalization of Potentials Between the Reservoirs and the Soil

In most of the experiments lactose solution was used in the end reservoirs, although attempts were made with supercooled water. There are two reasons for using lactose solution rather than pure water: (1) to prevent freezing in the reservoirs and (2) to equalize the chemical potential between the water in the reservoirs and the pore contents of the adjacent soil.

At any temperature below freezing, the chemical potential of the water and ice within the soil μ_p (T) is less than that of pure free water μ_w°(T) at the same temperature by an amount:

$$\mu_p (T) = \mu_w^\circ (T) - \frac{L \Delta T}{V_w T} \qquad (5.3)$$

Since the soil is subjected to a temperature gradient, μ_p (T) at the 'cold' end of the sample will be considerably lower than at the 'warm' end. Thus, the lactose concentration required to produce equilibrium will be greater in the 'cold' reservoir.

The chemical potential of the water at any solute concentration is given in equation 4.8. In theory, if the lactose concentration is adjusted precisely, the flow of moisture across the soil should be produced entirely by temperature induced osmotic gradients within the soil itself (i.e. there is no tendency for the sample to imbibe or expel water as a result of local osmotic gradients between the soil and the reservoirs).

The concentration required to equalize potentials can be more readily obtained from the freezing-point depression data for lactose (see Appendix D), rather than using equation 4.8. At any concentration, the freezing-point depression represents the temperature at which the water in

---

[5] For temperatures other than the values given in Appendix D, the lactose concentration was determined using lagrangian interpretation. (Hewlett Packard computer program in BASIC).

the solution is in exact chemical equilibrium with pure bulk ice at the same temperature. That is:

$$\mu_w^s(T) = \mu_i^\circ(T) \qquad (5.4)$$

where $\mu_w^s(T)$ = the chemical potential of the water in the solution

and $\mu_i^\circ(T)$ = the chemical potential of pure bulk ice.

Since, as noted earlier in Section 1:

$$\mu_p(T) = \mu_i^\circ(T), \qquad (5.5)$$

the chemical potential of the water in the solutuion should equal that of the pore contents of the adjacent soil.

A slight correction should be made for the fact that the data given in Appendix D is for anhydrous lactose (molecular weight = 340.3) whereas, the lactose that was used in the experiments was in the hydrated state (molecular weight = 360.3). The difference in molecular weight expressed as a fraction of the anhydrous solute is 0.05. Thus, the concentration of the hydrated solute required to produce a freezing-point depression is greater than the anhydrous concentration by an amount:

$$C_{hyd} = C_{anhyd} \times 0.05 \qquad (5.6)$$

where C = the concentration in g l^{-1}

Unfortunately, in most of the experiments this correction was not made and so a slight osmotic head probably exists between the reservoirs and the soil. This would result in a tendency for the pressure of the pore contents of the soil to rise slightly, counteracting the local osmotic head, by drawing in a small quantity of water at both ends of the soil sample. The net result would be a very small reduction in the rate of outflow at the 'cold' end of the sample and an increase in the rate of inflow at the 'warm' end.

5.6 Use of Polyethylene Glycol Instead of Lactose

One difficulty with the use of lactose solution in the end reservoirs is that the sugar molecules gradually enter the soil either by a process of molecular diffusion or by transport associated with the flow of water through the membranes. With the Castor soil, a thawed layer about 0.5 cm thick was observed at either end of the sample after 3 days. (0.25 cm with the Allendale). [6]

---

[6] The fact that the thawed layer was usually of equal thickness at either end of the soil sample suggests that lactose penetration is a diffusion process since it is largely independent of the direction of water movement through the system.

Figure 5.5

Beckmann's Freezing Point Depression Apparatus

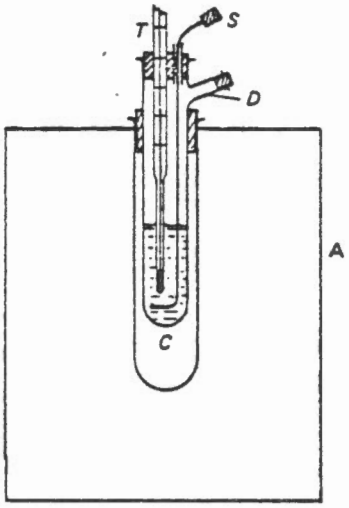

A Refrigerated Bath Circulator *

C Air Gap

D Nucleation Tube

S Stirring Rod

T Beckmann Thermometer

* temperature control accurate to ± 0.01°C

Levitt (1973)

Figure 5.6

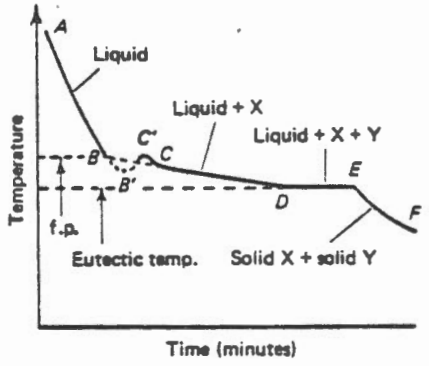

Typical cooling curve for a binary liquid mixture forming a eutectic.

Levitt (1973)

In principle, the membranes should be semipermeable allowing passage of the water molecules but restricting entry of the lactose. In practise, however, it is not possible to obtain membranes which are completely impermeable to non-ionic solutes with molecular weights less than about 10,000.

The presence of lactose within the soil comprises interpretation of the results to an unknown degree. Basically there are two possible solutions to the problem:

(1) Change the solute being used for a larger molecule; or
(2) Use a membrane with smaller pores.

Attempts were made to determine whether a very large molecule such as polyethene glycol 6,000 or 20,000 could be used as a viable substitute for lactose. One difficulty in using solutes with very large molecules is that, as the molecular weight increases, the maximum freezing-point depression that the solute is capable of producing, decreases. In other words, very large concentrations of solute are needed to produce even a small freezing-point depression. Moreover, tables of the equilibrium freezing temperatures of the solution as a function of solute concentration are not available. Values cannot be predicted from theory either since significant deviations from ideality would occur at the large concentraions being investigated and osmotic coefficients for the solute are unknown. To obtain this data, it is necessary to examine cooling curves for various concentrations of solute.

Several attempts were made to obtain cooling curves for both polyethylene glycol 6,000 and 20,000. This was done in the following manner.

A quantity of solute was dissolved in water. The solution was then placed in a well insulated container and allowed to cool very slowly (Figure 5.5). Initially the temperature of the solution should decrease along the curve AB until the freezing temperature is reached (Figure 5.6). As the water begins to crystallize, the rate of cooling is reduced somewhat by the release of latent heat during phase transition. The temperature should then fall along the curve BCD. The freezing temperature of the solution is represented by the break in the slope of the curve (f.p.).

With the polyethylene glycol although the solution was cooled extremely slowly, repeated attempts failed to produce any discernible break in the slope of the cooling curve. The most likely explanation for this result is that, at large concentrations, the solute becomes so completely polymerized that the water is unable to arrange itself in its normal solid configuration. Because of these difficulties, as well as the other disadvantages of using polyethylene glycol, the investigation was subsequently dropped.

5.7 Use of Cellulose Acetate Membranes

With the second approach to the problem, that is, changing the membranes, a somewhat greater degree of success was obtained. Originally a viskene membrane (regenerated cellulose) had been used in the early

Table 5.2

Physical Properties of the Cellulose Acetate Membranes Used in the Experiment

Classification:	SS AC-61
Pore Diameter*	<0.005 µm
Thickness*	80 µm
Hydraulic Conductivity*	2.10×10^{-8} cm s^{-1}
Freezing Temperature	-6°C
Upper Pore Size Limit	0.008 µm

* Data obtained from Schleicher and Schuell Catalogue

experiments. This is the same type of material that is used in dialyzing the blood of kidney patients. The membrane comes in sheets, in the dry state, and has on average pore size about 0.0024 μm. Most membranes do not have a uniforma pore size, the variation in pore diameters approximating a normal distribution. With the viskene membrane, although the average pore size is very small, the pore size distribution is probably fairly large, varying between 0.0002 μm and 0.02μm or more and it is the larger pores at the upper end of the distribution through which the lactose is moving (Dr S. Sourirajan, 1982). Sourirajan recommended the use of a cellulose acetate membrane (Schleicher and Schuell AC-61) instead of the viskene membrane since the pore structure is much more uniform, although the average pore diameter (0.005μm) is somewhat larger.[7]

The physical properties of the cellulose acetate membranes are listed in Table 5.2. Hydraulic conductivity values were calculated from data on flow rates listed in the Schleicher and Schuell catalogue. Note that the freezing temperature of the membrane (-6°C), which was roughly determined from laboratory experiments, indicates the the upper pore size limit is about 0.008μm (Values determined using equation 1.6).

With this type of membrane, lactose penetration has been reduced to about one-half the value that was previously observed with the viskene membrane. There is also a possibility that lactose penetration may be further reduced by heat treating the membrane, which causes shrinkage of the pores. However, further research is required on this point since, although a reduction in pore size inhibits the entry of lactose, it also reduces the permeability of the membrane to water flow as well. It is important that the permeability of the membrane exceeds that of the soil, otherwise it may seriously impede the flow of moisture between the reservoir and the soil.

5.8 Temperature Control Within the Sample Container

Initially some difficulty was experienced with the temperature control for the system. In many of the early experiments, there was a tendency for the temperature of the soil to be too warm (see example Figure 5.7). If this occurs, then the chemical potential of the water at the 'warm' end of the sample would exceed that of the adjacent soil, resulting in a local osmotic gradient. This would tend to counteract the temperature induced driving forces within the soil and may even be sufficient to produce outflow at the 'warm' end of the sample rather than inflow. It was suspected that this might be the cause of the outflow which was observed at the 'warm' end of the sample in many of the experiments.

At the 'cold' end of the sample, the converse situation would occur since the chemical potential of the water in the reservoir exceeds that of the soil.

---

[7] This is the smallest pore size that is commerically available.

Figure 5.7

Typical Temperature Profile In Soil Sample Before Modifications Were Made To Reduce Heat Convection Around The Cell

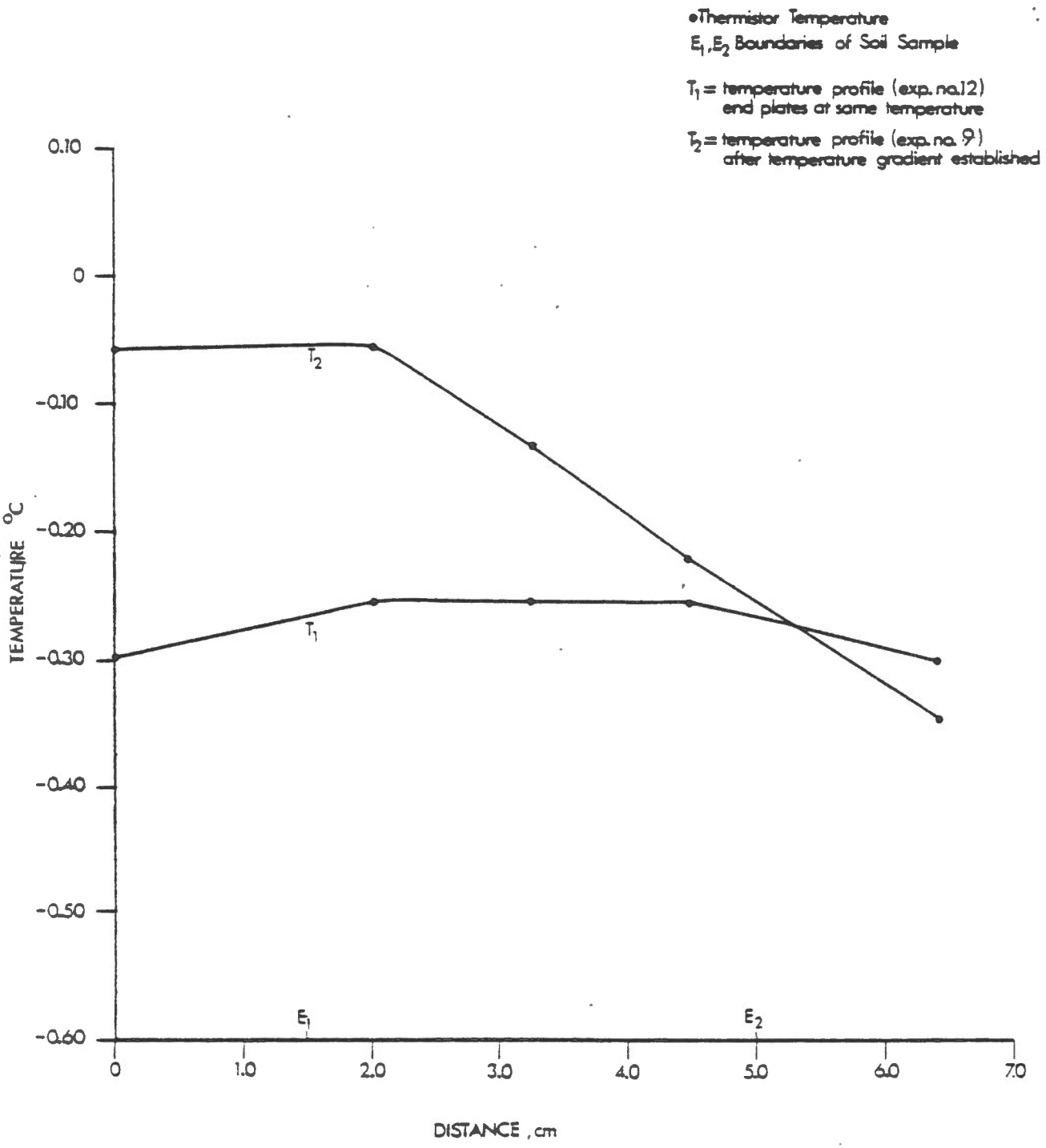

Figure 5.8

Typical Temperature Profile In Soil Sample After Modifications Were Made To Minimize Heat Convection Around The Cell

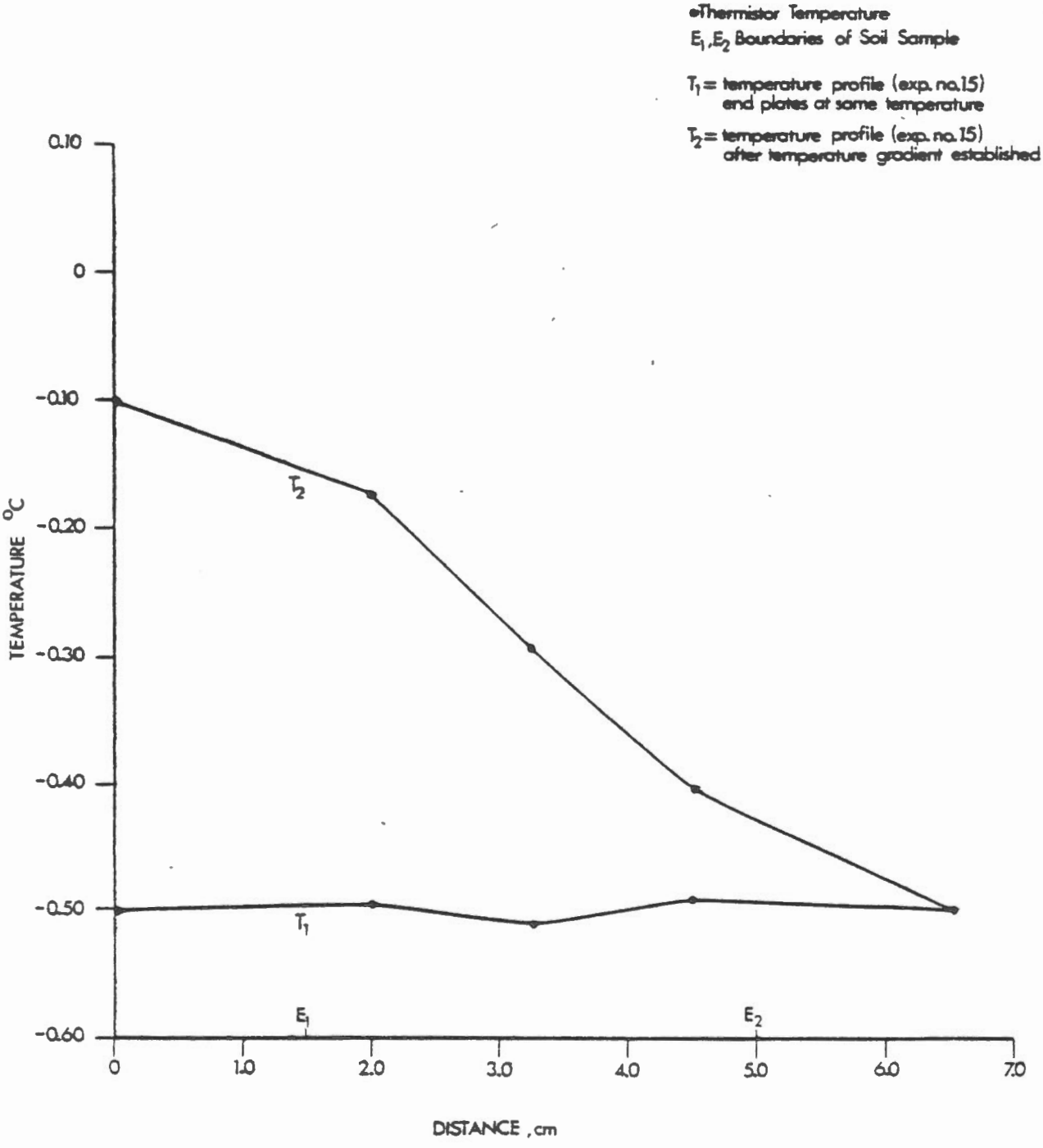

To eliminate the possibility that there might be some error in the measurement of temperatures within the sample, the thermistors were sent to the National Research Council of Canada and recalibrated against a platinum resistance thermometer. Calibration reports are shown in Appendix B. Once this had been completed, the temperature control for the system was examined for potential heat sources. Eventually it was determined that the excess heat was being produced by convection up around the walls of the sample container, through gaps in the insulating jacket, from the brass heat sinks attached to the 'hot' side of the peltier modules (see Figure 5.1). The problem has been eliminated by taking the following precautions:

(1) The temperature of the circulating fluid in the brass heat sinks has been lowered to 20°C, the minimum required for the thermo-electric cooling unit to function properly. If the temperature difference between the 'hot' and 'cold' junctions of the peltier modules is less than 20°C, the Seebeck effects begin to predominate and accurate temperature control can no longer be maintained.

(2) To prevent warm air from circulating up around the walls of the cell, a foam rubber pad 1.0 cm thick has been installed between the brass heat sinks and the aluminum end plates. The cell is also wrapped in a jacket of foam rubber insulation instead of fibreglass which had previously been used. Although the heat conducting properties are about the same for the two materials, overall, foam rubber has better insulating properties since convective heat transport is considerably lower.

(3) In addition, two small fans have been installed, one immediately above and the other below the cell, the direction of the air flow being away from the end plates. This tends to draw cooler air in from the incubator towards the cell, forcing the warmer air around the brass heat sinks away from the cell.

Examples of the temperature profiles that were obtained after these changes had been made are shown in Figure 5.8. As can be seen from the diagram, the temperature profile within the system is very nearly linear indicating that radial heat exchange is insignificant in comparison with axial heat transfer. The abrupt changes in the slope of the line T_2 indicate changes in the rate of heat transfer and are a result of the different thermal properties of the aluminium end plates and the frozen soil sample.

5.9. Mass Transfer In The Frozen Soil

The following generalizations can be made regarding mass transfer in the frozen soil.

In all of the tests, a large influx of water was initially observed at the 'warm' end of the soil sample, the rate of flow declining during the approach to a linear temperature profile. This was usually accompanied by a small amount of outflow at the 'cold' end of the sample, although occasionally the flow direction reversed and inflow was observed. The establishment of a linear temperature gradient was followed by

expulsion of water from the 'warm' end of the sample, and in almost all cases, the magnitude of the outflow exceeded that at the 'cold' end. The rate of outflow tended to decrease over two or three days but the experiment could not be continued to determine the ultimate situation.

An example of the initial influx of water at the 'warm' end of the sample is seen in experiment No. 15 (Figure 5.10a). The explanation for the influx is as follows.

Initially,the sample was brought to a uniform temperature of - 0.5°C. Following this, the temperature at one end of the system was raised to - 0.1°C and the reservoir was flushed with the appropriate concentration of lactose solution (see curves t_1 and t_2 Figure 5.9). Since the temperature of the soil immediately after the change is somewhat lower than the temperature of the reservoir, its chemical potential will also be lower. This results in the flow of water into the sample from the 'warm' reservoir which raises the pressure of the pore contents.

The Clapeyron equation indicates that at a temperature of - 0.5°C the equilibrium value of $P_i - P_w = 561$ KPa. The increase in the pressure of the sample is achieved by the enrichment of existing pore ice as well as the formation of ice lenses. As the rise in pressure is felt at the other end of the sample, its chemical potential now exceeds that of the 'cold' reservoir, resulting in outflow. (Figure 5.10a).

It was anticipated that once a linear temperature profile was established, a steady flux of water would occur in the direction of decreasing temperatures, the rate of flow being governed by the thermal driving force as well as the overall permeability of the sample. Therefore, it came as somewhat of a surprise that water was expelled from both ends of the soil sample, even after the temperature profile became linear. The following explanation is proposed.

As the soil warms up its chemical potential increases and the equilibrium pressures of the pore contents decrease. Since the pressure of the ice and water now equals its equilibrium value as a result of the initial influx of water, moisture must flow out of the soil, the pressure falling, until the equilibrium condition is attained. The lag between the temperature change within the soil sample (which dictates the equilibrium pressure of pore contents) and the actual pressure of the pore contents (which governs the direction of flow) is probably governed by the rheological properties of the pore ice as well as microscopic heat transfers within the soil pores. Outflow at the 'warm' end of the sample exceeds that at the 'cold' end for two reasons: (i) the discrepancy between the actual pressure of the pore contents and the equilibrium pressure is greatest at the 'warm' end of the sample and (ii) the permeability of soil increases towards the 'warm' end of the sample.

Evidence for the overall decline in pressure of the sample can be seen in Figures 5.10a-c. During the initial inflow period (cumulative time 185-425 minutes), the pressure at the 'cold' side of the sample was very high, varying between 60-130 KPa.[8] On the second day of the experiment

---

[8] The cumulative time denotes the total time in minutes since temperature control was first established within the system.

Therefore it is quite possible that the compressive strength of the soil on the 'warm' side of the sample may be so low that it is unable to sustain stresses of more than a few KPa.

(2) A second possibility is that the stresses originating on the 'cold' side of the system are transmitted entirely in a radial direction within the soil sample. This, however, seems unlikely since the temperature gradient is along the axis of the cell. That is, one would expect the heaving pressure to be maximum in this direction, since heaving is governed by the direction and rate of heat flow within the soil.

(3) It has also been suggested that the heaving stress is dictated entirely by thermodynamic conditions within the soil and can only be transmitted in the direction of colder temperatures. Once the system reaches a steady-state of heat and mass transfer, the pore contents of the soil are in a state of dynamic equilibrium with the surroundings. Since the driving force for moisture movement is in the direction of colder temperatures, any tendency for the pressure to rise towards the 'warm' end of the soil sample disturbs this equilibrium state. This results in a decline in the rate of moisture flow and a corresponding rise in the pressure on the 'cold' side of the sample until the dynamic equilibrium condition is re-established.

5.11 Results Obtained When the 'Warm' Side of the Sample was Above Freezing.

One experiment was run, in which the 'warm' end of the soil sample was maintained at +0.10° C. (See experiment no. 21, Figures 5.17 and 5.18.) In this instance, pure water rather than lactose solution was used in the 'warm' reservoir. Although the results appear similar to those obtained when the sample was completely frozen, there are a number of important differences.

First of all, once a linear temperature profile was attained, outflow from the 'cold' end of the sample remained remarkably stable, increasing almost linearly throughout the experiment. Secondly, although a small amount of outflow was observed at the 'warm' end of the sample on the second day of the test, the flow direction then reversed and an influx occurred for the remainder of the experiment. Flow rates at both ends of the soil sample appear to decline towards the end of the experiment. Thirdly, the cyclic pressure variation on the 'cold' side of the sample was much less pronounced than in the case where the sample was completely frozen, in most instances varying by less than 2 or 3 KPa. Note also, the sudden fall in the pressure on the 'cold' side, from about 18 KPa, during the first three days of the experiment, to atmospheric pressure for the remainder of the test. The fall in pressure coincides roughly with the flow reversal at the 'warm' end of the sample.

The fall in pressure on the 'cold' side of the sample is probably a result of internal yielding within the soil, although why the pressure does not show the pronounced cyclic variation that occurs when the sample is completely frozen, is not yet understood. The explusion of water from

the 'warm' end of the sample after a linear temperature gradient was established (cumulative time 1260 - 1620 minutes) probably represents a delayed reaction at the 'warm' end of the sample to the formation of segregation ice during the initial influx of water 30 - 330 minutes.

5.12 'Cold' End Reservoir Pressure

In many of the experiments, the change in the 'cold' end reservoir pressure was measured during the long time interval (approximately 18 hours) between flow reading sessions. Outflow from the 'cold' end of the sample was arrested by closing off the valves connected to the flushing ports on either side of the reservoir.

It was expected that reservoir pressure would rise over an extended period of time and stabilize at a value equal to the difference in the thermally induced osmotic pressure between the 'warm' and 'cold' ends of the soil sample. The rise in reservoir pressure (if it occurs) is not a direct measure of the heaving pressure since this represents the change in the total stress within the soil. However, it should provide a indication, in mechanical terms, of the thermally induced driving head and thus the overall gradient in the neutral stress exerted by the pore contents of the soil.[12]

It came as somewhat of a surprise to find that, in all of the tests, the reservoir pressure did not rise by more than 5 KPa above atmospheric pressure, even though substantial amounts of outflow were recorded, both before the reservoir was closed off and after it was reopened. For example, in experiment no. 20, the total rise in reservoir pressure during the time interval 3250 - 4305 minutes was 3.66 KPa. During this period, 1.41 cm of outflow were observed from the 'warm' end of the sample. Note the steady rate of outflow from the 'cold' end of the soil which occurred before the reservoir was closed off (2890 - 3250 minutes) and resumed after the valves were reopened (4305 - 4600 minutes). A possible explanation for these observations is outlined below.

After the reservoir valves are closed, the soil continues to expel water from the 'cold' end of the sample and the reservoir pressure begins to rise. This is accompanied by a corresponding rise in the pressure of unfrozen pore water within the soil. Since the value of $P_i - P_w$ is fixed, P_i adjusts accordingly. As the rise in the pressure of the soil is felt at the other end of the system, this results in yielding of the soil and outflow of water from the 'warm' end of the sample.

The question has also been raised whether the reservoir pressure rises initially to a somewhat higher value than the value indicated above and then gradually falls back to atmospheric pressure as a result of internal adjustments within the soil. To determine whether this does occur, in future tests, the reservoir pressure will be monitored continuously after the valves have been closed.

---

[12] The heaving pressure represents the reaction of the soil matrix (i.e. changes in the effective stress) to changes in the neutral stress exerted by the pore contents.

Figure 5.9

Temperature Profile Of The Soil Sample During The Approach To Steady State Heat Transfer Conditions (Experiment No. 15)

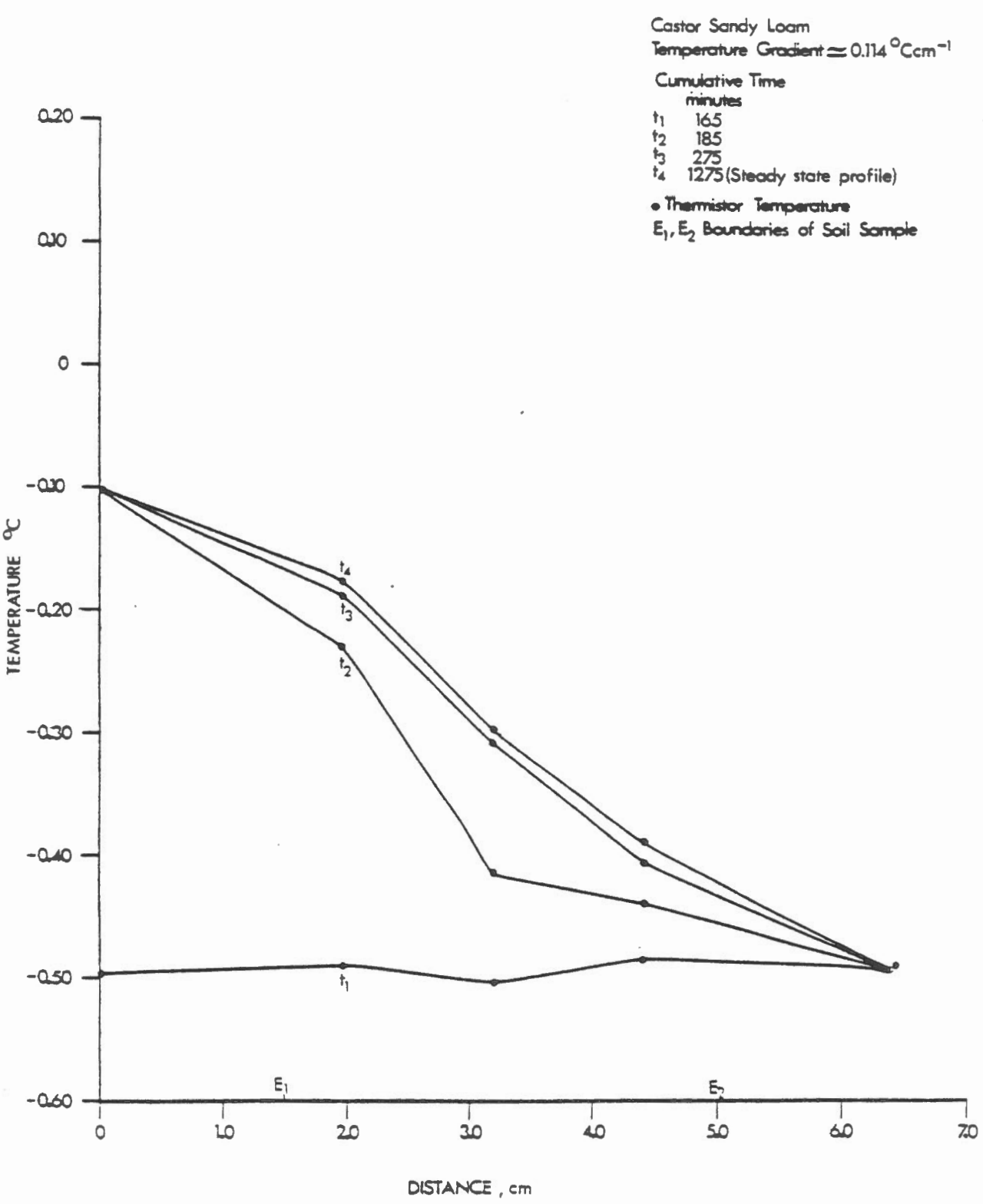

Plot of Pressure and Flow Vs. Cumulative Time During Temperature Induced Moisture Migration

Figure: 5.10a

Experiment No.: 16
Sample: Castor Sandy Loam
Mean Temperature Of Soil: -0.30°C
Temperature Gradient: 0.114°Ccm^{-1}
Atmospheric Pressure: 101.12KPa
Membrane: Cellulose Acetate (AC-61)

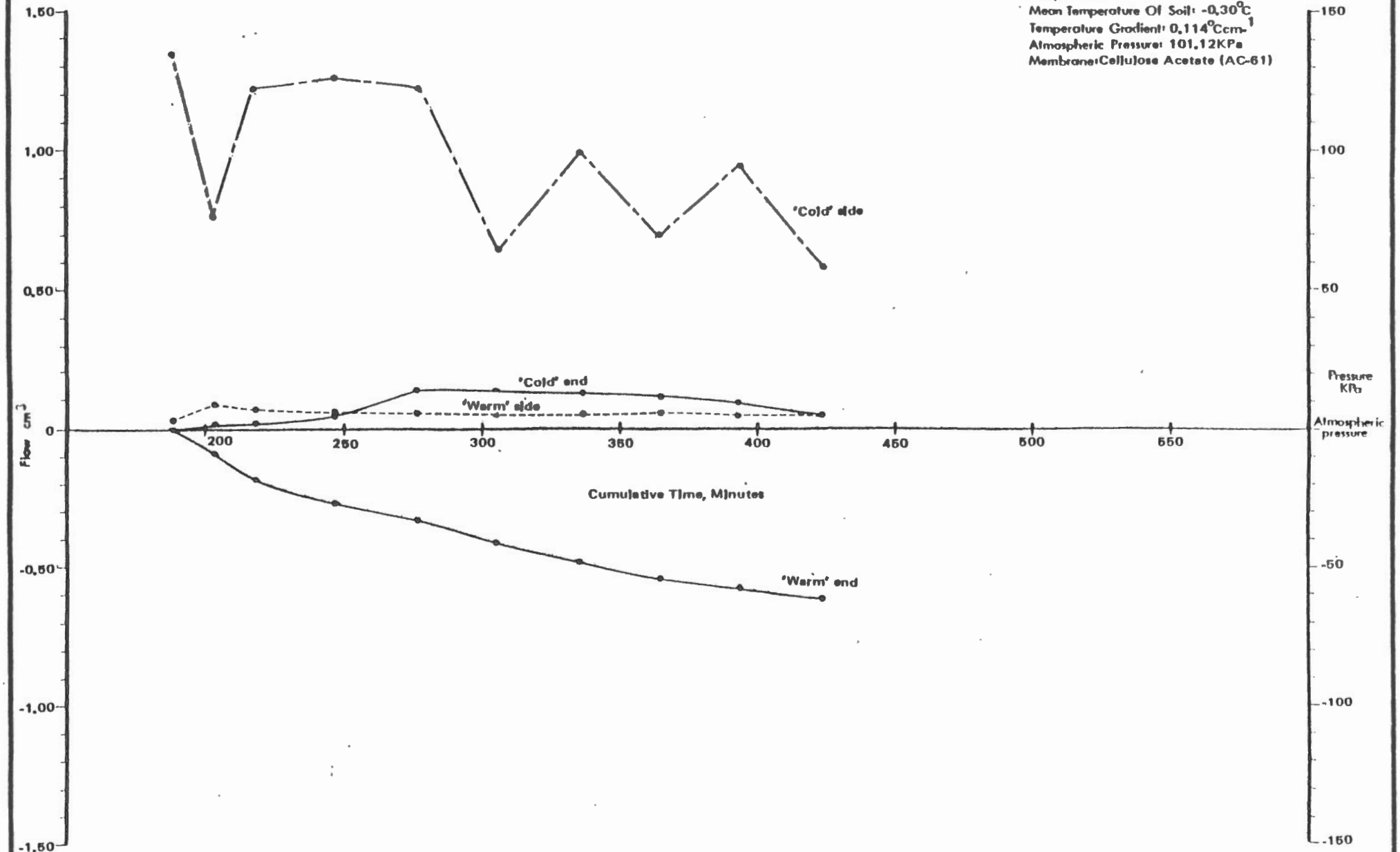

Cumulative Flow (Negative values indicate inflow, i.e. Moisture flow from the reservoir into the soil. Positive values indicate outflow).

Pressure (Total stress) relative to atmospheric pressure. (Negative values indicate pressures that are less than atmospheric).

	'Warm' Reservoir	'Cold' Reservoir
Temperature °C	-0.10	-0.50
Lactose Concentration gl^{-1}	17.95	83.20

Plot of Pressure and Flow Vs. Cumulative Time During Temperature Induced Moisture Migration

Figure: 5.10b

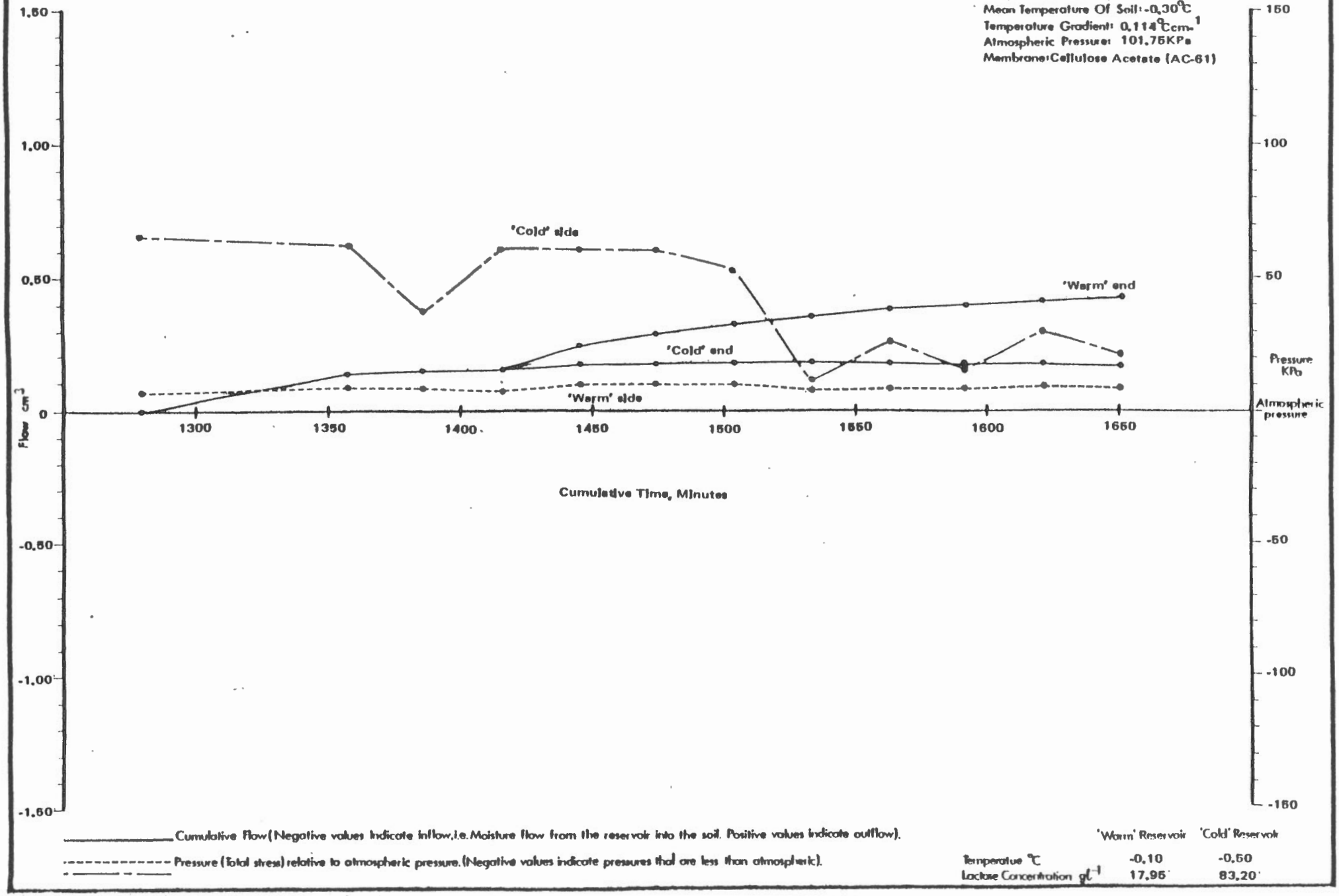

Plot of Pressure and Flow Vs. Cumulative Time During Temperature Induced Moisture Migration

Figure: 5.10e

Experiment No.: 15
Sample: Castor Sandy Loam
Mean Temperature Of Soil: -0.30 C
Temperature Gradient: 0.114 Ccm-1
Atmospheric Pressure: 101.76 KPa
Membrane: Cellulose Acetate (AC - 61)
Comments: 'Warm' End Flow Negligible

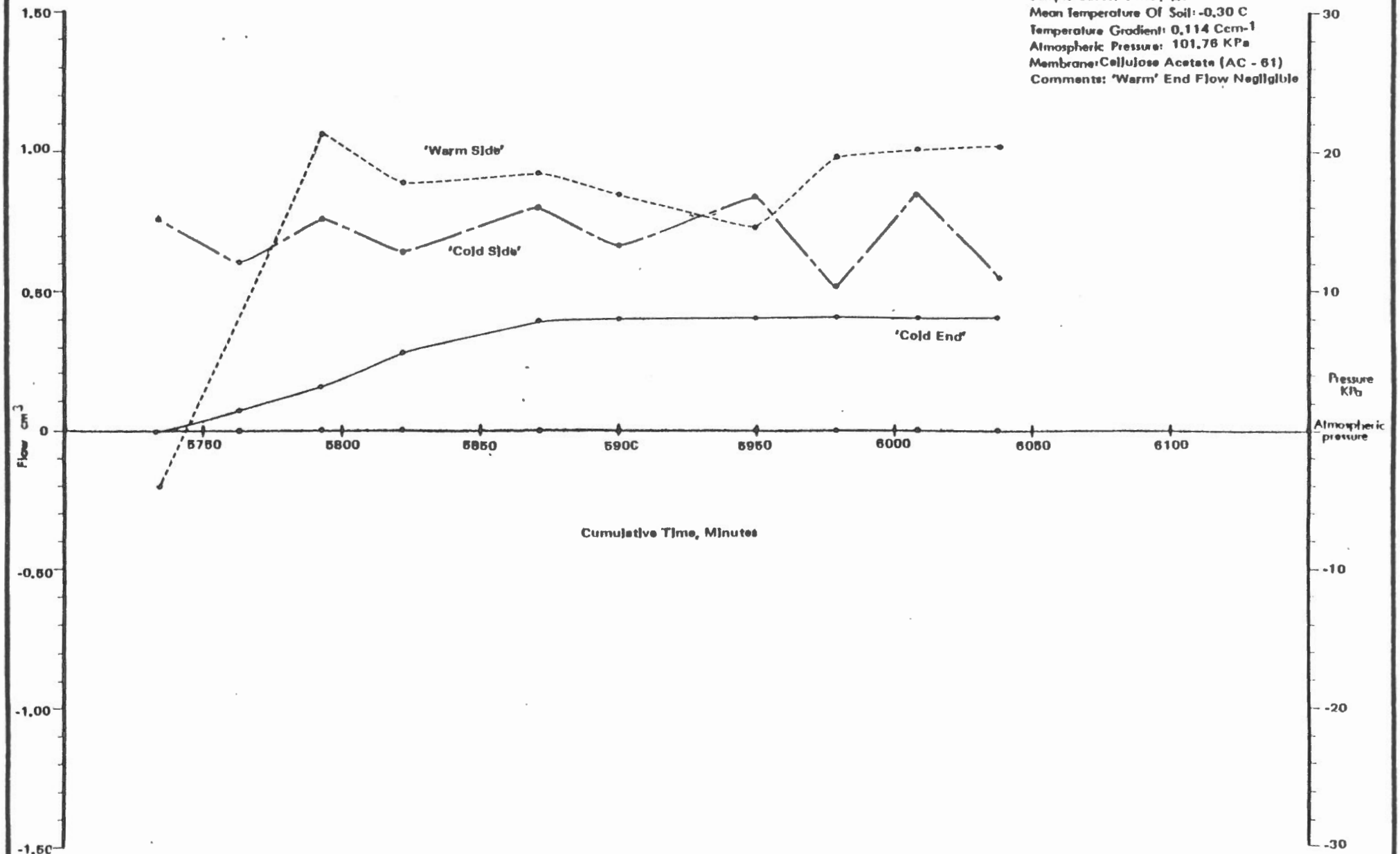

Cumulative Flow (Negative values indicate inflow, i.e. Moisture flow from the reservoir into the soil. Positive values indicate outflow).

Pressure (Total stress) relative to atmospheric pressure. (Negative values indicate pressures that are less than atmospheric).

	'Warm' Reservoir	'Cold' Reservoir
Temperature °C	-0.10	-0.50
Lactose Concentration gl^{-1}	17.95	83.50

Figure 5.11

Temperature Profile Of The Soil Sample During The Approach To Steady State Heat Transfer Conditions (Experiment No. 16)

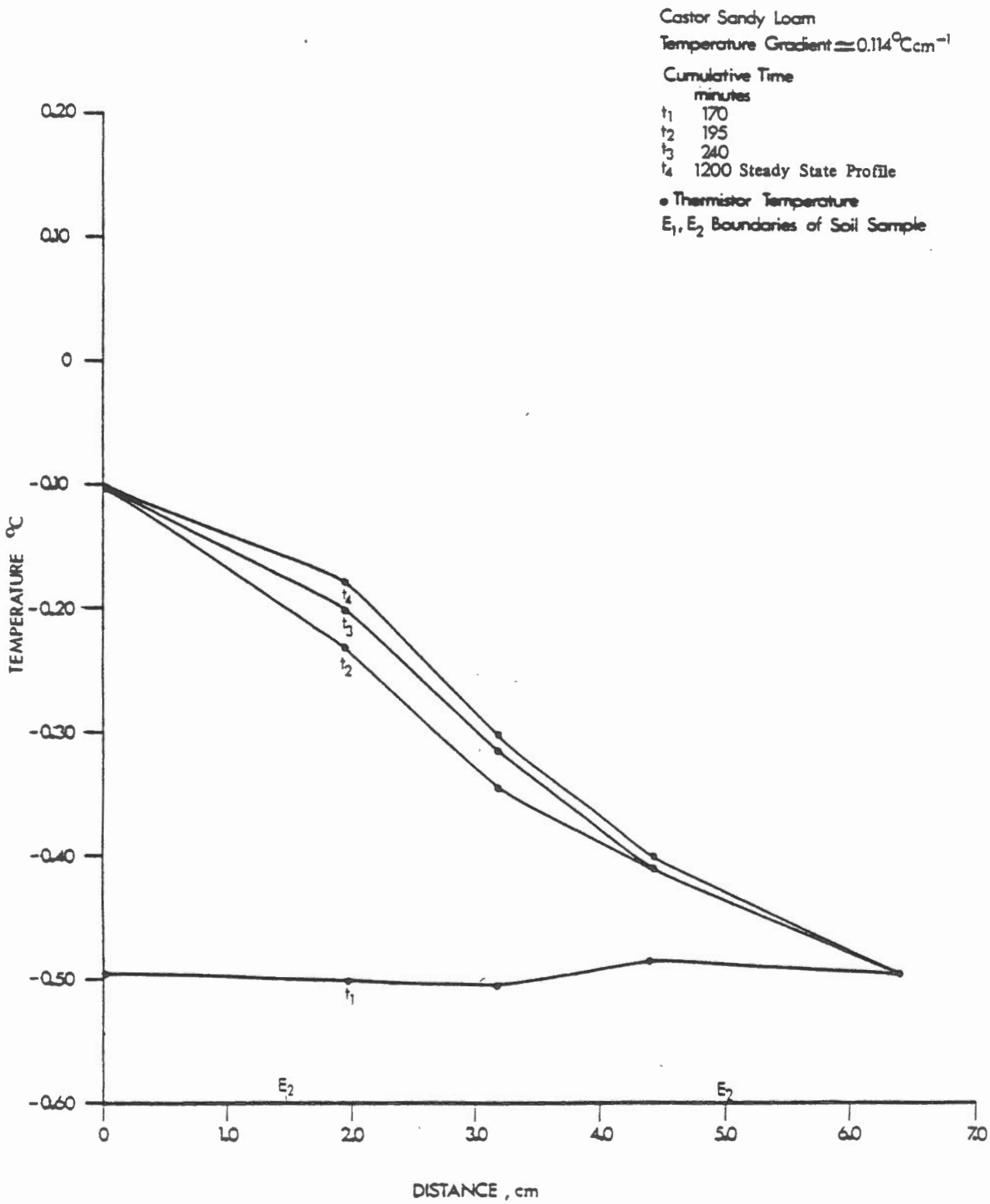

Plot of Pressure and Flow Vs. Cumulative Time During Temperature Induced Moisture Migration

Figure: 5.12a

Experiment No.: 16
Sample: Castor Sandy Loam
Mean Temperature Of Soil: -0.30 C
Temperature Gradient: 0.114 Ccm-1
Atmospheric Pressure: 102.39 KPa
Membrane: Cellulose Acetate (AC-61)
Comments: Pressure of the 'warm' side of the sample remained within ± 0.40 KPa of atmospheric pressure.

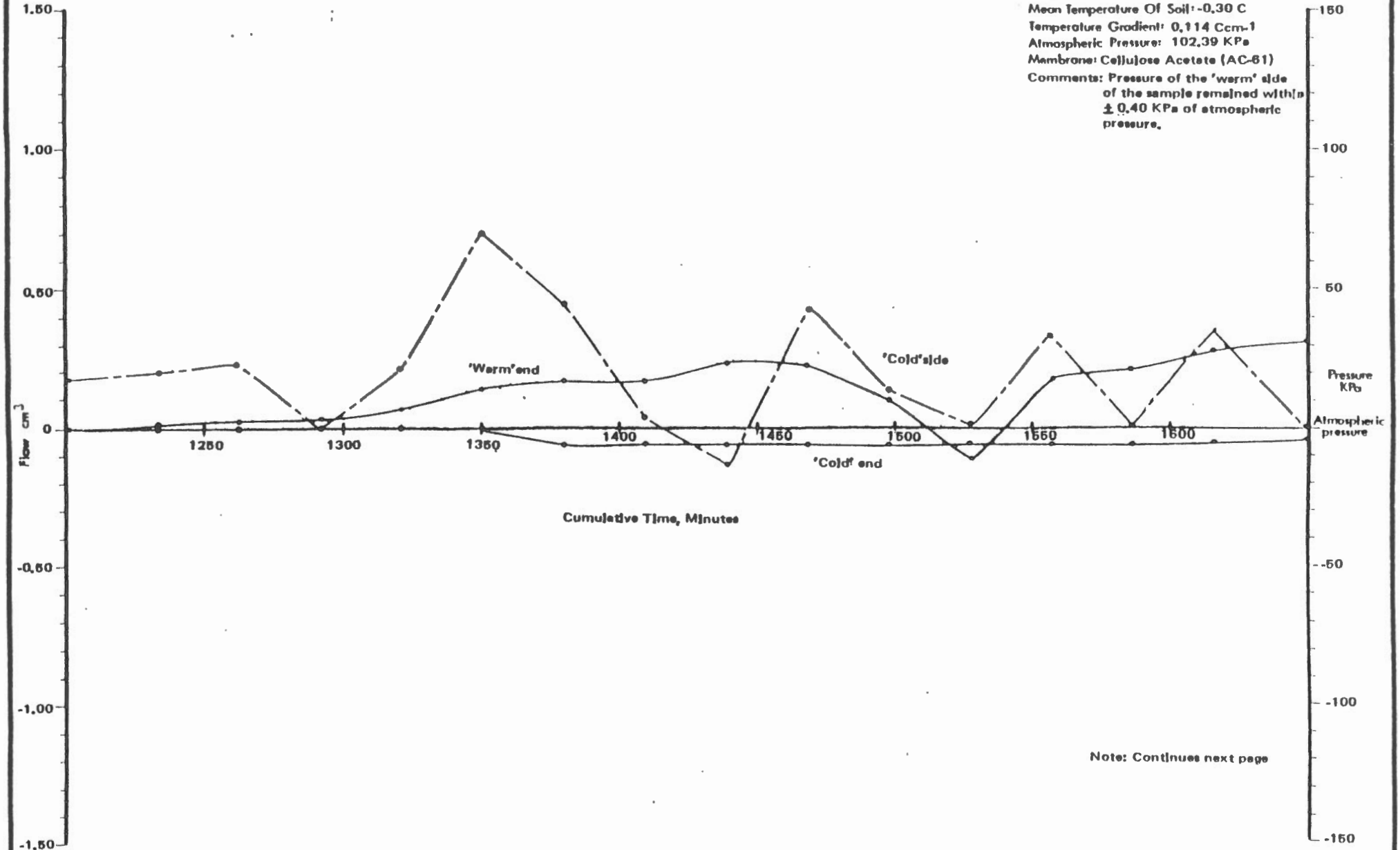

Note: Continues next page

Cumulative Flow (Negative values indicate inflow, i.e. Moisture flow from the reservoir into the soil. Positive values indicate outflow).

Pressure (Total stress) relative to atmospheric pressure. (Negative values indicate pressures that are less than atmospheric).

	'Warm' Reservoir	'Cold' Reservoir
Temperature °C	-0.10	-0.60
Lactose Concentration gl^{-1}	17.95	83.50

Plot of Pressure and Flow Vs. Cumulative Time During Temperature Induced Moisture Migration

Figure: 5.12b

Experiment No.: 16
Sample: Castor Sandy Loam
Mean Temperature Of Soil: -0.30°C
Temperature Gradient: 0.114°Ccm^{-1}
Atmospheric Pressure: 102.39KPa
Membrane: Cellulose Acetate (AC-61)
Comments: Pressure of the 'warm' side of the sample remained constant to within ± 1.0 KPa of atmospheric pressure.

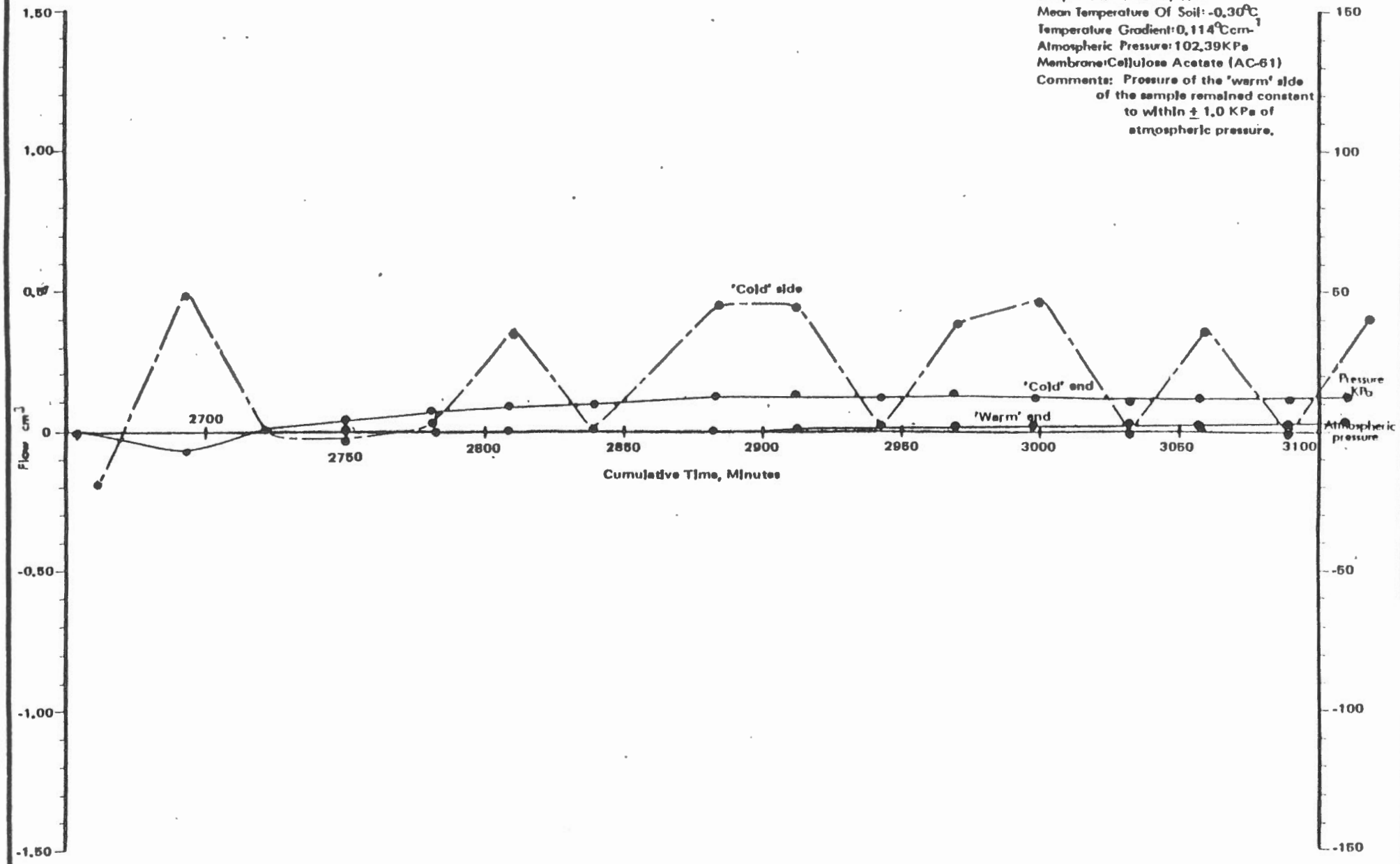

Cumulative Flow (Negative values indicate inflow, i.e. Moisture flow from the reservoir into the soil. Positive values indicate outflow).

Pressure (Total stress) relative to atmospheric pressure. (Negative values indicate pressures that are less than atmospheric).

	'Warm' Reservoir	'Cold' Reservoir
Temperature °C	-0.10	-0.50
Lactose Concentration gl^{-1}	17.95	83.50

Plot of Pressure and Flow Vs. Cumulative Time During Temperature Induced Moisture Migration

Figure: Figure 5.12c

Experiment No.: 16
Sample: Castor Sandy Loam
Mean Temperature Of Soil: -0.30°C
Temperature Gradient: 0.114°Ccm^{-1}
Atmospheric Pressure: 102.19KPa
Membrane: Cellulose Acetate (AC-61)
Comments: Negligible flow recorded at the 'warm' end of the sample Pressure at the 'warm' side of the sample remained constant within ± 0.90KPa of atmospheric pressure.

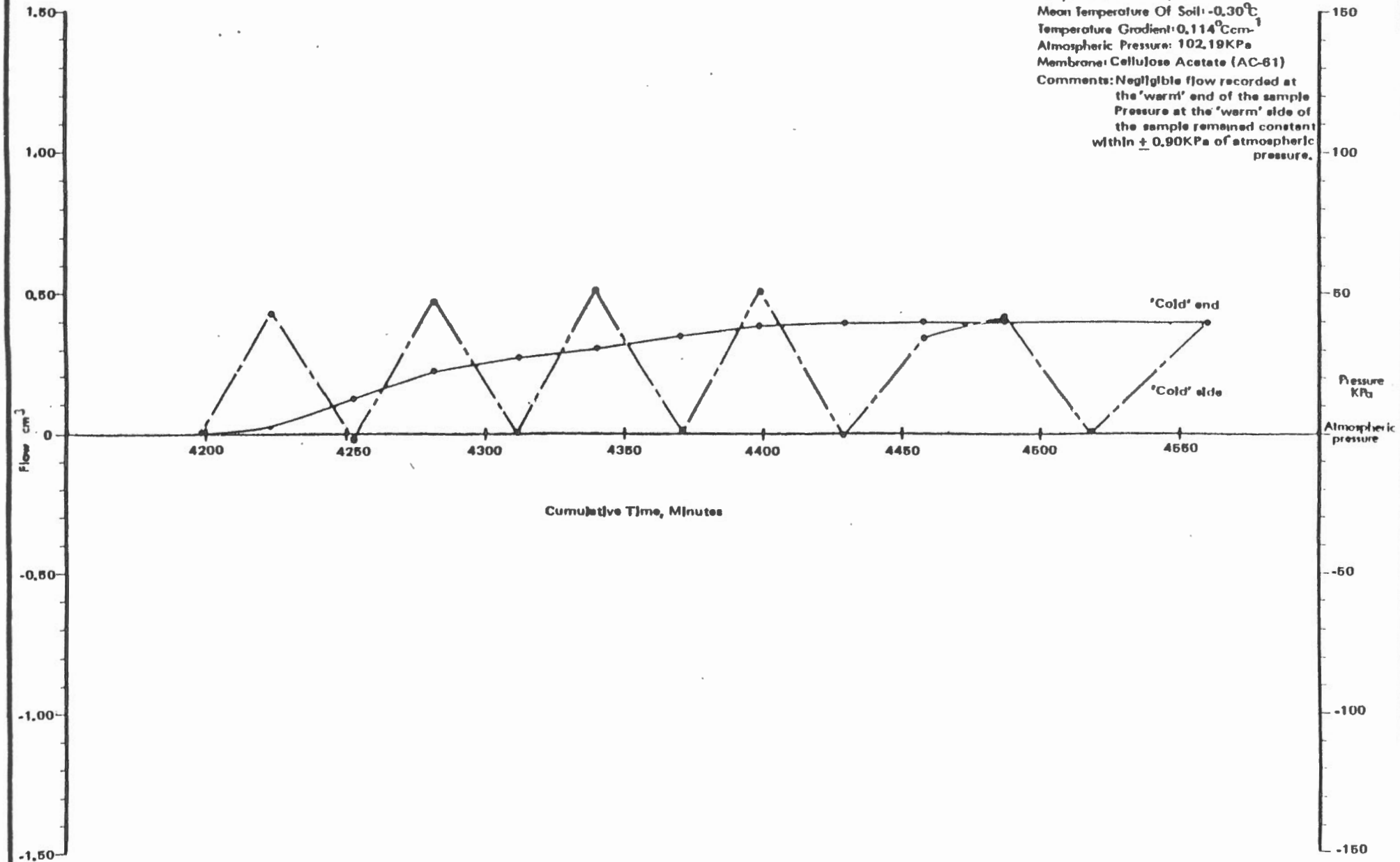

Cumulative Flow (Negative values indicate inflow, i.e. Moisture flow from the reservoir into the soil. Positive values indicate outflow).

Pressure (Total stress) relative to atmospheric pressure. (Negative values indicate pressures that are less than atmospheric).

	'Warm' Reservoir	'Cold' Reservoir
Temperature °C	-0.10	-0.50
Lactose Concentration gl^{-1}	17.95	83.50

Plot of Pressure and Flow Vs. Cumulative Time During Temperature Induced Moisture Migration

Figure: 5.12d

Experiment No.: 16
Sample: Castor Sandy Loam
Mean Temperature Of Soil: -0.30 C
Temperature Gradient: 0.114 Ccm^{-1}
Atmospheric Pressure: 100.49KPa
Membrane: Cellulose Acetate (AC-61)
Comments: Pressure at the 'warm' side of the sample remained constant to within + 0.50KPa of atmospheric pressure.

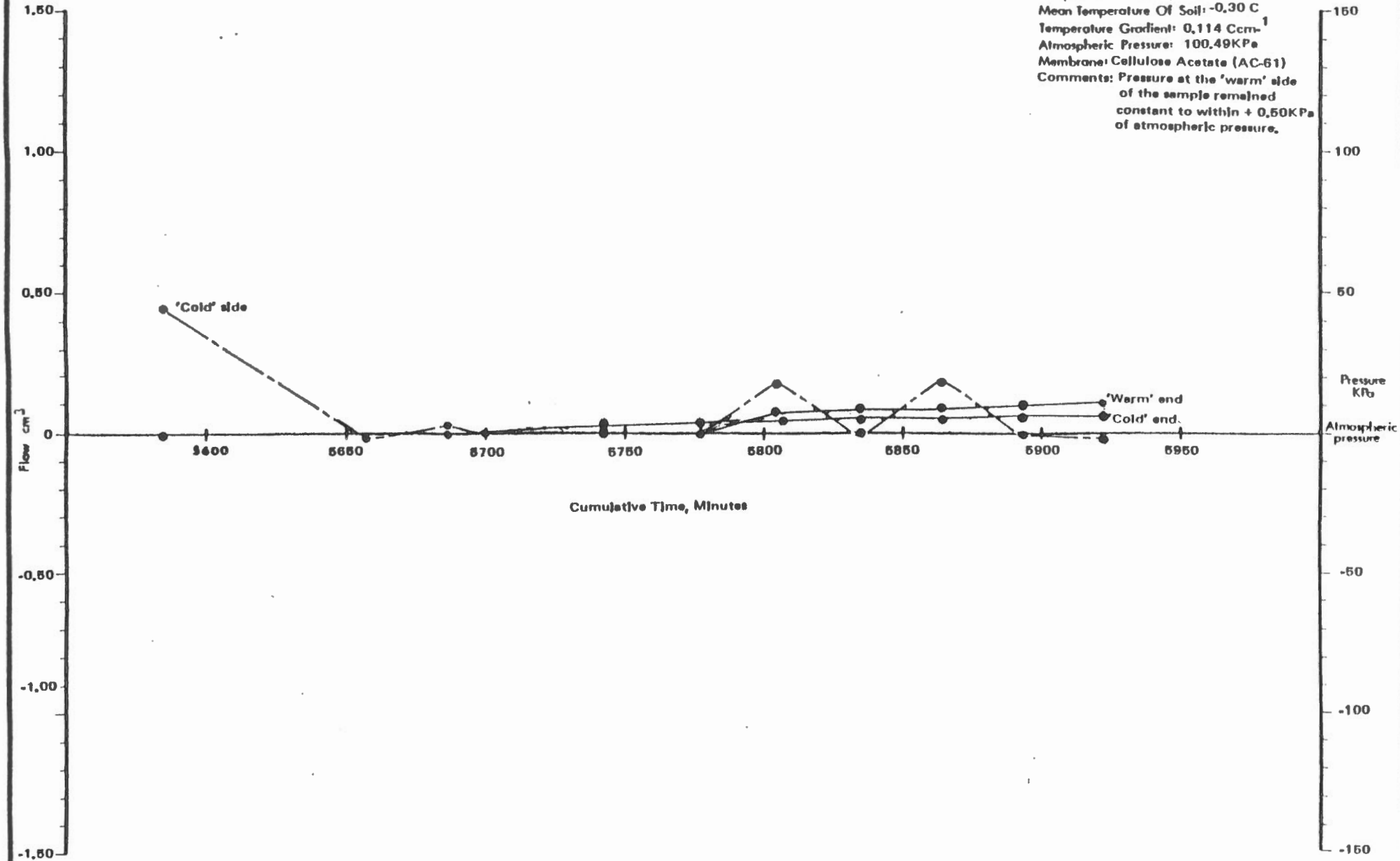

Cumulative Flow (Negative values indicate inflow, i.e. Moisture flow from the reservoir into the soil. Positive values indicate outflow).

Pressure (Total stress) relative to atmospheric pressure. (Negative values indicate pressures that are less than atmospheric).

	'Warm' Reservoir	'Cold' Reservoir
Temperature °C	-0.10	-0.50
Lactose Concentration gl^{-1}	17.95	83.50

Figure 5.13

Temperature Profile Of The Soil Sample During The Approach To Steady State Heat Transfer Conditions (Experiment No. 19)

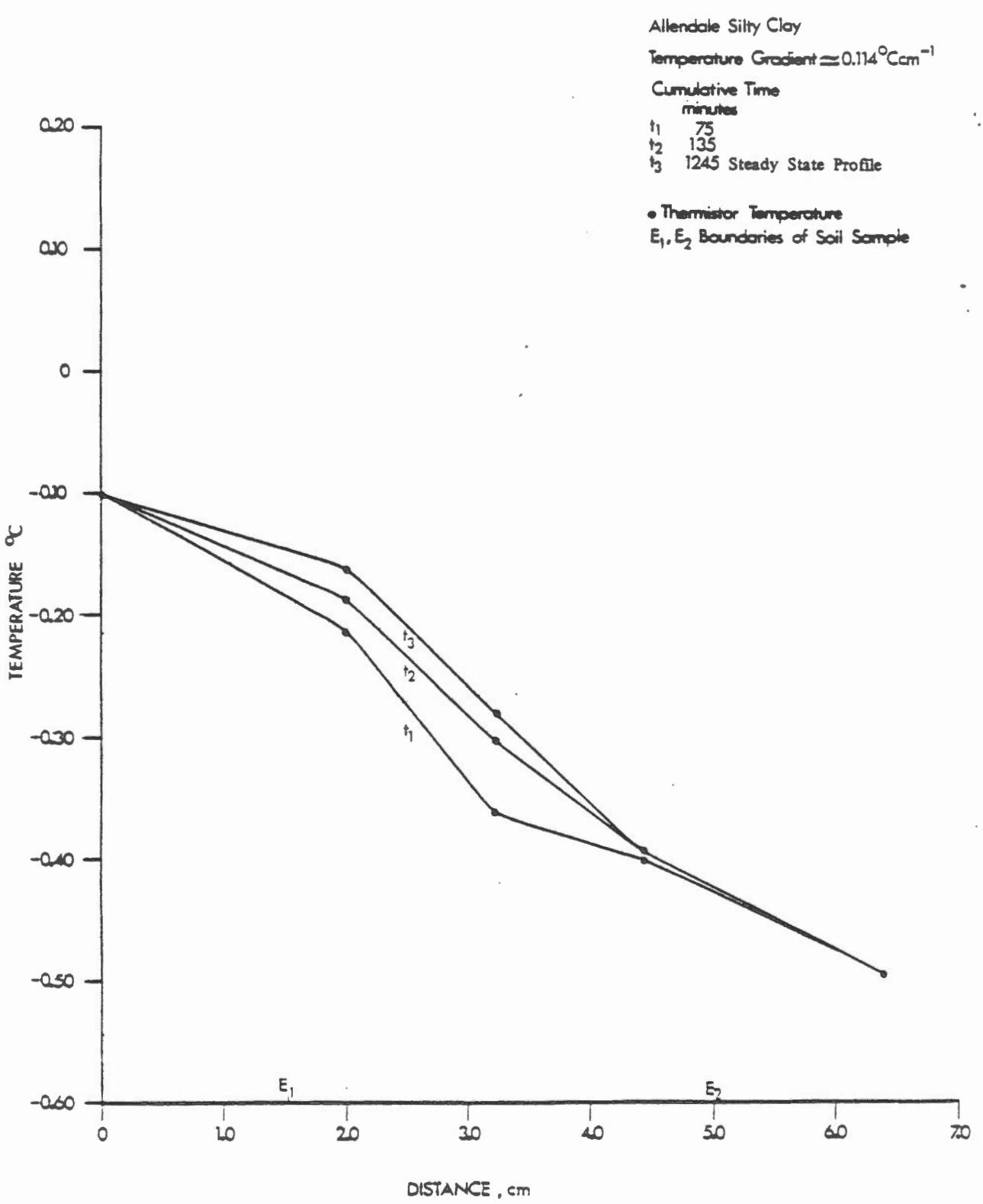

Plot of Pressure and Flow Vs. Cumulative Time During Temperature Induced Moisture Migration

Figure: 5.14a

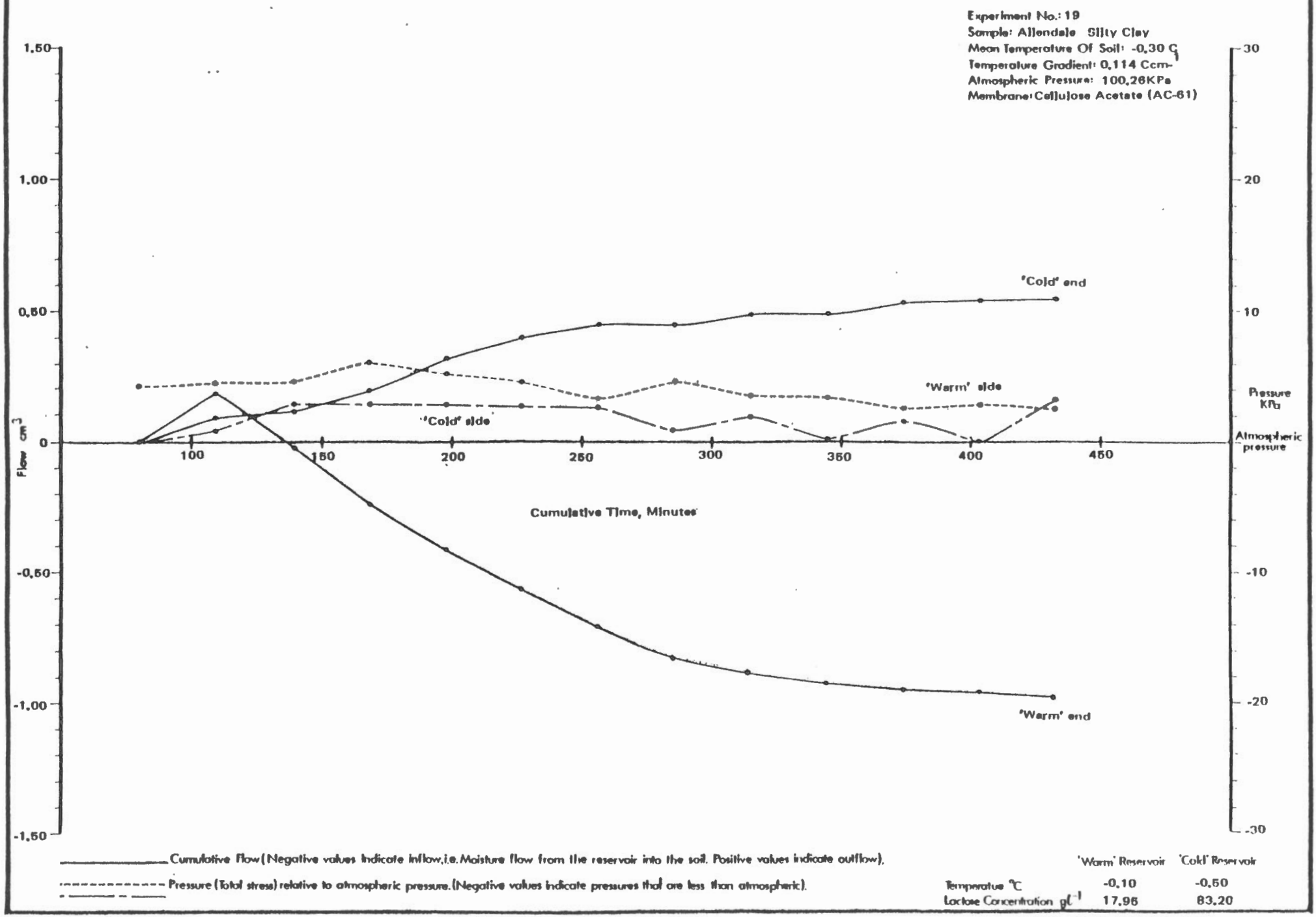

Plot of Pressure and Flow Vs. Cumulative Time During Temperature Induced Moisture Migration

Figure: 5.14b

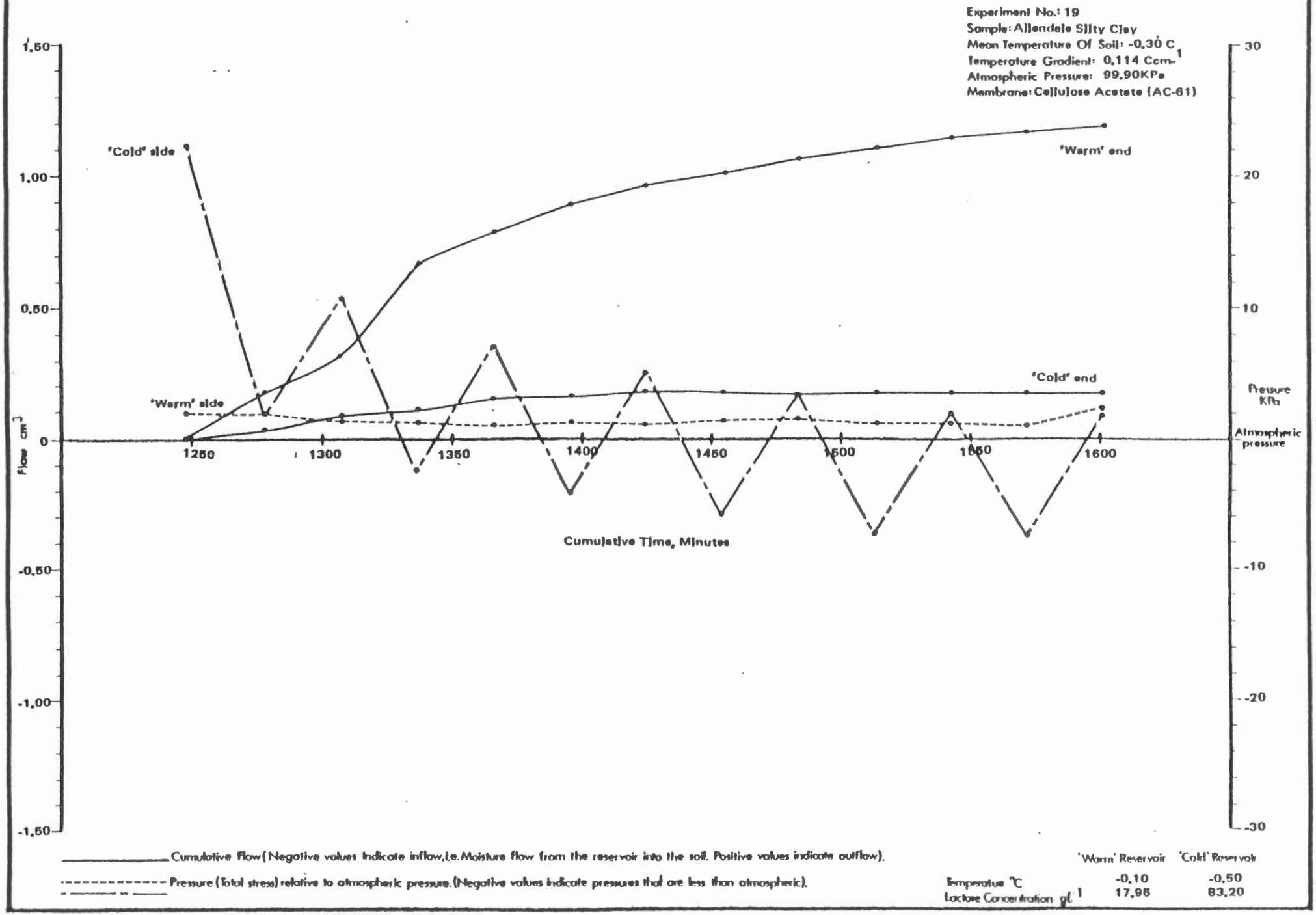

Plot of Pressure and Flow Vs. Cumulative Time During Temperature Induced Moisture Migration

Figure: 5.14c

Experiment No.: 19
Sample: Allendale Silty Clay
Mean Temperature Of Soil: -0.30 C
Temperature Gradient: 0.114 Ccm-1
Atmospheric Pressure: 100.37 KPa
Membrane: Cellulose Acetate (AC-61)
Comments: Pressure at the 'warm'side of the sample remained constant to within ± 1.00KPa of atmospheric pressure.

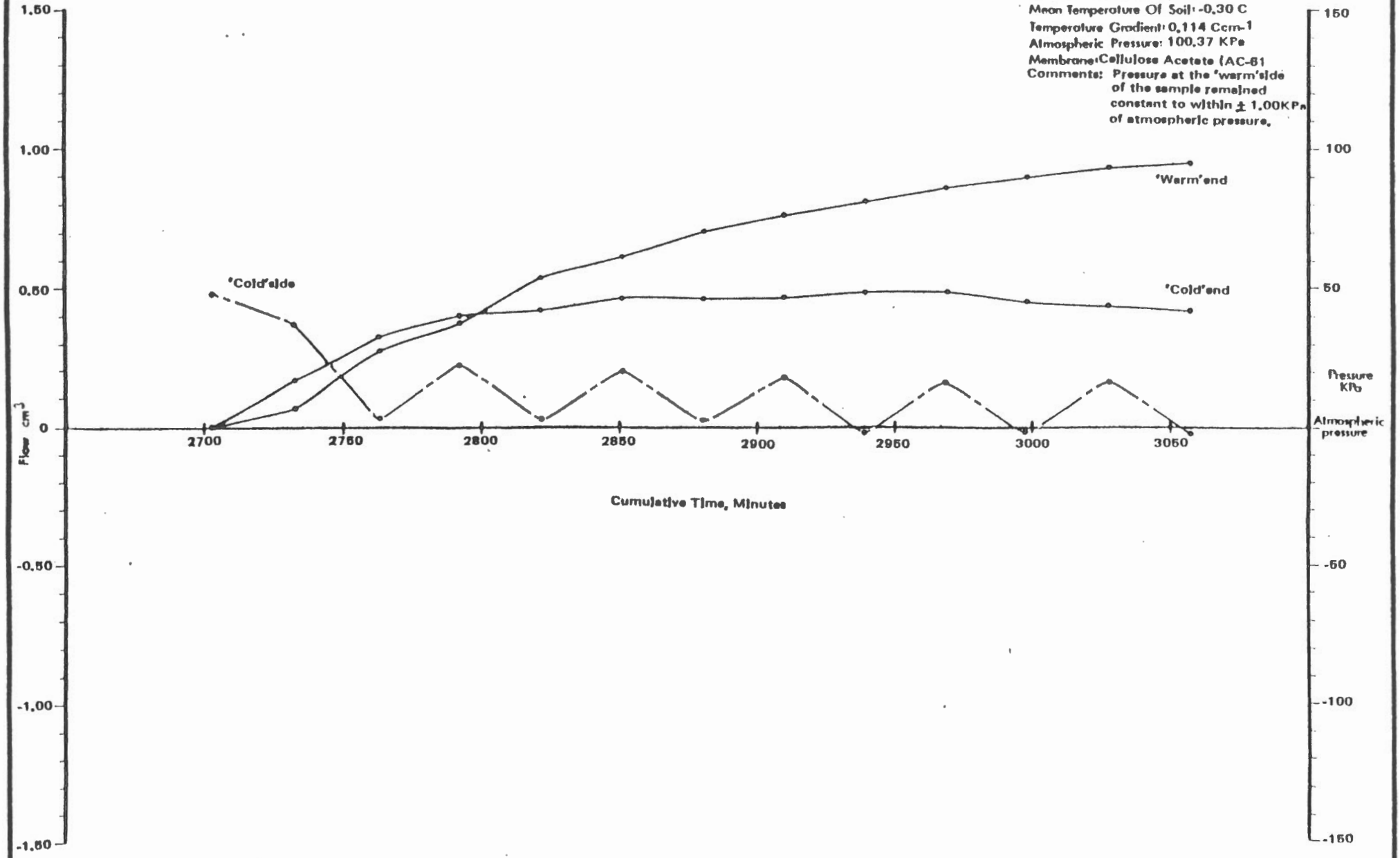

——————— Cumulative Flow (Negative values indicate inflow, i.e. Moisture flow from the reservoir into the soil. Positive values indicate outflow).

- - - - - - - - - - - - Pressure (Total stress) relative to atmospheric pressure. (Negative values indicate pressures that are less than atmospheric).

	'Warm' Reservoir	'Cold' Reservoir
Temperature °C	-0.10	-0.50
Lactose Concentration gL^{-1}	17.95	83.20

Figure 5.15

Temperature Profile Of The Soil Sample During The Approach To Steady State Heat Transfer Conditions (Experiment Number 20)

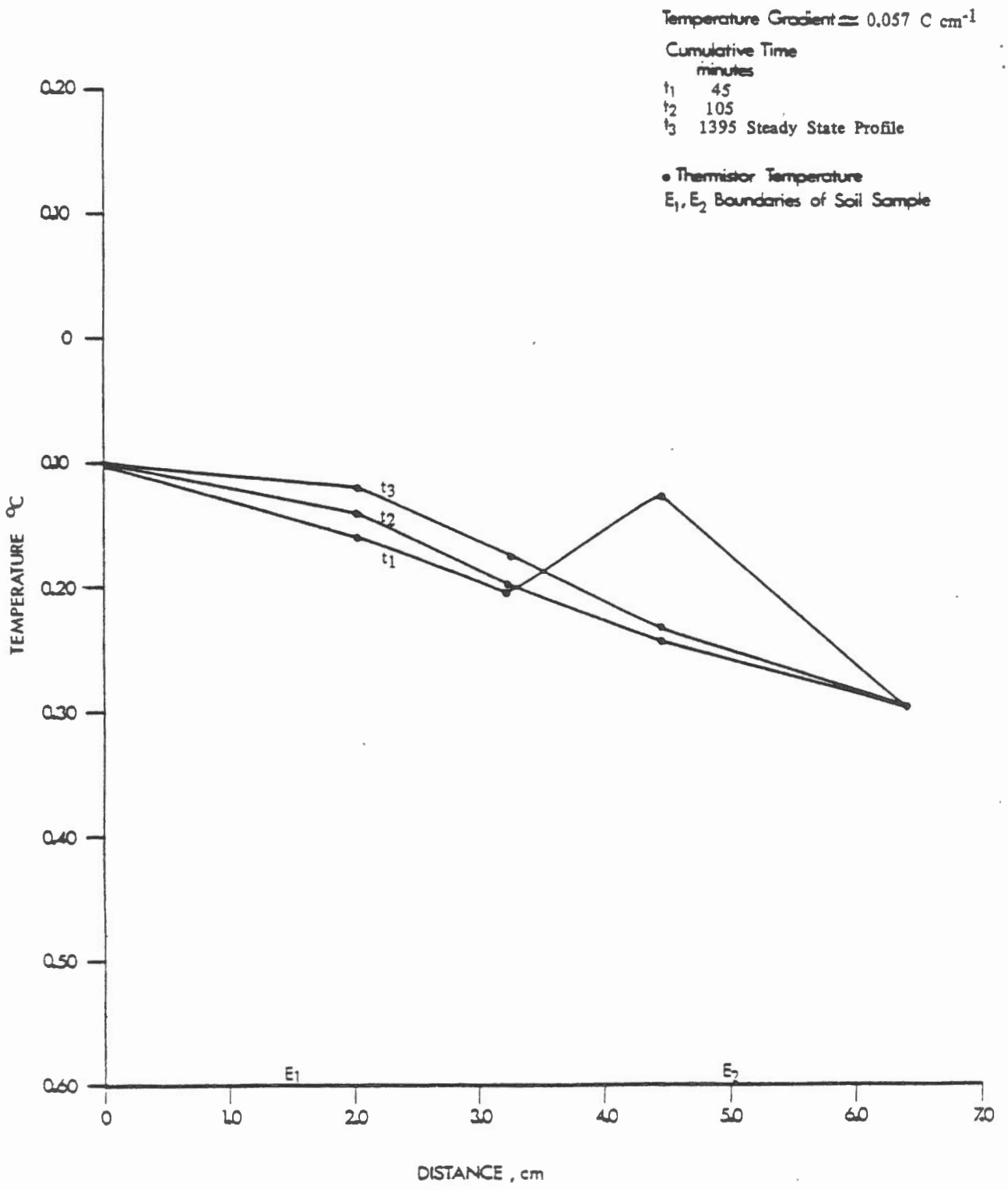

Plot of Pressure and Flow Vs. Cumulative Time During Temperature Induced Moisture Migration

Figure: 5.16a

Experiment No.: 20
Sample: Allendale Silty Clay
Mean Temperature Of Soil: -0.20 C
Temperature Gradient: 0.057 Ccm^{-1}
Atmospheric Pressure: 101.25KPa
Membrane: Cellulose Acetate (AC-61)

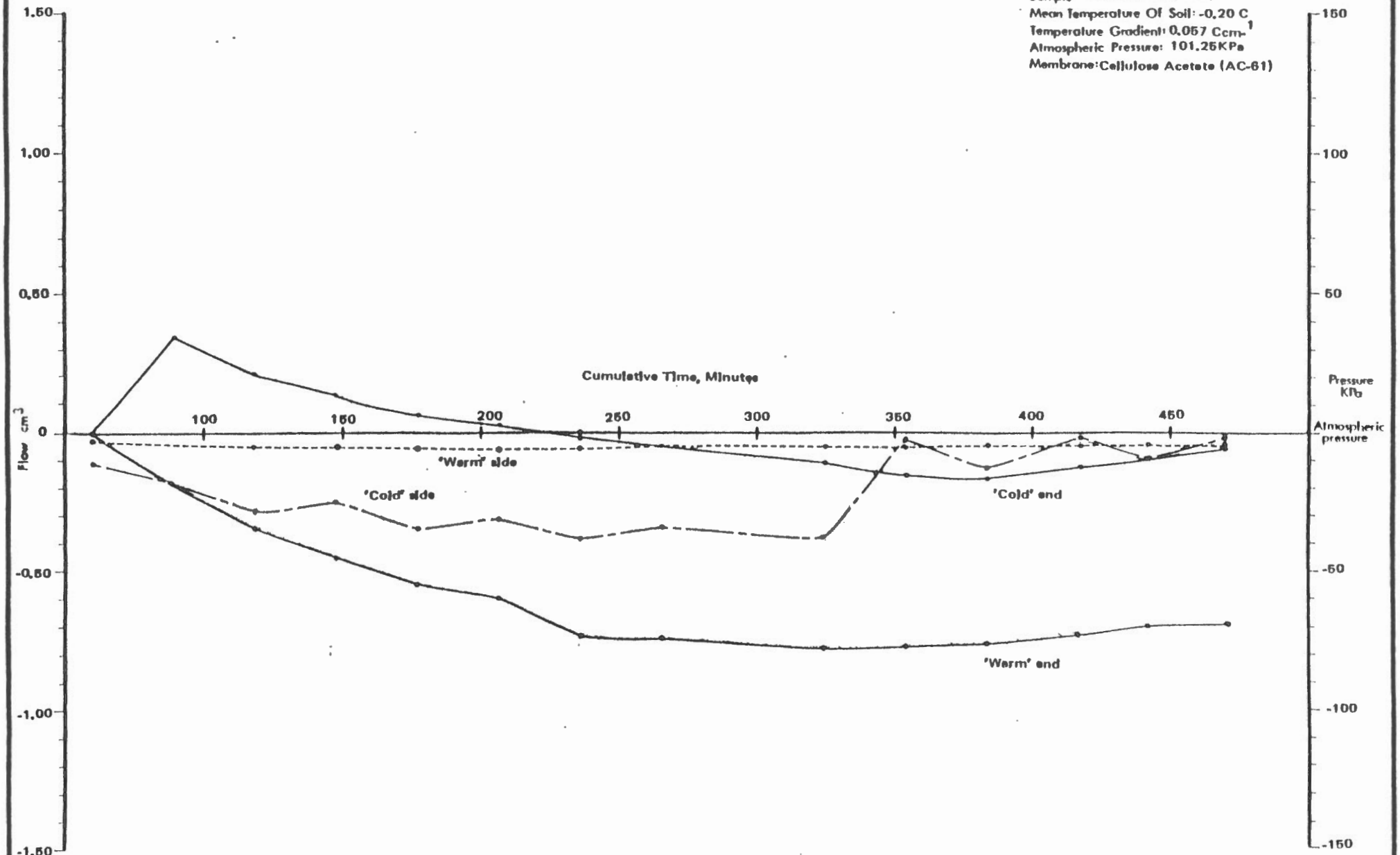

Cumulative Flow (Negative values indicate inflow, i.e. Moisture flow from the reservoir into the soil. Positive values indicate outflow).

Pressure (Total stress) relative to atmospheric pressure. (Negative values indicate pressures that are less than atmospheric).

	'Warm' Reservoir	'Cold' Reservoir
Temperature °C	-0.10	-0.30
Lactose Concentration gl^{-1}	17.94	62.94

Plot of Pressure and Flow Vs. Cumulative Time During Temperature Induced Moisture Migration

Figure: 5.16b

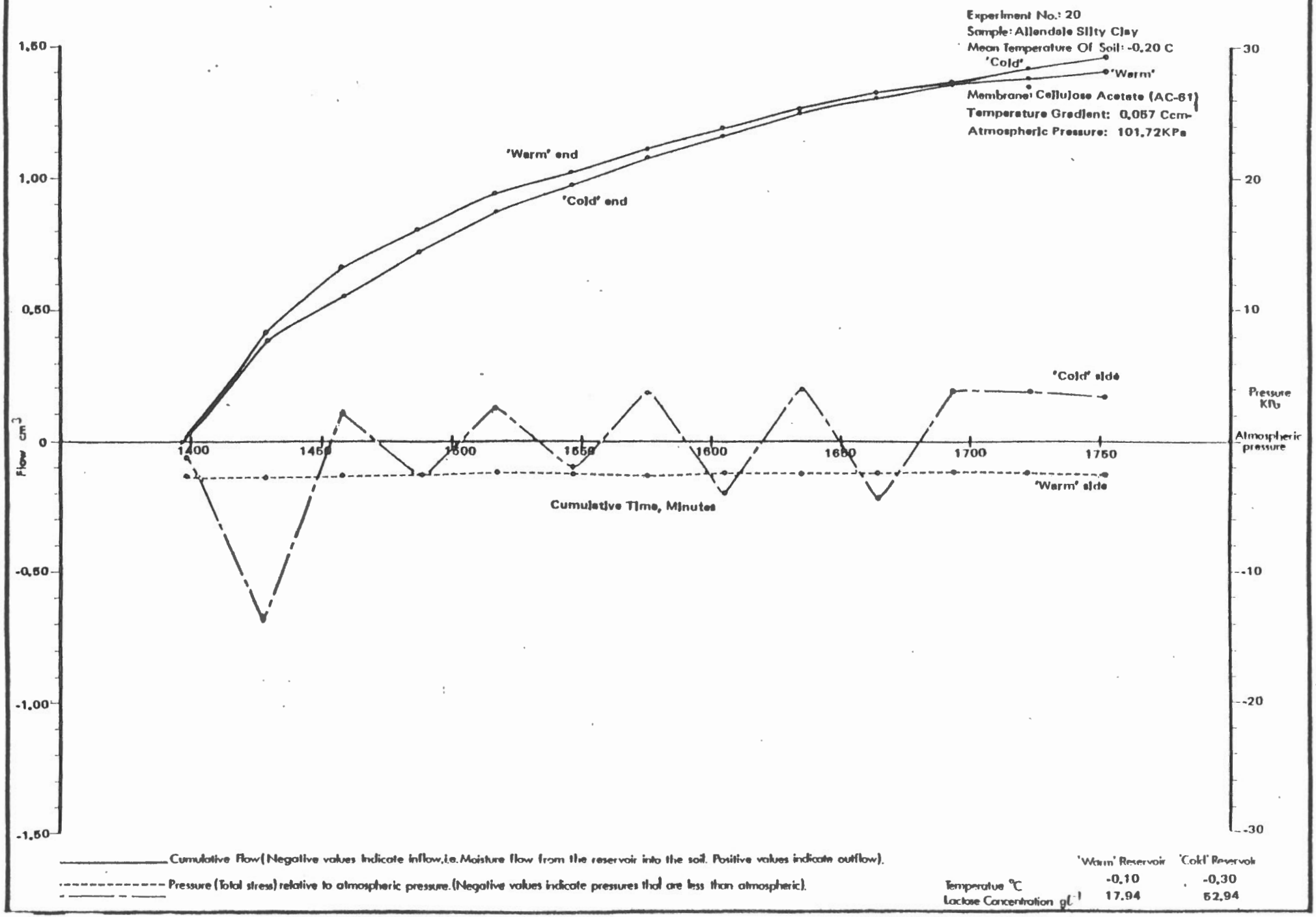

Cumulative Flow (Negative values indicate inflow, i.e. Moisture flow from the reservoir into the soil. Positive values indicate outflow).

Pressure (Total stress) relative to atmospheric pressure. (Negative values indicate pressures that are less than atmospheric).

	'Warm' Reservoir	'Cold' Reservoir
Temperature °C	-0.10	-0.30
Lactose Concentration g/l	17.94	52.94

Plot of Pressure and Flow Vs. Cumulative Time During Temperature Induced Moisture Migration

Figure: 5.16d

Experiment No.: 20
Sample: Allendale Silty Clay
Mean Temperature Of Soil: -0.20 C
Temperature Gradient: 0.057 Ccm^{-1}
Atmospheric Pressure: 99.69KPa
Membrane: Cellulose Acetate (AC-61)

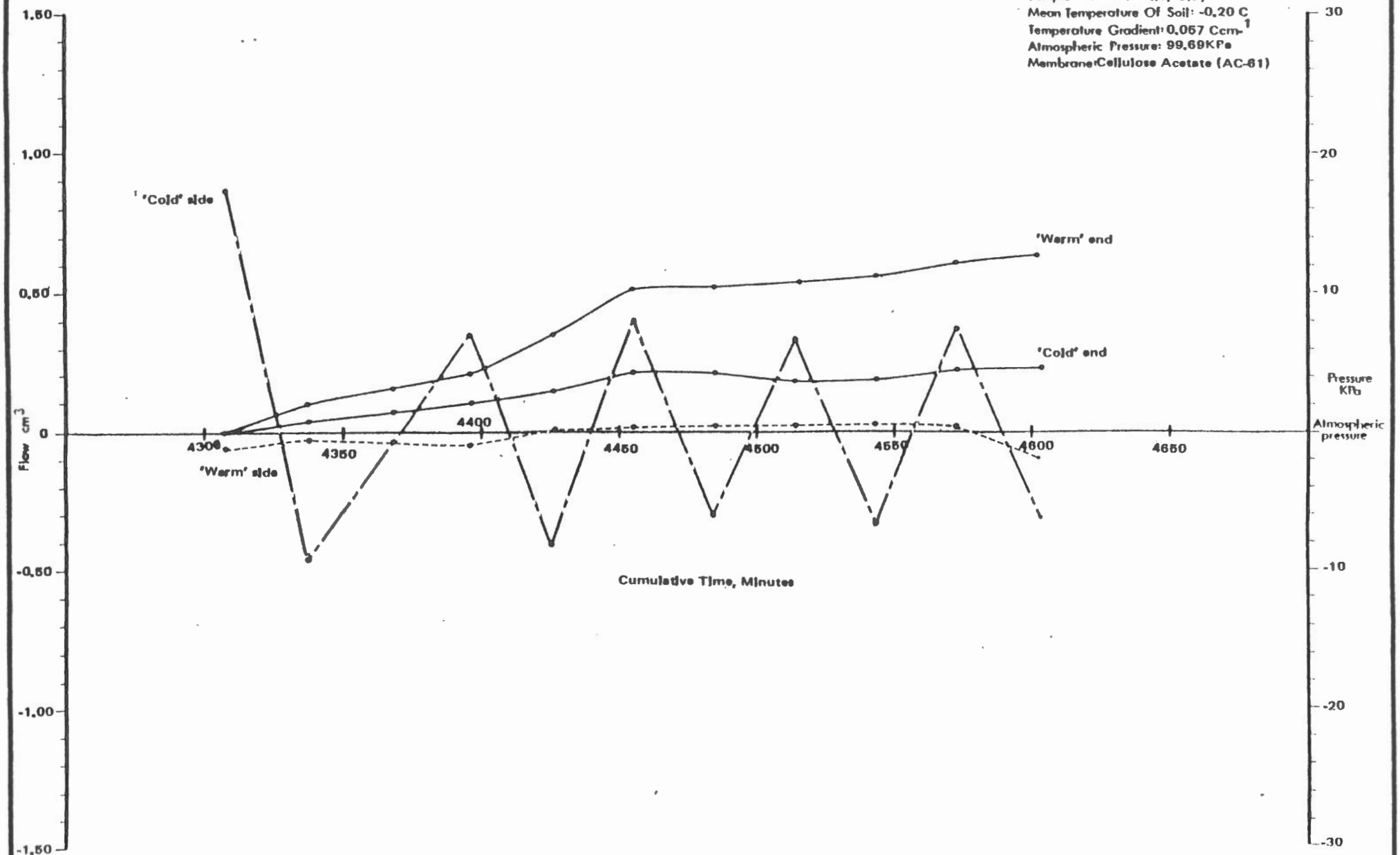

Cumulative Flow (Negative values indicate inflow, i.e. Moisture flow from the reservoir into the soil. Positive values indicate outflow).

Pressure (Total stress) relative to atmospheric pressure. (Negative values indicate pressures that are less than atmospheric).

	'Warm' Reservoir	'Cold' Reservoir
Temperature °C	-0.10	-0.30
Lactose Concentration gl^{-1}	17.94	52.94

Plot of Pressure and Flow Vs. Cumulative Time During Temperature Induced Moisture Migration

Figure: 5.16c

Experiment No.: 20
Sample: Allendale Silty Clay
Mean Temperature Of Soil: -0.20 C
Temperature Gradient: 0.057 Ccm^{-1}
Atmospheric Pressure: 101.10KPa
Membrane: Cellulose Acetate (AC-61)

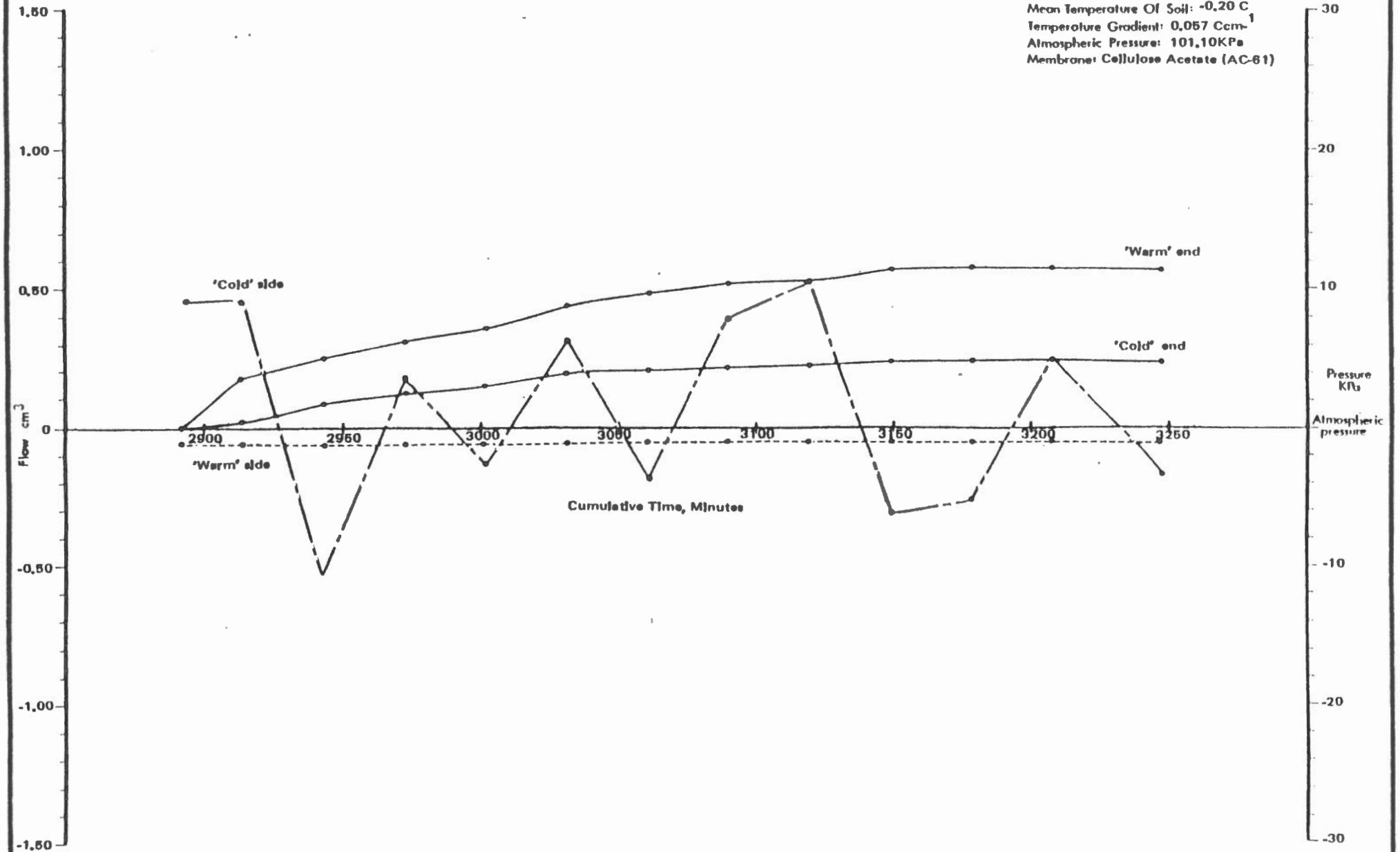

Cumulative Flow (Negative values indicate inflow, i.e. Moisture flow from the reservoir into the soil. Positive values indicate outflow).

Pressure (Total stress) relative to atmospheric pressure. (Negative values indicate pressures that are less than atmospheric).

	'Warm' Reservoir	'Cold' Reservoir
Temperature °C	-0.10	-0.30
Lactose Concentration gl^{-1}	17.94	52.94

Figure 5.17

Temperature Profile Of The Soil Sample During The Approach To Steady State Heat Transfer Conditions (Experiment No. 21)

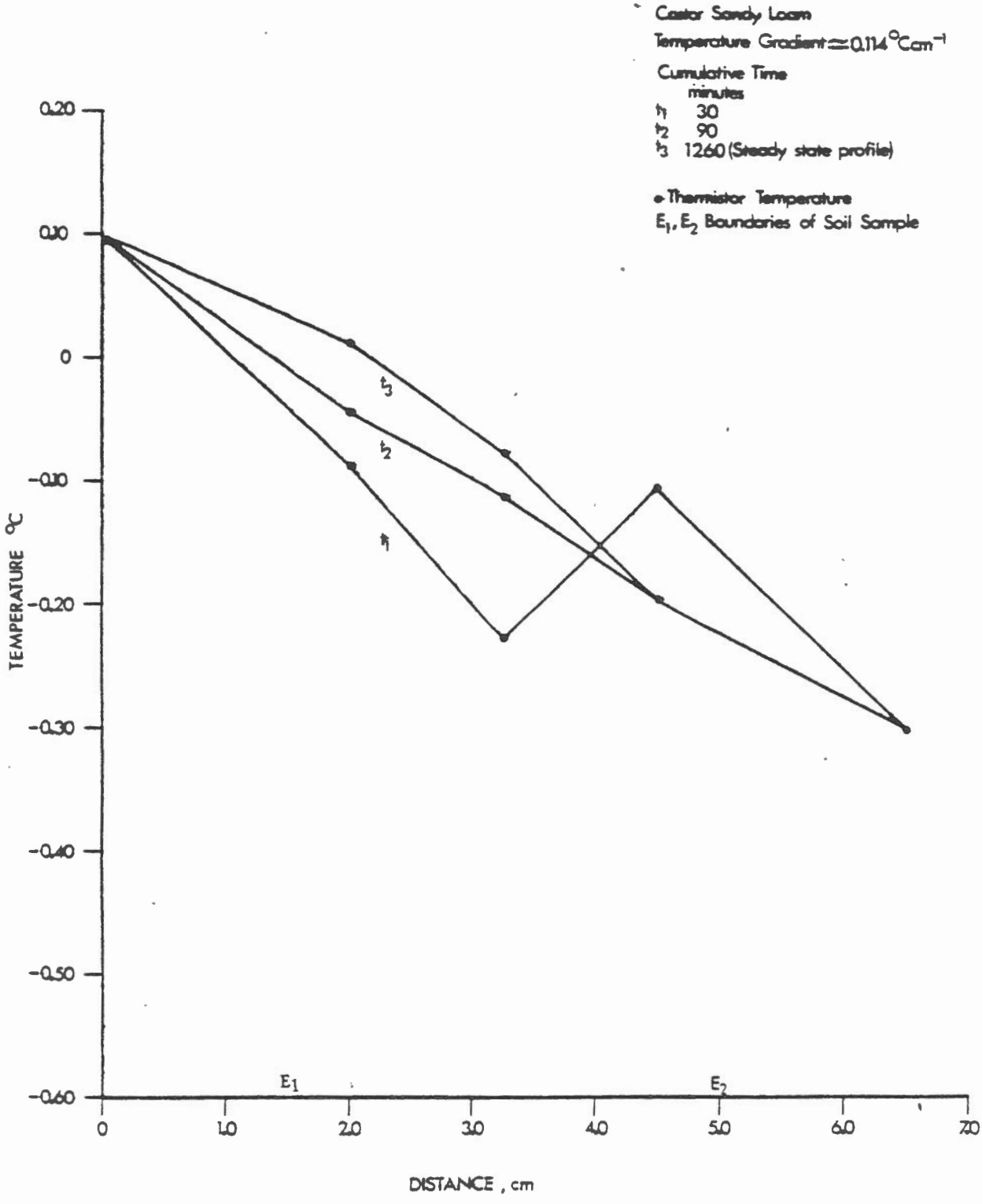

Plot of Pressure , and Flow Vs. Cumulative Time During Temperature Induced Moisture Migration

Figure: 5.18a

Experiment No.: 21
Sample: Allendale Silty Clay
Mean Temperature Of Soil: -0.10°C
Temperature Gradient: -0.114 °Cm^{-1}
Atmospheric Pressure: 100.56 KPa
Membrane: Cellulose Acetate (AC-61)

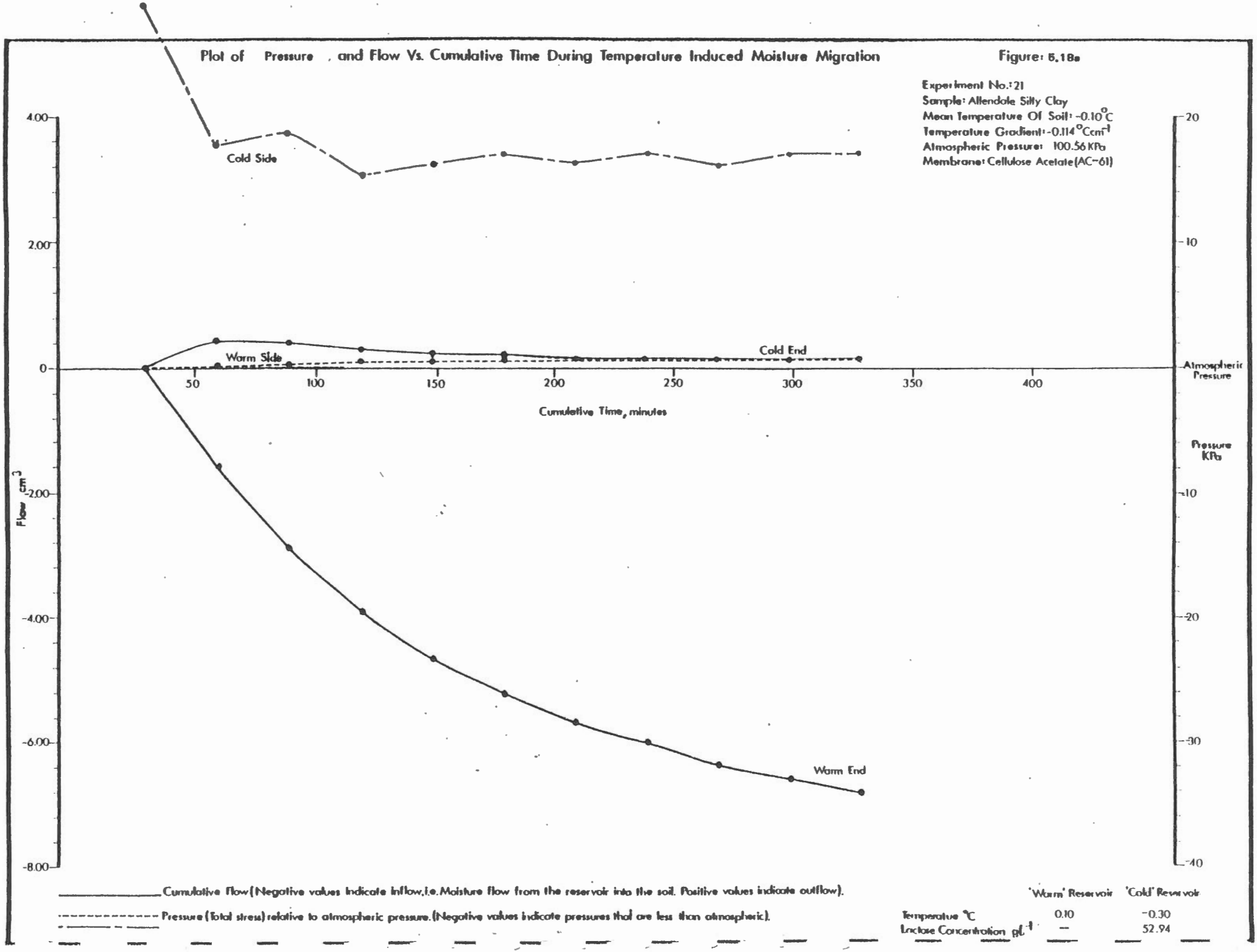

Cumulative Flow (Negative values indicate inflow, i.e. Moisture flow from the reservoir into the soil. Positive values indicate outflow).

Pressure (Total stress) relative to atmospheric pressure. (Negative values indicate pressures that are less than atmospheric).

	'Warm' Reservoir	'Cold' Reservoir
Temperature °C	0.10	-0.30
Lactose Concentration gL^{-1}	—	52.94

Plot of Pressure and Flow Vs. Cumulative Time During Temperature Induced Moisture Migration

Figure: 5.18b

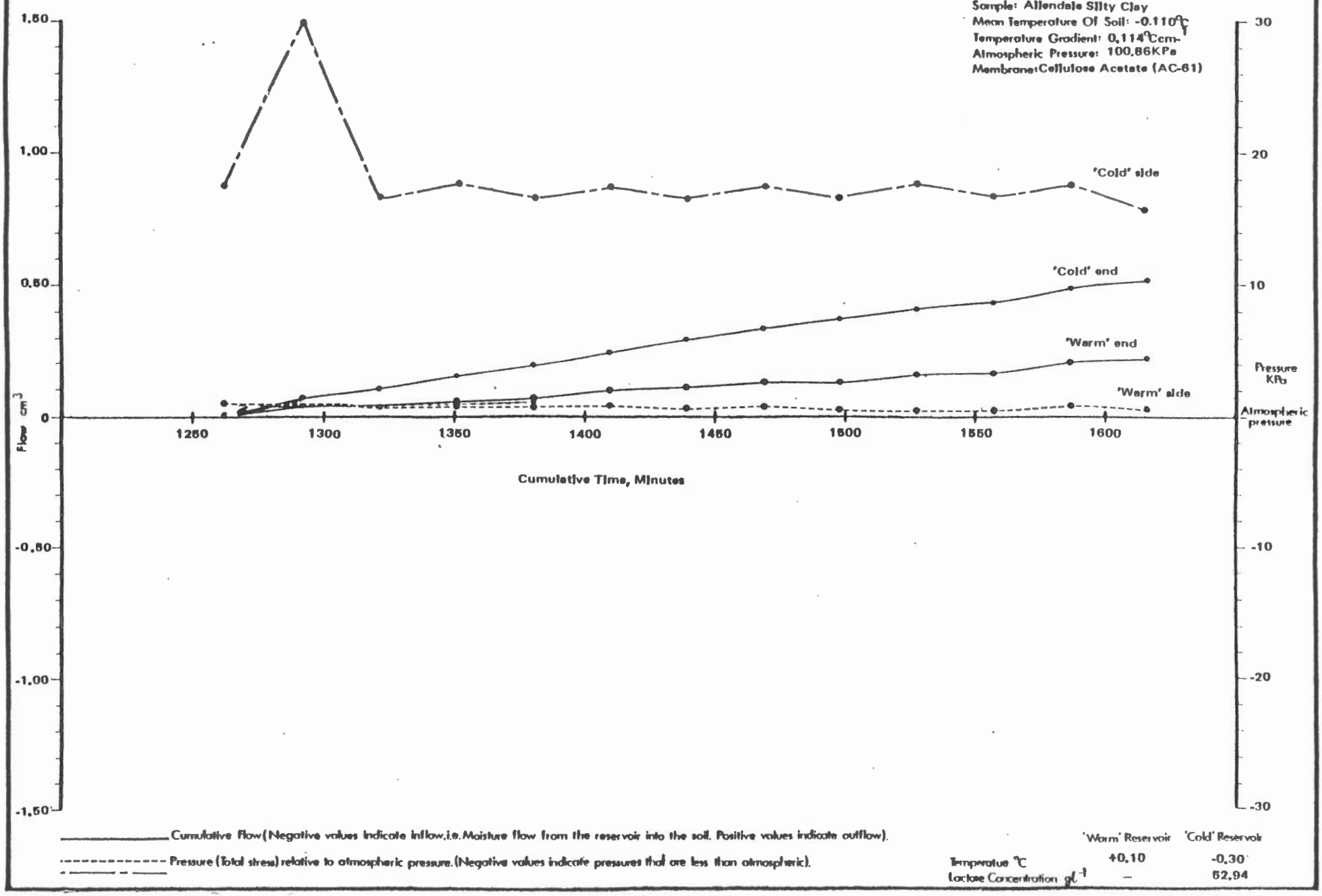

Plot of Pressure and Flow Vs. Cumulative Time During Temperature Induced Moisture Migration

Figure: 5.18c

Experiment No.: 21
Sample: Allendale Silty Clay
Mean Temperature Of Soil: -0.10 C
Temperature Gradient: 0.114 Ccm^{-1}
Atmospheric Pressure: 100.56KPa
Membrane: Cellulose Acetate (AC-61)

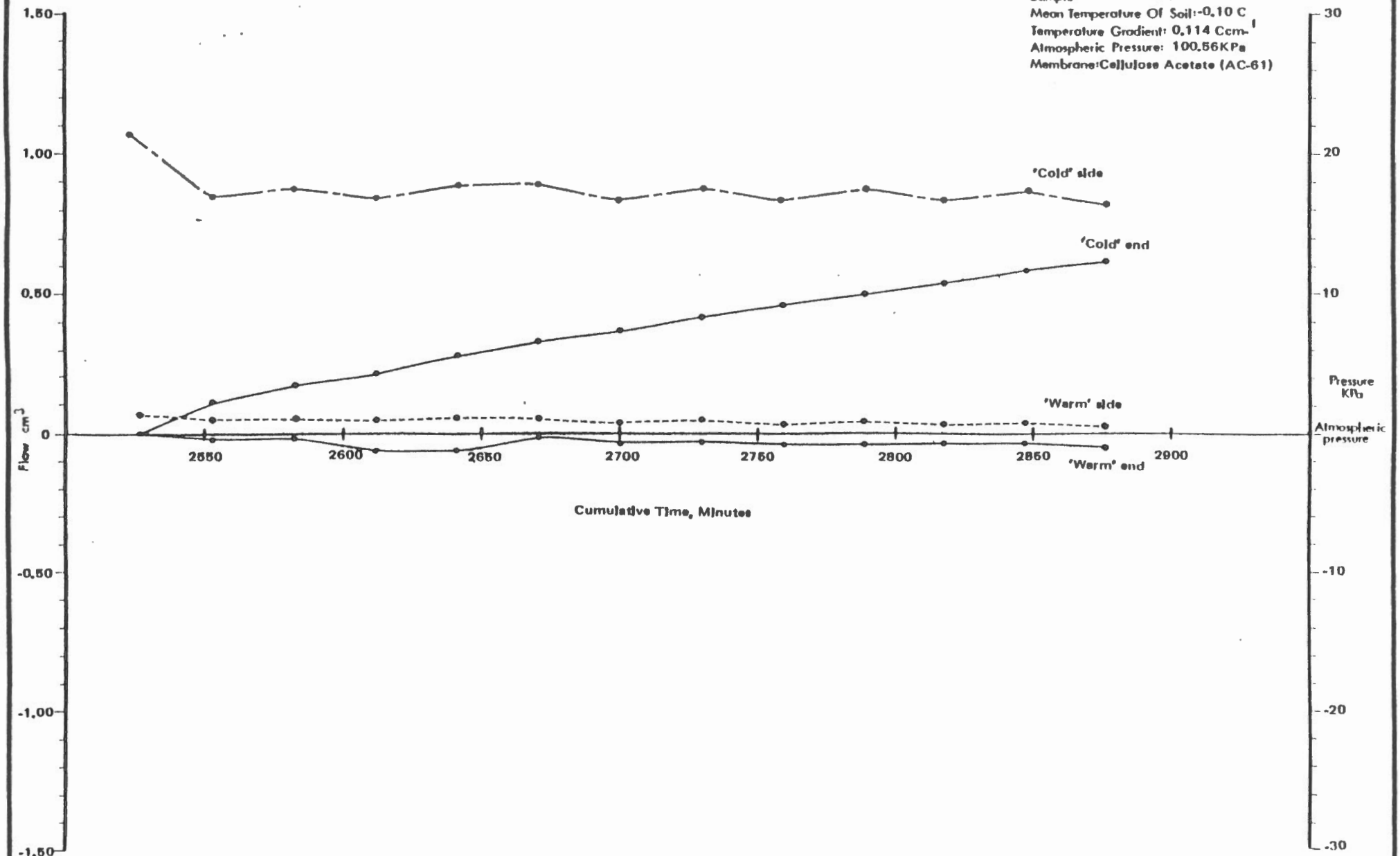

Cumulative Flow (Negative values indicate inflow, i.e. Moisture flow from the reservoir into the soil. Positive values indicate outflow).

Pressure (Total stress) relative to atmospheric pressure. (Negative values indicate pressures that are less than atmospheric).

	'Warm' Reservoir	'Cold' Reservoir
Temperature °C	+0.10	-0.30
Lactose Concentration gl^{-1}	—	52.94

Plot of Pressure and Flow Vs. Cumulative Time During Temperature Induced Moisture Migration

Figure: 5.18d

Experiment No.: 21
Sample: Allendale Silty Clay
Mean Temperature Of Soil: -0.10 C
Temperature Gradient: 0.114 Ccm^{-1}
Atmospheric Pressure: 101.01KPa
Membrane: Cellulose Acetate (AC-61)

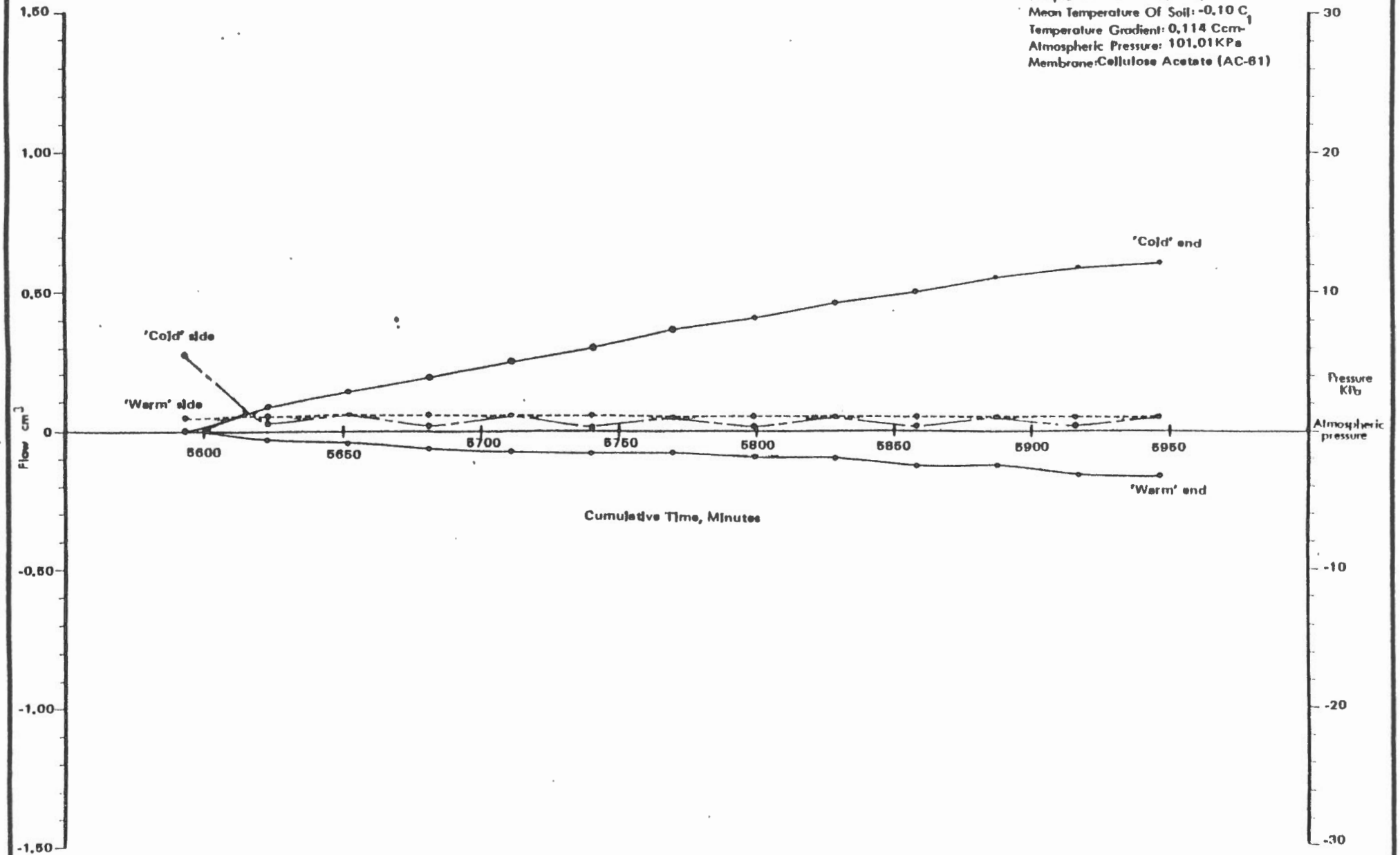

Cumulative Flow (Negative values indicate inflow, i.e. Moisture flow from the reservoir into the soil. Positive values indicate outflow).

Pressure (Total stress) relative to atmospheric pressure. (Negative values indicate pressures that are less than atmospheric).

	'Warm' Reservoir	'Cold' Reservoir
Temperature °C	+0.10	-0.30
Lactose Concentration gl^{-1}	—	52.94

Plot of Pressure and Flow Vs. Cumulative Time During Temperature Induced Moisture Migration

Figure: 5.18a

Experiment No.: 21
Sample: Allendale Silty Clay
Mean Temperature Of Soil: -0.10 C
Temperature Gradient: 0.114 Ccm^{-1}
Atmospheric Pressure: 100.95KPa
Membrane: Cellulose Acetate (AC-61)

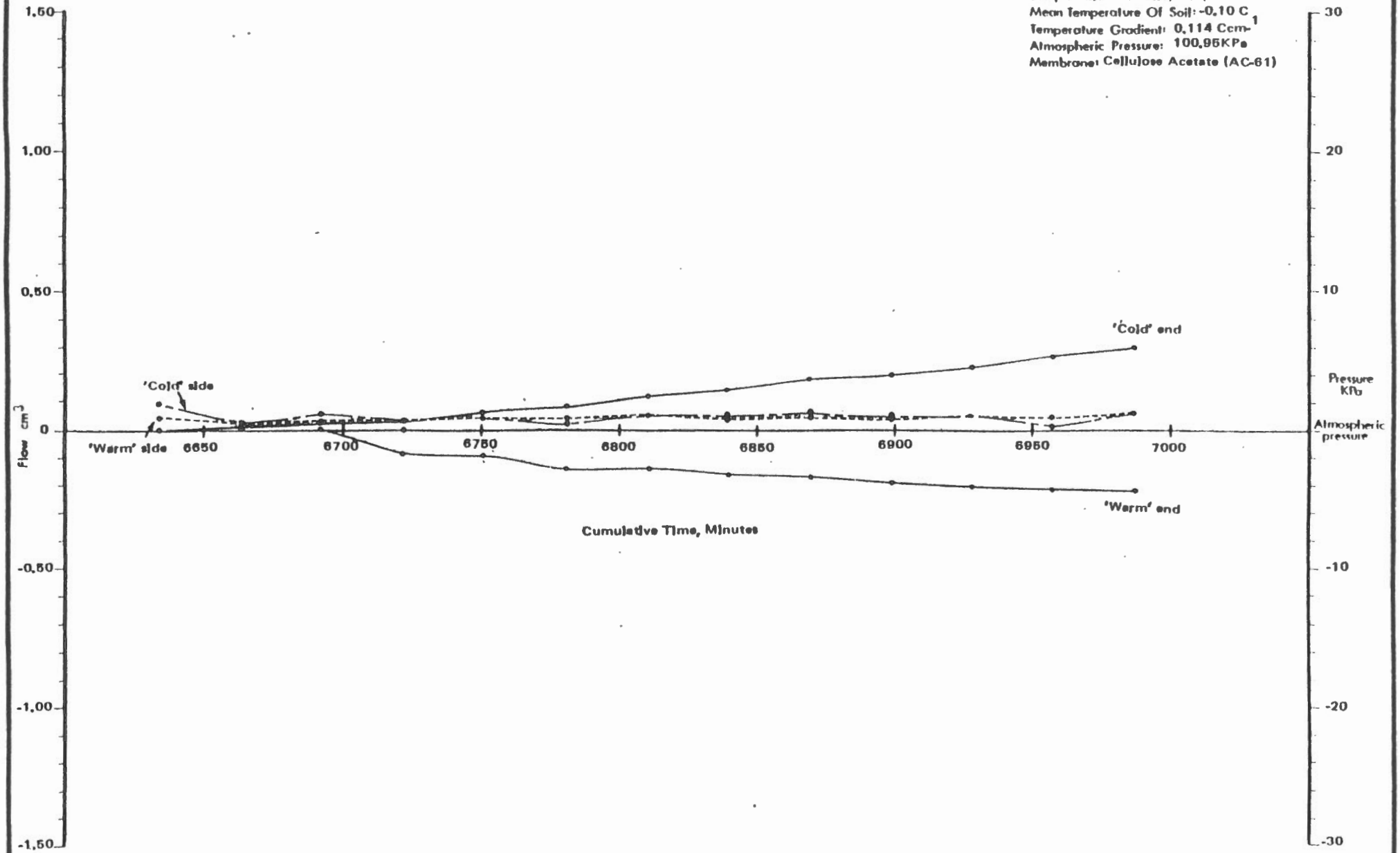

Cumulative Flow (Negative values indicate inflow, i.e. Moisture flow from the reservoir into the soil. Positive values indicate outflow).

Pressure (Total stress) relative to atmospheric pressure. (Negative values indicate pressures that are less than atmospheric).

	'Warm' Reservoir	'Cold' Reservoir
Temperature °C	+0.10	-0.50
Lactose Concentration gl^{-1}	—	52.94

Plot of Pressure and Flow Vs. Cumulative Time During Temperature Induced Moisture Migration

Figure: 5.18f

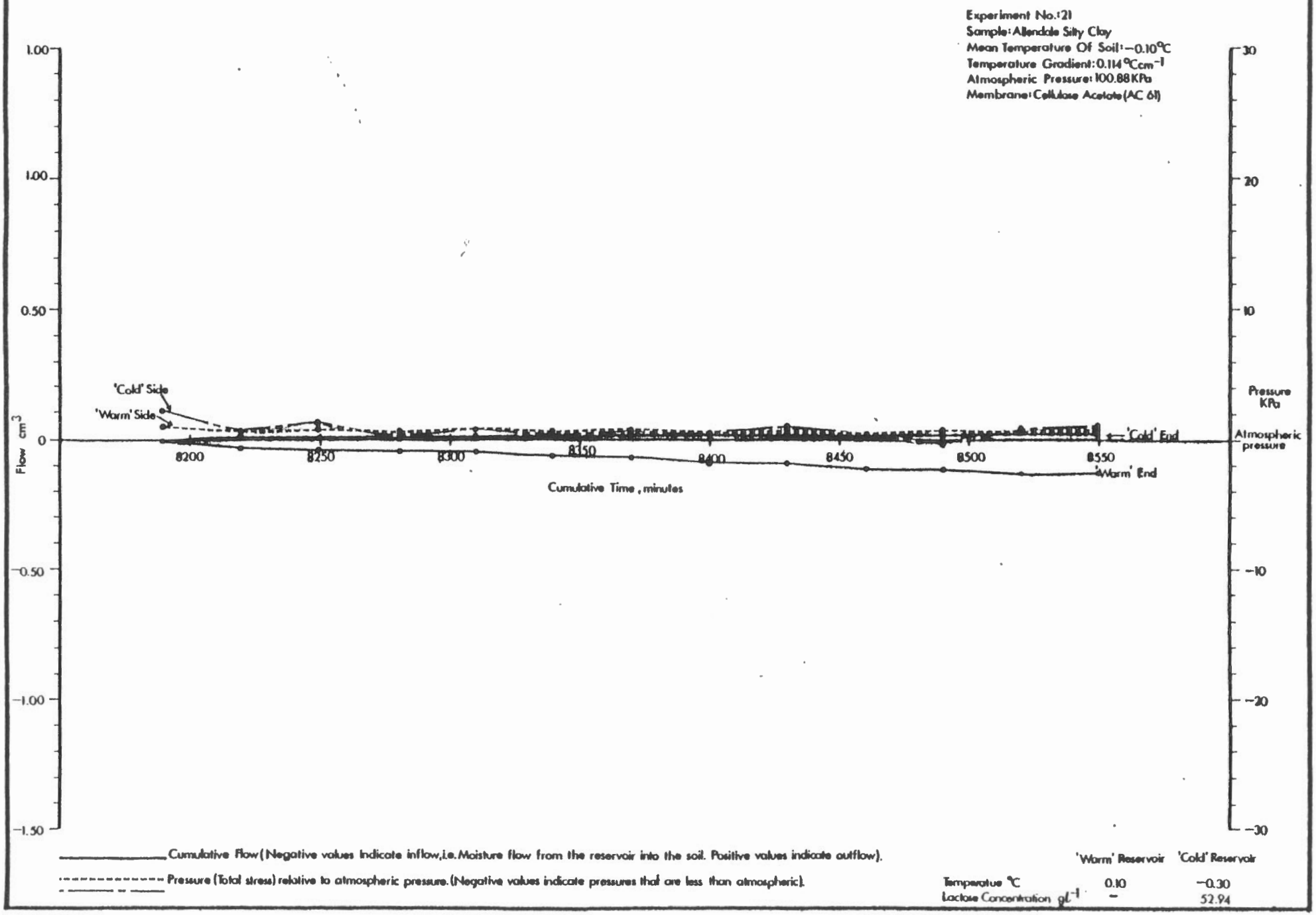

SUMMARY AND CONCLUSIONS

1. Of fundamental importance in describing the behaviour of frozen soils is the Clapeyron equation. This predicts the freezing-point depression for a system of water and ice, in thermodynamic equilibrium arising from an increase in ice pressure or a fall in water pressure or a combination of both changes.

2. Historically, the mechanism of frost heaving was first explained from a thermodynamic viewpoint. This is usually referred to as the capillary model. The realization that ice lenses actually form some distance behind the frost line in freezing soils, led to a description of the phenomenon in terms of the hydrodynamic conditions within the soil. More recently, there has been a growing awareness that the mechanism is more complicated than that envisaged by either of these models since the state of stress of the soil constituents must be taken into consideration as well. The secondary frost heaving model proposed by Miller (1975), represents the most advanced concept of frost heaving to date, combining elements of both the thermodynamic and hydrodyanmic approaches along with a description of the stress conditions within the soil.

3. The mechanism of moisture movement through frozen soils is still not fully understood and remains a subject of controversy. A U.S. group has proposed a series-parallel transport mechanism in which water moves through the soil pores in the direction of colder temperatures in both the solid and liquid phases. The movement is attributed to temperature induced gradients in the osmotic activity of the ions in the unfrozen films surrounding the soil particles. The parallel component of movement involves transport within the fluid films as well as plug movement and plasto-viscous flow of pore ice. The series component involves regelation-transport of pore ice. These effects are coupled with the localized recirculation of heat by conduction between temperature peaks and troughs with the soil pores.

   In earlier investigations of frozen soil, the regelation component of transport was assumed to be small and was generally ignored. However, a recent analysis indicates that regelation transport probably forms a large component of the total mass transfer in frozen soils.

4. Equations for coupled heat and mass transfer for frozen soils are based on the Onsager reciprocity relations which are utilized extensively in irreversible thermodynamics. In principle, direct and cross-coefficients for heat and mass transfer in frozen soils should be separated, to determine whether the rate of mass transfer is limited by the rate of heat transfer or by the intrinsic permeability of the soil itself. A major drawback with the existing methods of measuring the flow parameters in frozen soils is that mass transfer coefficients are

are not separated from heat transfer effects. In addition, the effect that the thermal properties of the permeameter have on the mass transfer in the frozen soil, is not known.

5. Experiments have been conducted to determine the rate of mass transfer for pure ice during regelation-transport. The apparatus simulates regelation-transport in a large pore. A disc of ice confined to a plexiglass ring was sandwiched between two reservoirs containing supercooled water. A microporous membrane separated the ice from the water. Application of a hydrostatic pressure to one reservoir resulted in a slow discharge of water from the other reservoir. The rate of mass transfer was found to be linearly related to the hydraulic head and exponentially related to the temperature. The latter result is in close agreement with existing theory on the rheological properties of polycrystalline ice. Overall, the mass transfer coefficient decreased by about 2 orders of magnitude for a temperature change of 0°C to -0.3 °C. The flow rates depend, in part, on the heat conducting properties of the ice-permeameter system.

   Ice pressures were measured once static equilibrium was attained between the solid and liquid phases. Down to about -0.2°C values agree closely with the values predicted by the Clapeyron equation. Beyond this limit, deviations from theory were caused by deformation of the apparatus.

6. Experiments were also carried out in which regelation-transport was induced by an osmotic gradient rather than a hydraulic gradient. The following observations were made.

   When lactose solution was used in one reservoir (supercooled water in the other), a continuous flow of water was observed in the direction of the solution. The explanation for the movement is that the osmotic gradient between the ice and the solution induces the movement of water towards the solution, resulting in a fall in the ice pressure. This disrupts the equilibrium between the ice and the supercooled water at the other end of the system, producing inflow.

   When lactose solution was used in both reservoirs, flow was observed towards the solution with the greater concentration. However, no flow was observed from the reservoir with the lower concentration. The explanation offered was that the gradient in osmotic pressure between the ice and the less concentrated solution was countered exactly by a pressure gradient within the ice, in the opposite direction, associated with flow towards the other reservoir.

7. An apparatus has been developed in which the pressure changes are measured in a frozen soil sample during temperature induced moisture migration. The soil sample is confined to a plexiglass cell which is sandwiched between metal end plates containing small reservoirs. These contain lactose solution, the concentration of which is adjusted according to the temperature of the reservoir. The temperature of the

end plates is controlled by a thermoelectric cooling system. Soil pressure is monitored with small pressure transducers mounted in the wall of the cell.

During the approach to a linear temperature profile, a large influx of water was observed at the 'warm' end of the soil sample and a small amount of outflow occurred at the 'cold' end. The subsequent establishment of a linear temperature gradient was accompanied by the expulsion of water from both ends of the soil sample, the flux being greater at the 'warm' end. Throughout the experiment, the pressure on the 'warm' side of the soil sample remained constant and very close to atmospheric pressure. In contrast, the pressure on the 'cold' side showed a marked cyclic variation, changing by about 20-30 KPa in a 1-2 hour period.

The explanation is that the initial influx of water results in the formation of segregation ice towards the 'cold' end of the soil. The stress generated by the growing ice lenses rises until it exceeds the long-term strength of the soil, at which point, the soil begins to yield and the pressure falls. Peak pressures occurring on the 'cold' side of the system are in close agreement with values given for the long-term strength of a similar soil at the same temperature. The outflow on the 'warm' end of the sample can be explained by the fact that yielding and the displacement of water is probably greater towards the 'warm' end owing to the rapid decline in the long-term strength of frozen soil with warmer temperatures.

Similar results were also obtained when the 'warm' end of the soil was above freezing, although there were two important differences: (1) The pressure on the 'cold' side of the sample did not show the cyclic variation that occurred when the soil was completely frozen; (2) an influx of water was observed at the 'warm' end of the soil sample rather than outflow. Experiments could not be continued long enough to determine the ultimate (long-term) migrations of water.

8. Provisions were also made to allow measurement of the change in reservoir pressure at the 'cold' end of the system when the outlet was closed. The reservoir pressure did not rise significantly above atmospheric pressure even over an extended period of time. This probably occurs as a result of internal yielding within the soil sample.

Although preliminary results are encouraging, a more detailed analysis awaits further testing. Experiments will continue throughout the summer, and a further report prepared.

REFERENCES

Anderson D.M. and Tice A.R., 1973, "The Unfrozen Interfacial Phase in Frozen Soil Water Systems", In: Physical Aspects of Soil Water and Salt In Ecosystems, Springer Verlag, Berlin, p. 107-124.

Aquirre-Puente J., 1982, personal communication.

Atkins P.W., 1978, "Physical Chemistry", Oxford University Press, Great Britain, p. 151-247.

Barnes D., Tabor F.R.S. and Walker J.C.R., 1971, "The Friction and Creep of Polycrystalline Ice," Proc. Roy. Soc. London V.A324, p. 127-155.

Bishop A.W. and Blight, G.E., 1963, "Some Aspects of Effective Stress in Saturated and Partly Saturated Soils," Geotechnique, V. 13, p. 177-197.

Bowes W.H., 1982, Civil Engineering Dept., Carleton University, Personal communication.

Buil M. and Aquirre-Puente J., 1981, "Thermodynamic And Experimental Study of the Crystal Growth of Ice," Am. Soc. Mech. Eng., Winter Meeting, Wash.

Burt T.P., 1974, "A Study of the Hydraulic Conductivity in Frozen Soils", Unpubl. M.A. Thesis, Carleton University, Ottawa, 78 p.

Burt T.P. and Williams P.J., 1976, "Hydraulic Conductivity in Frozen Soils", Earth Surface Processes, V. 1, p. 349-360.

Edlefsen N.E. and Anderson A.B.C., 1943, "Thermodynamics of Soil Moisture", Hilgardia, V. 15, No. 2, 298 p.

Everett D.H., 1961, "Thermodynamics of Frost Damage to Porous Solids", Trans. Far. Soc., V. 57, p. 1541-1551.

Everett D.M. and Haines J.M., 1965, "Capillary Properties of Some Model Pore Systems with Special Reference to Frost Damage", Bull. RILEM, No. 27, p. 31-36.

Glen L.W., 1975, "The Mechanics of Ice," U.S. Army CRREL Report No. MII-C2b, 43 pp.

Gold L.W., 1963, "Deformation Mechanisms in Ice," in Ice and Snow; Properties Processes and Applications (W.D. Kingery, ed.), Cambridge Mass.:MIT Press, p. 8-27.

Gray H.J. and Issacs A. (eds.), 1975, "A New Dictionary of Physics", Longman Group, London, p. 391.

Harlan, R.L., 1971, "Water Transport in Frozen and Partly Frozen Porous Media", Can. Hydro. Symp. Proc. 8th, V. 1, p. 109-129.

Harlan, R.L., 1973, "Analysis of Coupled Heat-Fluid Transport in Partially Frozen Soil", Water Resourses Res., V. 9, p. 1314-1322.

Hillel, D., 1971, "Soil And Water, Physical Principles and Processes", Academic Press, London, p. 119.

Hoekstra, P. and Miller, R.D., 1967, "On the Mobility of Water Molecules in the Transition Layer Between Ice and a Solid Surface", Journ. Colloid Interface Sci., V. 25, p. 166-173.

Horiguchi K. and Miller, R.D., 1980, "Experimental Studies with Frozen Soil in an 'Ice Sandwich' Permeameter", Cold Reg. Sci and Tech., V. 3, p. 177-183.

Koopmans, R.W.R. and Miller R.D., 1966, "Soil Freezing and Soil Water Characteristic Curves", Soil Sci. Soc . Am. Proc., V. 30, N. 6, p. 680-685.

Levitt, B.P., 1973, ed. Findlay's Practical Physical Chemistry, Longman, London, p. 113-125, 158-161.

Loch, J.P.G., 1975, "Secondary Heaving: Experiments and Analysis of Frost Heaving Pressure in Soils", Ph.D. Thesis, Cornell University, 102 pp.

Loch, J.P.G. and Kay, B.D., 1978, "Water Distribution in Partially Frozen Saturated Silt Under Several Temperature Gradients and Overburden Loads", Soil Sci. Soc. Am. Journ., V. 42, p. 400-406.

Miller, R.D., 1970, "Ice Sandwich: Functional Semipermeable Membrane", Science, V. 169, p. 584-585.

Miller, R.D., 1976, "Reviewers Comments: The Variation of Hydraulic Conductivity in Frozen Soils", T.P. Burt and P.J. Williams, personal communication.

Miller, R.D., 1977, "Lens Initiation in Secondary Frost Heaving", Proc. of the International Symposium on Frost Action in Soils, Lulea Sweden, V. 2, p. 68-74.

Miller, R.D., 1978, "Frost Heaving in Non-Colloidal Soils", Proc. 3rd Int. Conf. on Permafrost, V. 1, p. 708-713.

Miller, R.D., 1980, "The Adsorbed Film Controversy", Agronomy Paper No. 1327, Cornell University, 9 p.

Miller, R.D.,1981, Personal communication.

Miller, R.D. and Koslow, E.E., 1980, "Computation of Rate of Heave vs. Load Under Quasi-Steady State", Cold Reg. Sci. Tech., V. 3, p. 243-251.

Miller, R.D., Loch, J.P.G. and Bresler, E., 1975, "Transport of Water and Heat in a Frozen Permeameter", Soil Sci. Soc. Am. Proc., V. 39, p. 1029-1036.

Nye, J.F., 1957, "The Distribution of Stress in Glaciers and Ice Sheets", Proc. Royal Society, V.A 239, p. 113-133.

Patterson, W.S.B., 1969, "The Physics of Glaciers", Pergamon Press, Oxford, 247 p.

Penner, E., 1967, "Heaving Pressure in Soils During Unidirectional Freezing", Can. Geotech. Journ., V. 4, p. 398-408.

Penner, E., 1982, "Aspects of Ice Lens Formation", Proc. of the Third International Symposium on Ground Freezing., Hanover, N.H.

Perfect, E., 1980, "Temperature Induced Water Migration in Saturated Frozen Soils", Unpub. M.A. Thesis, Carleton University, Ottawa, 81 pp.

Perfect, E., and Williams, P.J., 1980, "Thermally Induced Water Migration in Frozen Soils", Cold Reg. Sci. and Tech., V. 3, p. 101-109.

Philip, J.R., 1980, "Thermal Fields During Regelation", Agronomy Paper No. 1320, Dept. of Agronomy, Cornell University, Ithaca, N.Y.

Philip, J.R. and De Vries, D.A., 1957, "Moisture Movement in Porous Materials Under Temperature Gradients", Trans. Am. Geophys. Un., V. 38, p. 222-231.

Römkens, M.J,M. and Miller, R.D., 1973, "Migration of Mineral Particles in Ice With a Temperature Gradient", J. Colloid Interface Sci., V. 42, p. 103-111.

Schleicher and Schuell Catalogue.

Sheeran, D.E. and Yong, R.N., 1975, "Water and Salt Redistribution in Freezing Soils", Proc. Conf. on Soil-Water Problems in Cold Regions, Calgary, Alta., p. 61-69.

Sourirajan, S., 1982, Chemical Engineering Division, N.R.C. Canada, Personal Communication.

Sutherland, H.B. and Gaskin, P.N., 1973, "Pore Water and Heaving Pressures Developed in Partially Frozen Soils", 2nd Int. Conf. on Permafrost Proceedings, Nat. Acad. Sci., p. 409-419.

Taylor, G.S. and Luthin, J.N., 1976, "Numeric Results of Coupled Heat-Mass Flow During Freezing and Thawing", Proc. 2nd Conf. on Soil-Water Problems in Cold Regions, Edmonton Alta., p. 155-172.

Tsytovitch, N.A., 1975, "The Mechanics of Frozen Ground", (G.K. Swinzow ed.), Scripta Books Co., Washington D.C., p. 152.

Washburn, A.L., 1979, "Geology: A Survey of Periglacial Processes and Enviroments", Edward Arnold Ltd, London, 406 pp.

Williams, P.J., 1967, "Properties and Behaviour of Freezing Soils", Norwegian Geotechnical Institute, Publ. N. 72, 119 p.

Williams, P.J., 1979, "Pipelines and Permafrost", Geography and Development in the Circumpolar North," Longmans Inc., N.Y., p. 33.

Williams, P.J. and Perfect, E., 1979, "Investigation of Rates of Water Movement through Frozen Soils", Final Report for Dept. Energy, Mines and Resources, Ottawa, DSS File No. 02SU-KL229-7-1562, 36 pp.

Williams, P.J. and Perfect, E., 1980, "Investigation of Thermally Actuated Water Migration in Frozen Soils", Final Report for Dept. Energy, Mines and Resources, Ottawa, DSS File No. 05SU-23235-9-0484, 57 pp.

Williams, P.J. and Wood, J.A., 1981, "Investigation of Pressure Charges in Frozen Soils during Thermally Induced Moisture Migration", Final Report for Dept. of Energy, Mines and Resources, Ottawa, DSS File No. 05SU-23235-0-0496, 128 pp.

Woodruff, D.P., 1963, "The Solid-Liquid Interface", Cambridge University Press, Great Britain, p. 21-25.

Zemansky, M.W. and Dittman R.H., 1981, 'Heat and Thermodynamics', McGraw Hill, U.S.A., p. 204-206.

APPENDIX A

ONSAGER RECIPROCITY PRINCIPLE

Classical thermodynamics deals primarily with reversible processes and equilibrium states. It allows prediction of whether a spontaneous process will occur and its direction, but not the rate. Irreversible thermodyanmics deals with the rate at which processes occur. In natural systems, a variety of forces X_i may operate in such a manner so as to produce mutually interacting fluxes J_i (Hillel, 1971). If a system is relatively close to an equilibrium state, the fluxes can be assumed to be linearly related to the forces causing them. Hence:

$$J_1 = L_{11}X_1 + L_{12}X_2 + \ldots + L_{1n}X_n$$

$$J_2 = L_{21}X_1 + L_{22}X_2 + \ldots + L_{2n}X_n$$

$$\vdots$$

$$J_n = L_{n1}X_1 + L_{n2}X_2 + \ldots + L_{nn}X_n$$

That is:

$$J_i = \sum_{k=1}^{n} L_{ik} X_n$$

where L_{ik} = the transmission coefficients of the various fluxes

The Onsager principal of reciprocity states that the phenomenological cross-coefficients are equal (i.e. $L_{ik} = L_{ki}$), Zemansky and Dittman (1981). Note that if the system differs significantly from equilibrium, the fluxes may no longer be linearly related to the forces and the above relations are not applicable.

APPENDIX B

CALIBRATION REPORT FOR THERMISTORS AND THERMOMETER

DATE ...27 January 1982.....

REPORT NO. APH 2426.....
RAPPORT NO.

Calibration of 7 thermistors

for/pour
Carleton University
Geography Dept., Loeb Bldg, Rm. 8347
Ottawa, Ontario
Attn: John Wood

AUTHOR ... Don Lawlor.....
AUTEUR

APPROVED Ronald E. Stafford
APPROUVÉ for Director/pour le directeur

The thermistors were calibrated in a stirred liquid bath between -0.6° and 0.1°C with the readings listed in the table below. The thermistor (serial number 0) was calibrated with a Keithley digital multimeter model 177 serial number 096877 and readings were taken on the 20 K ohm range. The remaining thermistors were calibrated with a Keithley digital multimeter model 191 serial number 17059 and the readings were taken on the 200 K ohm range.

Temp	No.0	No.1	No.12	No.14	No.16	No.15	No.13
-0.641	10.115	10.152	10.134	10.168	10.139	10.153	10.149
-0.607	10.097	10.134	10.117	10.151	10.123	10.135	10.132
-0.503	10.043	10.080	10.063	10.097	10.069	10.081	10.077
-0.421	10.001	10.038	10.021	10.054	10.026	10.039	10.035
-0.310	9.944	9.981	9.964	9.997	9.969	9.982	9.978
-0.198	9.887	9.923	9.906	9.940	9.911	9.924	9.921
-0.077	9.826	9.863	9.845	9.879	9.850	9.863	9.860
-0.021	9.799	9.835	9.818	9.851	9.822	9.836	9.832
-0.005	9.790	9.826	9.808	9.842	9.813	9.827	9.823
0.111	9.733	9.768	9.751	9.784	9.756	9.769	9.765

National Research Council Canada | Conseil national de recherches Canada

REPORT

Liquid-in-Glass Thermometer

Serial No.: 112213

Manufacturer: Brooklyn Thermo. Co.

Submitted By: Carleton Univ. (Geography Dept.)
Ottawa, Ontario

Description: Liquid in Glass, 4 inch immersion

Range: -6 to 0.1°C

Graduation: .01°C

THE ABOVE DESCRIBED THERMOMETER HAS BEEN COMPARED WITH THE STANDARDS OF THE NATIONAL RESEARCH COUNCIL AND FOUND, AT THIS DATE, TO HAVE THE CORRECTIONS LISTED BELOW.

Thermometer Reading	Correction
-5°C	-0.070°C
-4°	-0.068°
-3°	-0.065°
-2°	-0.064°
-1°	-0.066°
0	-0.062°

TO USE THE CORRECTIONS PROPERLY REFERENCE SHOULD BE MADE TO THE FOLLOWING NOTES ON THE REVERSE SIDE OF THIS SHEET: A & D

REMARKS: The estimated limit of accuracy was ±0.01°C. Corrections apply to a partial immersion. The average temperature between theimmersion and the next 1.5in. of thermometer stem was (20°C + Thermometer Reading)/2. The temperature of the remaining graduation region was 20°C.

Ronald E Bell.
for the Director, Division of Physics, Ottawa.

REPORT No. APH 2426/1

DATE 27 January 1982

APPENDIX C

TEST REPORTS FOR PRESSURE TRANSDUCERS

DURHAM
INSTRUMENTS
division of BUCHAN INSTRUMENTS INC
P.O. BOX 426·PICKERING ONT. L1V 2R7· TELEX: 06-981474
TAWA: (613) 238-4200 — TORONTO: (416) 839-9960

PRESSURE TRANSDUCER TEST REPORT

(ORDERED AS XTM-1-190-100 SG)

MODEL NO. XTM-190-100 SG NEW MODEL SERIAL NO. 375-5-114 (R4-40)

CUSTOMER DURHAM CUSTOMER P.O. No. 1890

STANDARD ELECTRICAL CONNECTIONS: (Per ISA 37.1)

Red	-	+ Input	Green	-	+ Output
Black	-	– Input	White	-	– Output

SPECIAL CONNECTIONS:

TEST CONDITIONS:

Rated Pressure 100 psi SG ____ Gage X Sealed Gage
Maximum Pressure 200 psi SG
Maximum Reference Pressure ____ psi ____ Absolute ____ Differential
Tested at 5 VDC Excitation Maximum Excitation: 7.5 VDC

SPECIFICATIONS:

Sensitivity: .403 mV/psi
Zero Pressure Output: < ±3% F.S.
Thermal Effect on Zero: < ±2 % FS/100°F ____ Not Compensated
Thermal Effect on Sensitivity: < ±2 %/100°F ____ Not Compensated*
Compensated Temperature Range: 14°F to 86°F (-10°C to +30°C)
Output Impedance 328 ohms Input Impedance 965 ohms
*See Bulletin ____ for external compensation method.

REMARKS:

O-RING SUPPLIED.

MAXIMUM TORQUE 15 INCH POUNDS.

QUALITY ASSURANCE:

Tested by M. S. Inspected by

Date 12-29-81 Date DEC 30 1981

DURHAM INSTRUMENTS
division of BUCHAN INSTRUMENTS INC
P.O. BOX 426-PICKERING ONT. L1V 2R7 · TELEX: 06-981474
OTTAWA: (613) 238-4200 — TORONTO: (416) 839-9960

PRESSURE TRANSDUCER TEST REPORT

MODEL NO. VQS-250-50 SG SERIAL NO. 4505-5-76

CUSTOMER DURHAM CUSTOMER P.O. No. 1890

STANDARD ELECTRICAL CONNECTIONS: (Per ISA 37.1)

Red - + Input
Black - - Input
Green - + Output
White - - Output

SPECIAL CONNECTIONS:

TEST CONDITIONS:

Rated Pressure 50 psi SG ____ Gage X Sealed Gage
Maximum Pressure 100 psi SG
Maximum Reference Pressure ____ psi ____ Absolute ____ Differential
Tested at 5 VDC Excitation Maximum Excitation: 7.5 VDC

SPECIFICATIONS:

Sensitivity: .904 mV/psi
Zero Pressure Output: < ±3% F.S.
Thermal Effect on Zero: < ±1 % FS/100° F ____ Not Compensated
Thermal Effect on Sensitivity: < ±2 %/100° F ____ Not Compensated*
Compensated Temperature Range: 14°F to 86°F (-10°C to +30°C)
Output Impedance 362 ohms Input Impedance 734 ohms
*See Bulletin ____ for external compensation method.

REMARKS:

SILASTIC COATING ON DIAPHRAGM.

O-RING SUPPLIED.

UNIT PARYLENE COATED.

QUALITY ASSURANCE:

Tested by H. S. Inspected by

Date 1-7-81 Date

DURHAM
INSTRUMENTS
division of BUCHAN INSTRUMENTS INC
BOX 426 • PICKERING • ONTARIO • L1V 2R7 • TELEX 06-981474
(416)839-9960, Ottawa(613)238-4200, Montreal(514)286-9797

PRESSURE TRANSDUCER TEST REPORT

MODEL NO. VQS-250-50 SG SERIAL NO. 4505-5-81

CUSTOMER DURHAM CUSTOMER P.O. No. 2085

STANDARD ELECTRICAL CONNECTIONS: (Per ISA 37.1)

Red - + Input
Black - – Input
Green - + Output
White - – Output

SPECIAL CONNECTIONS:

TEST CONDITIONS:

Rated Pressure 50 psi SG ____ Gage X Sealed Gage
Maximum Pressure 100 psi SG
Maximum Reference Pressure ____ psi ____ Absolute ____ Differential

Tested at 5 VDC Excitation Maximum Excitation: 7.5 VDC

SPECIFICATIONS:

Sensitivity: .908 mV/psi
Zero Pressure Output: < ±3% F.S.
Thermal Effect on Zero: < ±1 % FS/100°F ____ Not Compensated
Thermal Effect on Sensitivity: < ±2 %/100°F ____ Not Compensated*
Compensated Temperature Range: 14°F to 86°F (-10°C to +30°C)
Output Impedance 372 ohms Input Impedance 705 ohms
*See Bulletin ____ for external compensation method.

REMARKS:

O-RING SUPPLIED.

SILASTIC COATING ON DIAPHRAGM.

QUALITY ASSURANCE:

Tested by H. S. Inspected by ____

Date 2-26-82 Date ____

DURHAM INSTRUMENTS
Division of BUCHAN INSTRUMENTS INC.
P.O. BOX 426·PICKERING ONT. L1V 2R7· TELEX: 06-981474
TAWA: (613) 238-4200 — TORONTO: (416) 839-9960

PRESSURE TRANSDUCER TEST REPORT

MODEL NO. VQS-250-50 SG SERIAL NO. 4505-5-79

CUSTOMER DURHAM CUSTOMER P.O. No. 1890

STANDARD ELECTRICAL CONNECTIONS: (Per ISA 37.1)

Red - + Input Green - + Output
Black - – Input White - – Output

SPECIAL CONNECTIONS:

TEST CONDITIONS:

Rated Pressure 50 psi SG ____ Gage X Sealed Gage
Maximum Pressure 100 psi SG
Maximum Reference Pressure ____ psi ____ Absolute ____ Differential

Tested at 5 VDC Excitation Maximum Excitation: 7.5 VDC

SPECIFICATIONS:

Sensitivity: .906 mV/psi

Zero Pressure Output: < ±3% F.S.

Thermal Effect on Zero: < ±1 % FS/100° F ____ Not Compensated

Thermal Effect on Sensitivity: < ±2 %/100° F ____ Not Compensated*

Compensated Temperature Range: 14°F to 86°F (-10°C to +30°C)

Output Impedance 365 ohms Input Impedance 687 ohms

*See Bulletin ____ for external compensation method.

REMARKS:

SILASTIC COATING ON DIAPHRAGM.

O-RING SUPPLIED.

UNIT PARYLENE COATED.

QUALITY ASSURANCE:

Tested by H. S. Inspected by

Date 1-7-81 Date

APPENDIX D

EQUILIBRIUM FREEZING TEMPERATURE OF A SOLUTION AS A FUNCTION OF LACTOSE CONCENTRATION

Reference: Handbook of Chemistry and Physics, 58th ed.
Pages D232-233

LACTOSE, $C_{12}H_{22}O_{11} \cdot 1H_2O$

Molecular weight = 342.30

Formula weight = 360.31

Anhydrous Solute Concentration g/l	Molar Concentration g - mol/l	Freezing Point Depression Δ°C
0.50	5.0	0.027
1.00	10.0	0.055
1.50	15.1	0.083
2.00	20.1	0.112
2.50	25.2	0.140
3.00	30.3	0.169
3.50	35.4	0.198
4.00	40.6	0.228
4.50	45.7	0.258
5.00	50.9	0.288
5.50	56.1	0.319
6.00	61.4	0.351
6.50	66.6	0.385
7.00	71.9	0.420
7.50	77.2	0.456
8.00	82.5	0.495
8.50	87.8	No value given
9.00	93.1	" " "
9.50	98.5	" " "
10.00	103.9	" " "

APPENDIX E

CUMULATIVE OUTFLOW VS. TIME FOR ICE DURING REGELATION TRANSPORT EXPERIMENT NO. A8

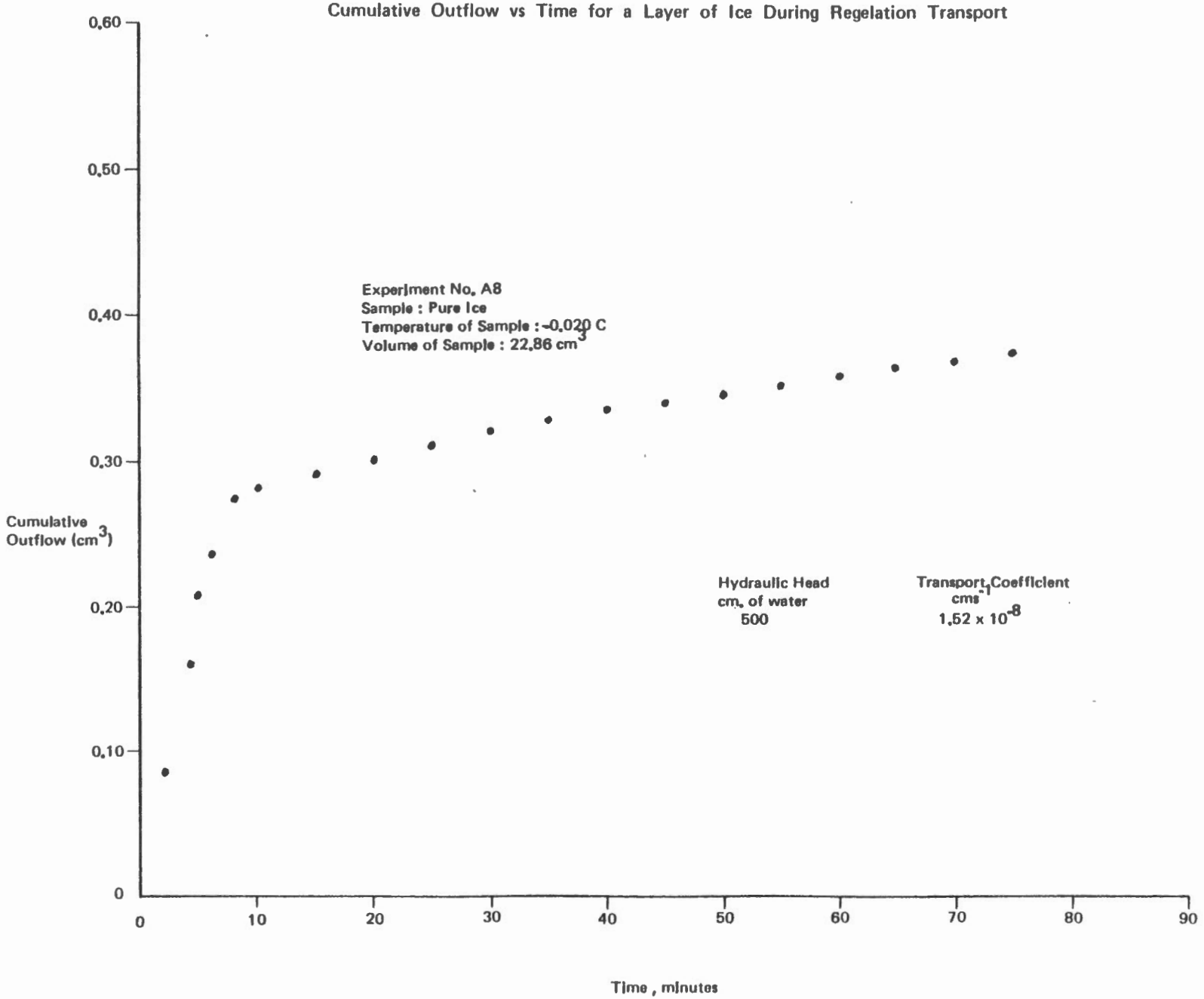
Cumulative Outflow vs Time for a Layer of Ice During Regelation Transport
0.60
0.50
0.40
0.30
0.20
0.10
0
Experiment No. A8
Sample : Pure Ice
Temperature of Sample : -0.020 C
Volume of Sample : 22.86 cm3
Cumulative Outflow (cm3)
Hydraulic Head cm. of water
500
Transport Coefficient cms-1
1.52 x 10-8
0
10
20
30
40
50
60
70
80
90
Time , minutes

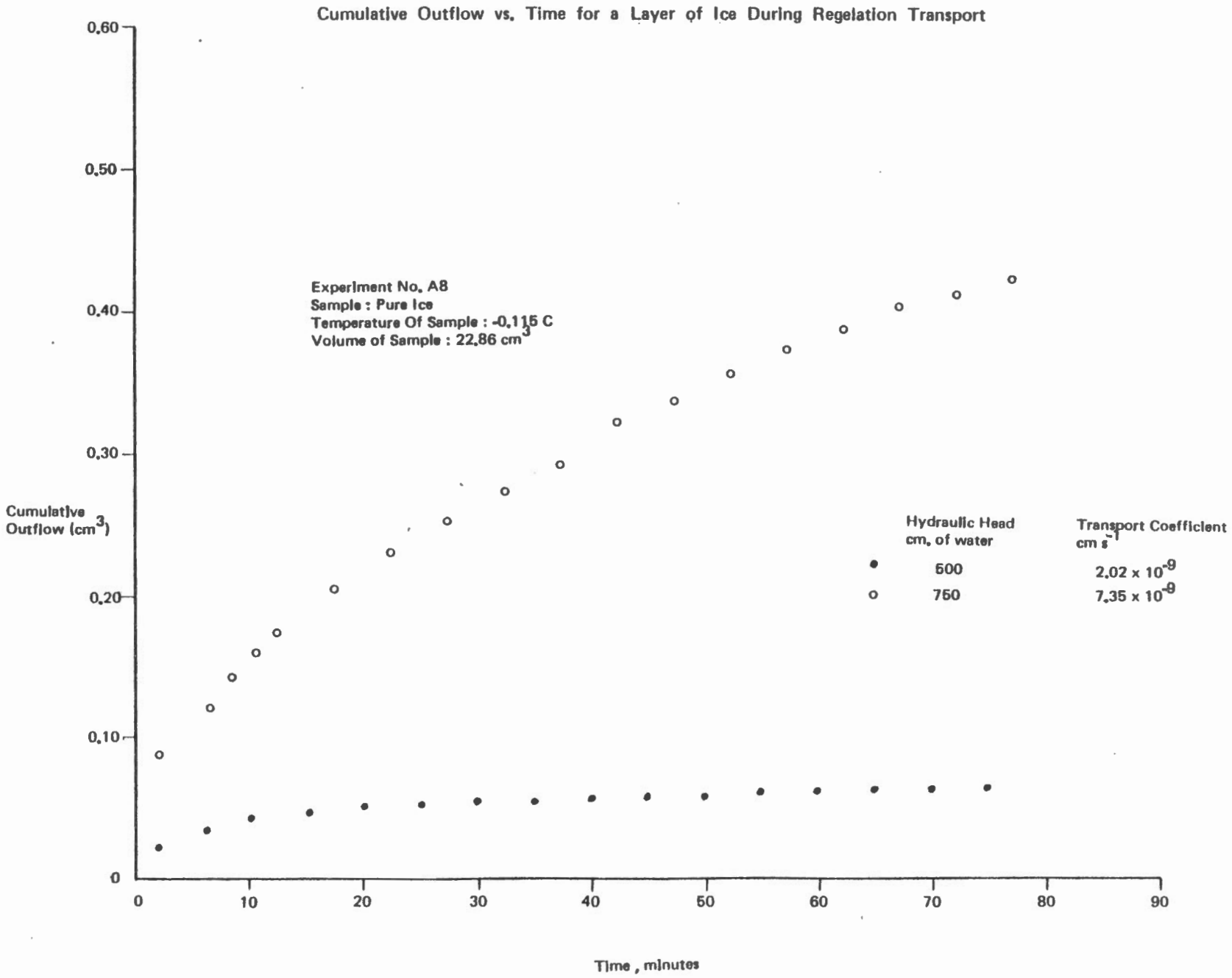
Cumulative Outflow vs. Time for a Layer of Ice During Regelation Transport
Experiment No. A8
Sample : Pure Ice
Temperature Of Sample : -0.115 C
Volume of Sample : 22.86 cm3
Hydraulic Head cm. of water
Transport Coefficient cm s-1
500
2.02 x 10-9
750
7.35 x 10-9
Cumulative Outflow (cm3)
0.60
0.50
0.40
0.30
0.20
0.10
0
0
10
20
30
40
50
60
70
80
90
Time , minutes

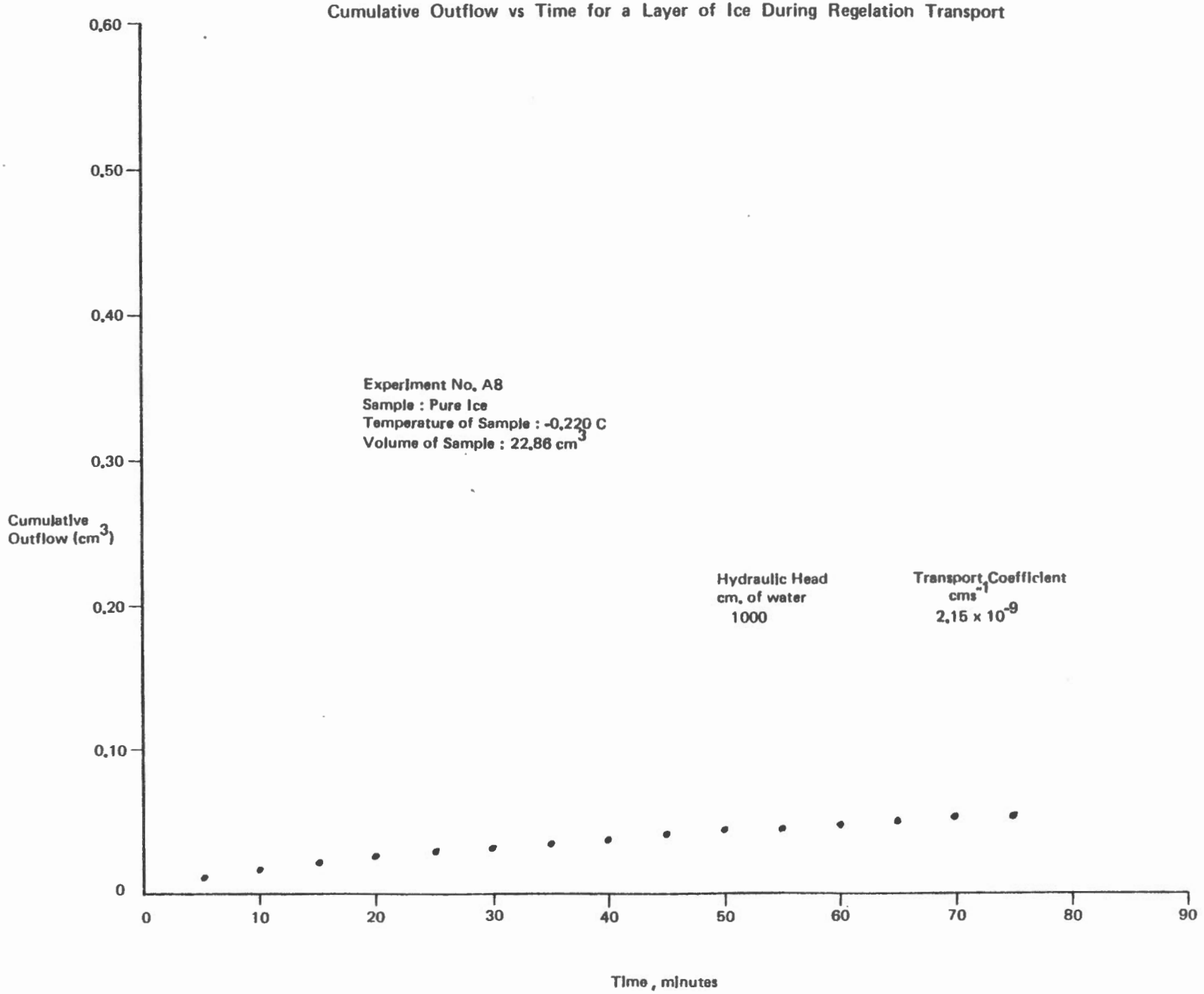
Cumulative Outflow vs Time for a Layer of Ice During Regelation Transport
0.60
0.50
0.40
0.30
0.20
0.10
0
Cumulative Outflow (cm3)
Experiment No. A8
Sample : Pure Ice
Temperature of Sample : -0.220 C
Volume of Sample : 22.86 cm3
Hydraulic Head cm. of water
1000
Transport Coefficient cms-1
2.15 x 10-9
0
10
20
30
40
50
60
70
80
90
Time , minutes

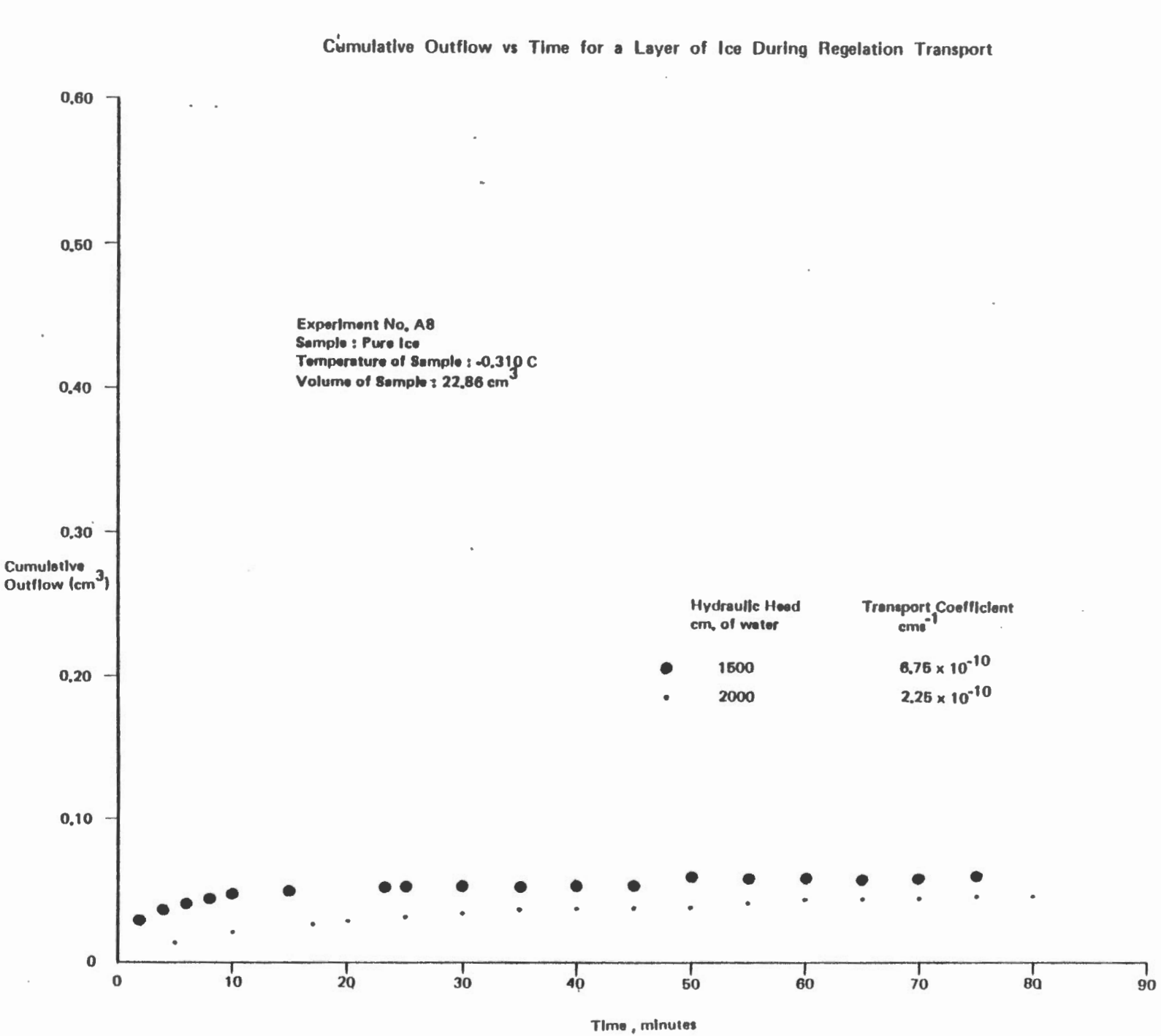
Cumulative Outflow vs Time for a Layer of Ice During Regelation Transport
0.60
0.50
0.40
0.30
0.20
0.10
0
Experiment No. A8
Sample : Pure Ice
Temperature of Sample : -0.310 C
Volume of Sample : 22.86 cm3
Cumulative Outflow (cm3)
Hydraulic Head cm. of water
Transport Coefficient cms-1
1500
6.75 x 10-10
2000
2.25 x 10-10
0
10
20
30
40
50
60
70
80
90
Time , minutes